DERIVED EXPRESSIONS TO COMPARE ATOMIC FLUORESCENCE FLAME SPECTROMETRY WITH OTHER FLAME SPECTROMETRIC METHODS

By

MICHAEL LOEWEN PARSONS

A DISSERTATION PRESENTED TO THE GRADUATE COUNCIL OF
THE UNIVERSITY OF FLORIDA
IN PARTIAL FULFILLMENT OF THE REQUIREMENTS FOR THE
DEGREE OF DOCTOR OF PHILOSOPHY

UNIVERSITY OF FLORIDA

June, 1966

ACKNOWLEDGMENTS

First and foremost, the author is indebted to Dr. J. D. Winefordner, his research director, who has been a true leader and friend and who has the proverbial patience of Job.

Sincere thanks must also go to Dr. Winefordner's many graduate students: Bill McCarthy for his assistance with the computer programs; John Cetorelli for his knowledge of phototubes; Joe Mansfield for his interest and friendship; and all of the others for their good humor.

Technical assistance was received from Bill Luckhurst, the machinest, and Dick Logdsdon, the glass blower. Financial aid was received from N.A.S.A. and the U.S.A.F. All computer work was made possible by the University of Florida Computing Center.

Last, to my wife, Karen, my son, Stevie, and my father, O. L. Parsons, M.D., I dedicate this work.

TABLE OF CONTENTS

Page

ACKNOWLEDGMENTS ii

LIST OF TABLES. viii

LIST OF FIGURES ix

Chapter

I. INTRODUCTION. 1

II. THE INTENSITY OF THE SIGNAL IN ATOMIC FLUORESCENCE FLAME SPECTROMETRY AS A FUNCTION OF ATOMIC CONCENTRATION 4

Theory. 6

Part I 9

Simplified intensity expression 9

General intensity expression for resonance fluorescence 12

General intensity expression for stepwise- and direct-line fluorescence 12

Evaluation of total absorption, A_T, for specific cases 15

Part II. 16

Atomic absorption line half-width is narrow compared to the source line half-width: low atomic concentration. 16

Atomic absorption line half-width is narrow compared to the source line half-width: high atomic concentration. 17

Part III 20

Atomic absorption line half-width is large compared to the source line half-width: low atomic concentration. 20

Chapter Page

Atomic absorption line half-width is large compared to the source line half-width: high atomic concentration. 21

Evaluation of Integrated Intensity Expressions for Specific Cases 24

Discussion of Equations 27

III. DERIVATION OF EXPRESSIONS FOR CALCULATION OF THE LIMIT OF DETECTABILITY IN ATOMIC FLUORESCENCE FLAME SPECTROMETRY 35

Theory. 36

Part I 37

The fluorescence signal 37

Part II. 41

The total noise expression, $\overline{\Delta i_T}$ 41

Part III 43

The phototube shot noise expression . . 43

Part IV. 46

The flame background noise expression . 46

Part V 46

The reflection and Rayleigh scattering (from water droplets) noise expression 46

Part VI. 48

The amplifier-readout noise expression. 48

Part VII 49

The signal-to-noise expressions 49

Part VIII. 52

Calculation of the limiting detectable atomic concentration and the optimum slit width 52

Chapter Page

Use of Derived Expressions and Sample Concentrations 55

Discussion. 58

Part I 58

Comparison of sources and amplifier-readout systems. 58

Part II. 61

The optimum slit width and flame. . . . 61

Part III 70

Methods of lowering the limiting detectable atomic concentration in atomic fluorescence flame spectrometry 70

IV. THEORETICAL COMPARISON OF ATOMIC FLUORESCENCE, ATOMIC EMISSION, AND ATOMIC ABSORPTION FLAME SPECTROMETRY. 74

Theory and Calculations 74

Results 75

Discussion. 100

Part I. Comparison of Calculated $W_{opt.}$ and $N_{min.}$ Values for Atomic Fluorescence, Atomic Emission, and Atomic Absorption Flame Spectrometry as a Function of Flame Type and Conditions. 100

Elements by atomic absorption flame spectrometry 100

Zinc by atomic fluorescence and atomic emission flame spectrometry. 102

All other elements in Table 4.2 by atomic fluorescences and atomic emission flame spectrometry. 102

Chapter Page

Optimum monochromator slit width 103

Part II. The Calculated Range of Near-Linearity for Atomic Fluorescence and Atomic Emission Flame Spectrometry . . . 105

Part III. Variation and Comparison of r.m.s. Noise Terms with Monochromator Slit Width in Atomic Fluorescence, Atomic Emission, and Atomic Absorption Flame Spectrometry 106

Atomic fluorescence flame spectrometry . 107

Atomic emission flame spectrometry . . . 109

Atomic absorption flame spectrometry . . 109

Part IV. Comparison of Experimental Designs in Atomic Fluorescence, Atomic Emission, and Atomic Absorption Flame Spectrometry 110

Sources of excitation. 110

Flame sample cells and entrance optics . 112

Monochromators and detection systems . . 114

APPENDICES 117

I. Symbols and Definitions of Terms Used. 118

II. Evaluation of f_X, f_Y, f_Z, and the Total Absorption, A_T 126

III. Noise Terms Which Do Not Generally Contribute to the Total Noise in Atomic Fluorescence Flame Spectrometry 131

IV. Spectral Constants 134

V. Procedures Used to Obtain the Experimental Parameters Needed for All Calculations 139

VI. Calculated Values of $N_{min.}$ and $W_{opt.}$ for Analytically Useful Lines of Sixty Elements Under Six Flame Conditions in Atomic Emission and Atomic Absorption Flame Spectrometry . . . 163

Page

VII. Factors Concerning the Conversion of Atomic Concentration to Solution Concentration . . . 193

VIII. Computer Programs 199

LITERATURE CITED. 229

BIOGRAPHICAL SKETCH 232

LIST OF TABLES

Table Page

2.1 Intensity Expressions for an Isolated Atomic Fluorescence Line 25

3.1 Derived Signal-to-Noise Expressions for Atomic Fluorescence Flame Spectrometry 50

3.2 Derived Expressions for $N_{min.}$ for Atomic Fluorescence Spectrometry 53

3.3 Calculated Values of $N_{min.}$ and $W_{opt.}$ for Zn, Cd, Hg, Cu, Tl, and Na. 56

4.1 Equations Needed for This Chapter 76

4.2 Calculated Values of W(opt.) and N(min.) for the Resonance Lines of Zn, Cd, Hg, Cu, Tl, and Na as a Function of Flame Type for Atomic Fluorescence, Atomic Emission, and Atomic Absorption Flame Spectrometry 78

4.3 Approximate Range of Near-Linearity of Analytical Growth Curves for Optimum Oxyhydrogen or Air-Hydrogen Flames. 89

IV.1 Values of Atomic Spectral Constants for Some Analytically Important Lines of Sixty Elements. 135

V.1 Data Used for Calculations in Text. 140

VI.1 Calculated Values for the Minimum Atomic Concentration at the Optimum Slit Width for Some Analytically Important Lines of Sixty Elements Under Several Flame Types and Conditions for Atomic Emission and Atomic Absorption Flame Spectrometry 165

LIST OF FIGURES

Figure Page

2.1 Schematic representation of resonance (A), stepwise-line (B), and direct-line (C) fluorescence 5

2.2 Schematic representation of flame cell and light paths. 8

2.3 Representation of variation of total absorption of radiation from a continuous source with atomic concentration 19

2.4 Representation of variation of total absorption of radiation from a narrow line source with atomic concentration 23

2.5 Some possible growth curve shapes: A. Absorption line half-width much less than source line half-width. B. Absorption line half-width much greater than source line half-width 34

3.1 Typical $N_{min.}$ versus monochromator slit width curves for Cd, Cu, and Na when excited by a continuous source. 63

3.2 Typical $N_{min.}$ versus monochromator slit width curves for Cd, Cu, and Na when excited by a narrow line source 65

3.3 Typical variation of $N_{min.}$ versus monochromator slit width curves with variation in flame background intensity 67

4.1 Curves of $N_{min.}$ versus monochromator slit width for atomic fluorescence flame spectrometry using a continuous source with five flame types. 84

Figure Page

4.2 Typical curves of $N_{min.}$ versus monochromator slit width for atomic fluorescence flame spectrometry using a narrow line source with four flame types 86

4.3 Typical curves of $N_{min.}$ versus monochromator slit width for atomic emission and atomic absorption flame spectrometry with four flame types. 88

4.4 Typical r.m.s. noise versus monochromator slit width curves for atomic fluorescence flame spectrometry using a continuous source 91

4.5 Typical r.m.s. noise versus monochromator slit width curves for atomic fluorescence flame spectrometry using a normal intensity narrow line source. 93

4.6 Typical r.m.s. noise versus monochromator slit width curves for atomic fluorescence flame spectrometry using a very high intensity narrow line source 95

4.7 Typical r.m.s. noise versus monochromator slit width curves for atomic emission flame spectrometry 97

4.8 Typical r.m.s. noise versus monochromator slit width curves for atomic absorption flame spectrometry 99

V.1 Schematic diagrams of entrance optics assumed for atomic emission (A), atomic fluorescence (B), and atomic absorption (C) flame spectrometry 145

V.2 Measured γ versus wavelength curve at 900 volts on the phototube 147

V.3 Measured flame background intensity versus wavelength curves for oxyhydrogen and air-hydrogen flames as a function of flame gas composition and height above the burner tip. . 151

Figure Page

V.4 Measured flame background intensity versus wavelength curves for the argon-hydrogen-entrained air flame as a function of the height above the burner tip 153

V.5 Measured intensity versus wavelength curve for 150 watt xenon arc. 156

V.6 Measured fraction of incident radiation reflected and scattered by water droplets in the flame versus wavelength curves. 159

CHAPTER I

INTRODUCTION

In 1964 atomic fluorescence flame spectrometry was first used as an analytical technique for trace metal analysis (25,26), and an initial theoretical treatment of the fluorescence signal as a function of the atomic concentration of the metallic species in the flame was given (28). Since that time, two articles have appeared which have given the method a firm footing as a useful analytical tool. Mansfield, Winefordner, and Veillon (13) determinzed zinc, cadmium, and thallium in the parts per billion, ppb (millimicrograms per gram of solution), range and mercury, indium, and gallium in the parts per million, ppm (micrograms per gram of solution), range using intense, narrow line sources of excitation. Veillon, Mansfield, Parsons, and Winefordner (21) determined nine elements in the ppm range using a continuous source of excitation.

Because atomic fluorescence flame spectrometry is proving to be complementary to the other flame spectrometric methods, atomic emission and atomic absorption, it has become desirable to complete the theoretical treatment started by Winefordner and Vickers (28). The theoretical treatment of both atomic emission and atomic absorption flame spectrometry has been given by Winefordner and Vickers (29, 30) and Winefordner and Veillon (27). Thus, the completion of the theory of atomic fluorescence permits the comparison of all three methods as well as the prediction of relative sensitivities, minimum atomic concentrations, ranges of near-linearity, optimum monochromator slit widths, and the best experimental designs for analysis.

The atomic concentration (atoms per cm.^{3} of flame gases) has been related to the solution concentration (moles per liter of solution) by Winefordner and Vickers (29), and therefore, if certain information is available about the compounds formed in the flame, the theoretical treatment of any flame method can be used to predict the minimum solution concentration of sample which is detectable in a given flame.

The purpose of this dissertation is therefore threefold: (1) A theoretical derivation of the equations needed to predict the intensity of atomic fluorescence as a function of atomic concentration will be given. This is done for narrow line and continuous sources of excitation using both D.C. and A.C. amplifier-readout systems. Knowledge of these equations enables the experimenter to predict the shape of analytical growth curves for any experimental design. (2) Derivation of equations for all of the noises contributing to the total noise in atomic emission, atomic absorption, and atomic fluorescence flame spectrometry. The limit of detectability can then be calculated for the limiting detectable signal-to-noise ratio (usually 2). From these equations the variation of each noise term, as well as the total noise term, with the monochromator slit width can be predicted, and the optimum slit width determined. (3) A comparison of atomic fluorescence, atomic emission, and atomic absorption flame spectrometry can then be made on a theoretical level, including limits of detectability, dominate noises, ranges of near-linearity of analytical curves, optimum monochromator slit widths for maximum signal-to-noise ratios, and experimental designs.

Sample calculations are given for cases where sufficient data exist or logical assumptions of unknown values can be made. In the process of gathering the data for the sample calculations, many experimental parameters have been measured. The procedures and techniques for making these measurements are given in the Appendices and will be referred to at appropriate places in the text. Finally, procedures for obtaining information about the parameters needed to convert atomic concentration into solution concentration are given in the Appendices; this allows the experimenter to take the final step from theory to practice.

CHAPTER II

THE INTENSITY OF THE SIGNAL IN ATOMIC FLUORESCENCE FLAME SPECTROMETRY AS A FUNCTION OF ATOMIC CONCENTRATION

Atomic fluorescence results when an atom is excited to some energy level above the ground energy level by the absorption of radiation and emits radiation upon deactivation. There are three basic types of atomic fluorescence produced by radiational excitation (15), and they are illustrated in Figure 2.1. These are resonance fluorescence, stepwise-line fluorescence, and direct-line fluorescence. Resonance fluorescence is defined as the process resulting when an atom is excited by and re-emits the same spectral line. The resonance transition always involves the ground energy level. Direct-line fluorescence consists of excitation of an atom to an energy level with a radiational deactivation to an energy level above the ground energy level. Stepwise-line fluorescence consists of excitation to an energy level higher than the first energy level, a non-radiational deactivation to a lower energy level, and a radiational deactivation to an even lower (usually ground) energy level.

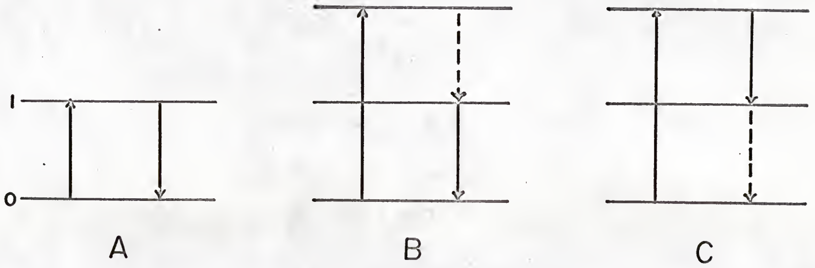

Fig. 2.1.-Schematic representation of resonance (A), stepwise-line (B), and direct-line (C) fluorescence. (The solid line represents a radiational transition, and the dashed line represents a radiationless transition.)

Theory

The basic experimental setup for atomic fluorescence flame spectrometry is assumed to be the same as that described by Winefordner and Vickers (28), which consisted of an intense source of radiation focused on a flame sample cell containing atomic vapor of the element of interest; the resulting fluorescence radiation is observed at right angles to the incident exciting radiation; the fluorescence radiation is focused on the entrance slit of a monochromator; and the amplified signal from a multiplier phototube is displayed on a meter or recorder. In order to make the theory as general as possible, it is assumed that only a portion of the flame is illuminated with the exciting radiation and only a portion of the resulting atomic fluorescence is collected by the monochromator (see Figure 2.2). Although the top diagram in Figure 2.2 is an exact representation of the flame cell and path lengths, it will be simpler to deal with the dimensions and arrangements shown in the lower diagram. The lower diagram is drawn so that the areas X, Y, and Z are the same as in the upper diagram, and therefore the path lengths d, l, L, and b are average values for the trapezoidal areas in the top diagram in Figure 2.2. This simplified representation should introduce only a negligible error into the final expressions and so will be used throughout the remainder of the chapter. It will be

Fig. 2.2.-Schematic representation of flame cell and light paths.

Actual Representation of Flame Cell + Light Paths

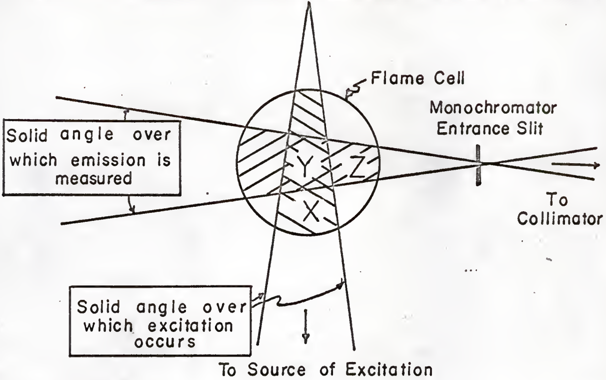
Flame Cell
Monochromator Entrance Slit
Solid angle over which emission is measured
Y
Z
X
To Collimator
Solid angle over which excitation occurs
To Source of Excitation

Simplified Representation of Flame Cell - Light Paths

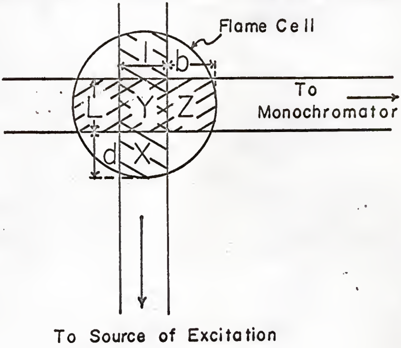

convenient to divide the theory into three parts. In the first part, the basic intensity of fluorescence expressions will be derived. In the second part, the intensity expressions for low and high atomic concentrations will be given for the case where the excitation source line half-width is much wider than the absorption line half-width of the atoms in concern in the hot flame gases. This case results when using a continuous source of excitation, such as the xenon arc, or perhaps when using a wide-line metal vapor discharge lamp, such as the Osram or Philip's lamps. In the third part, the intensity expressions for low and high atomic concentrations will be given for the case where the excitation source line half-width is much narrower than the absorption line half-width of the atoms in concern in the hot flame gases. This case will often be encountered when using narrow line sources, such as electrodeless discharge tubes or hollow cathode discharge tubes. The case where the absorption line half-width is similar to the excitation source line half-width is considerably more difficult to treat, should seldom be important in most analytical studies, and so will not be treated here. All symbols are defined in Appendix I.

Part I

Simplified intensity expression.-The integrated atomic fluorescence intensity expression for an isolated spectral line is given by

$$I_F = I_A \frac{\Phi_T}{4\pi} f_Z \text{ , watts cm.}^{-2} \text{ ster.}^{-1} \qquad (2.1)$$

where I_A is the intensity absorbed by the resonance line in watts cm.$^{-2}$; Φ_T is the total power or energy efficiency for fluorescence, that is, the ratio of the power (or energy per second) emitted per second to the power (or energy per second) absorbed per second; and is related to ϕ_T, and the total quantum efficiency, that is, the ratio of the number of photons emitted per second by fluorescence to the number of photons absorbed per second, by $\Phi_T = (\nu_f/\nu_a)\phi_T$, where ν_f and ν_a are the frequencies in sec.$^{-1}$ of the fluorescence (f) and absorbed (a) photons, respectively; 4π is the number of steradians (unit solid angles, no units) in a sphere; and f_Z is a factor (no units) to account for the decrease in fluorescence intensity in region Z of Figure 2.2 by absorbing particles. Refer to the article by McCarthy, Parsons, and Winefordner (12) for a discussion of factors influencing the quantum and power efficiencies.

The intensity absorbed by a spectral line, I_A, is given by

$$I_A = I^\circ f_x \Omega_a A_T \text{ , watts cm.}^{-2} \qquad (2.2)$$

where I° is the incident intensity of the exciting radiation from a continuous source in watts cm.$^{-2}$ ster.$^{-1}$ sec., that is, the radiant power per unit source area per unit solid angle per frequency interval. If the exciting radiation is a narrow line source, then I° must be replaced by $I_L\, 2\sqrt{\ln 2}/\sqrt{\pi}\, \Delta \nu_L$, where I_L is the intensity of the source line in watts cm.$^{-2}$ ster.$^{-1}$, and $\Delta \nu_L$ is the source line half-width in sec.$^{-1}$ for a line with a Gaussian contour (the $2\sqrt{\ln 2}/\sqrt{\pi}$ is necessary to convert the Gaussian half-width to a triangular half-width -- this procedure simplifies the calculation of line profile areas). The other parameters in equation 2.2 are defined as follows: f_X is a factor (no units) to account for the decrease in the intensity of the exciting radiation in region X of Figure 2.2 by absorbing particles, Ω_a is the solid angle (ster.) of incident radiation used for excitation of the atomic vapor (see Figure 2.2), and A_T is the total absorption factor, that is, the fraction of incident radiation (in the flame cell region which is being studied, that is, region Y of Figure 2.2) absorbed in sec.$^{-1}$ and is defined (15,20) as

$$A_T = \int_0^{\infty} \frac{I^{\circ}_{\nu} - I\nu_t}{I^{\circ}_{\nu}}\, d\nu = \int_0^{\infty} [1 - \exp(-k_{\nu} L)]\, d\nu \text{ , sec.}^{-1} \tag{2.3}$$

where I°_{ν} is the intensity of the exciting radiation as a function of frequency (units of watts cm.$^{-2}$ ster.$^{-1}$ sec.), $I\nu_t$ is the intensity transmitted through the flame of average width L at frequency ν, k_{ν} is the atomic absorption coefficient in cm.$^{-1}$ as a function of frequency, ν, and L is the average path length over which absorption occurs and the resulting atomic fluorescence is measured (see Figure 2.2). The factors f_X and f_Z are related to the distances over which absorption occurs and to the atomic absorption coefficient, $\overline{k}$, averaged over all frequencies and all absorbing atoms. The factors f_X and f_Z approach unity as the solid angle over which excitation occurs is increased to cover the entire flame cell and as the solid angle over which the fluorescence is measured is increased to include the entire flame cell. Expressions for the factors f_X and f_Z are given in Appendix II.

General intensity expression for resonance fluorescence.-For an isolated atomic resonance line excited by the same line, the intensity of fluorescence can be found by combining equation 2.1 and 2.2, and so

$$I_F = I^{\circ} f_X \frac{\Omega_a}{4\pi} A_T \Phi_T f_Z \text{ , watts cm.}^{-2} \text{ ster.}^{-1} \qquad (2.4)$$

General intensity expression for stepwise- and direct-line fluorescence (15,28).-For an isolated fluorescence line produced by stepwise-line fluorescence, the intensity of fluorescence expression can be found by combining equations 2.1 and 2.2, but in doing this the various absorption lines (other than resonance absorption) which are effective in exciting the fluorescence energy level must be considered as well as the influence of re-absorption of the fluorescence radiation by atoms of the same kind within the region of observation (region Z of Figure 2.2). If there are j absorption lines (other than resonance absorption) resulting in excitation of an atom to the fluorescence energy level, then the intensity of fluorescence is given by

$$I_F = \frac{\Omega_a}{4\pi} f_Z f_Y \Phi_T \sum_j I^{\circ}_j f_{X_j} A_{T_j} \text{ , watts cm.}^{-2} \text{ ster.}^{-1} \tag{2.5}$$

where the f_Y term accounts (10) for re-absorption of the fluorescence radiation produced by non-resonance absorption within region Y in Figure 2.2 by atoms of the same kind as the fluorescent ones (see Appendix II for derivation of the re-absorption factor). For the case of resonance fluorescence, re-absorption is inherently considered in the A_T factor, and so f_Y is unity for resonance fluorescence (that is, $f_Y = 1 + \exp(\bar{k}l)$, where $\bar{k}$ is the average atomic absorption coefficient for absorption of radiation produced by means other than resonance absorption; therefore, if resonance fluorescence is produced by resonance absorption, then f_Y is unity. The summation in equation 2.5 is necessary because the fluorescence energy level (the excited energy level which undergoes a radiational deactivation to produce a fluorescence line) can be populated by a variety of routes, that is, there may be j absorption transitions other than the resonance transition which ultimately result in populating the fluorescence energy level. All of the terms within the summation sign concern the absorption line (22) which produces the fluorescence line, that is, I°_{j} is the intensity of the exciting radiation at the frequency of the absorption line j, f_{X_j} is the fraction of radiation transmitted through region X of Figure 2.2 by the absorption line j, A_{T_j} is the total absorption for the absorption line j, and Φ_T is the total power efficiency for the fluorescence line resulting from absorption of radiation (refer to McCarthy, Parsons, and Winefordner (12) for a thorough discussion of the power efficiency).

For resonance fluorescence f_Y is unity (in the absence of any other fluorescence emission and in the absence of any excitation to energy levels other than the resonance energy level); the terms within the summation are then defined only for the resonance line; the total power efficiency is simply given by the quantum efficiency for resonance fluorescence; and equation 2.5 reduces to equation 2.4.

Equation 2.5 is also a general expression for evaluating the intensity of atomic fluorescence for the case of direct-line fluorescence and so is a general expression whatever the mechanism of excitation and whatever emission transition is involved. For the case of direct-line fluorescence, there may still be j absorption routes of excitation, but the fluorescence transition does not ever involve the ground electronic state.

If more than one fluorescence transition is involved, for example, a multiplet or closely spaced lines, then a summation of expressions like equation 2.5 can be added together to give the total fluorescence intensity. Hyperfine splitting of spectral lines due to the isotopes or nuclear spin effects can also be considered using equation 2.5.

Evaluation of total absorption, A_T, for specific cases.-The intensity of atomic fluorescence can be calculated for specific cases by evaluating the A_T factor and substituting into equations 2.4 or 2.5. The value of A_T depends upon the line-width of the atomic absorption line compared to the line-width of the exciting radiation and upon the product of NL (the number of atoms in the ground energy level per cm.^{3} of flame gases times the flame absorption path length of region Y of Figure 2.2, that is, the region being viewed by the spectrometric system). In Parts II and III the extreme cases will be considered, that is, very high and very low values of NL and very narrow and very wide atomic absorption lines compared to the excitation source line half-width. These cases are ordinarily the most useful in analytical work. Refer to Appendix II for the derivation of A_T.

Part II

Atomic absorption line half-width is narrow compared to the source line half-width: low atomic concentration.- For this case the total absorption factor, A_T, can be given by the expression

$$A_T = \int_0^\infty [1-\exp(-k_\nu L)]\, d\nu = \int_0^\infty k_\nu L d\nu \quad , \text{sec.}^{-1} \;, \qquad (2.6)$$

and so A_T can be shown (20) to be given by

$$A_T = \frac{k^\circ L \Delta\nu_D \sqrt{\pi}}{2\sqrt{\ln 2}} \;, \text{sec.}^{-1} \;. \qquad (2.7)$$

The atomic absorption coefficient, k°, at the absorption line center for a purely Doppler broadened line (that is, for small $k^\circ L$ or small NL, the contour of an absorption line near the line center is determined entirely by Doppler broadening) is given (15) by

$$k^\circ = \frac{2\sqrt{\ln 2}\, \lambda_o^2\, g_u\, NA_t}{8\pi^{3/2}\, \Delta\nu_D\, g_1}, \text{cm.}^{-1} \;, \qquad (2.8)$$

where λ_o is the wavelength of the center of the absorption line in concern, g_u and g_1 are the statistical weights of the upper (u) and ground (1) energy levels involved in the absorption transition, respectively, N is the number of atoms in the lower energy level per cm.^{3} of flame gases (ground for the lower energy level of the absorption lines which are effective in exciting fluorescence), A_t is the transition probability in sec.$^{-1}$ for the transition u to 1, and $\Delta\nu_D$ is the Doppler half-width in sec.$^{-1}$ and is given (15) by

$$\Delta\nu_D = \frac{2\sqrt{2R\ln 2}}{c}\ \nu_o\sqrt{\frac{T}{M_x}}\ , \qquad (2.9)$$

where R is the gas constant, ν_o is the frequency of the line center in sec.$^{-1}$, T is the temperature of the hot gas in °K, c is the speed of light in cm. sec.$^{-1}$, and M_x is the atomic weight of the absorbing atom.

Qualitatively, the variation of A_T with NL is shown in Figure 2.3. As NL increases (for small NL values), the area under the curves in Figure 2.3 (that is, A_T) increases linearly with NL, and so I_F will increase linearly with NL.

Atomic absorption line half-width is narrow compared to the source line half-width: high atomic concentration.- At large values of NL, that is, large $k^{\circ}L$, the value of A_T is given (20) by

$$A_T = \sqrt{\frac{k^{\circ}L\ \Delta\nu^2_D\ a\sqrt{\pi}}{\ln 2}} = \sqrt{\frac{\lambda^2_o\ \Delta\nu_D\ aNA_tLg_u}{4\pi\sqrt{\ln 2}\ g_1}}\ ,\ \text{sec.}^{-1} \qquad (2.10)$$

where the expression on the right results when equation 2.8 is substituted for k° in the left hand expression. The factor, a, in equation 2.10 is called the damping constant and is given (15,20) by

Fig. 2.3.-Representation of variation of total absorption of radiation from a continuous source with atomic concentration.

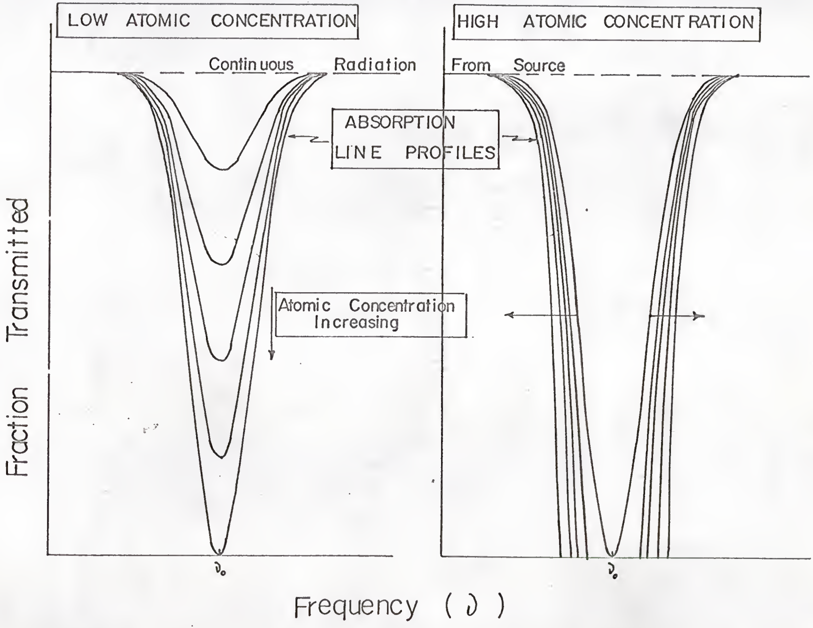
LOW ATOMIC CONCENTRATION
HIGH ATOMIC CONCENTRATION
Continuous Radiation From Source
ABSORPTION LINE PROFILES
Atomic Concentration Increasing
Fraction Transmitted
ν_o
ν_o
Frequency (ν)

$$a = \frac{\Delta\nu_C}{\Delta\nu_D}\sqrt{\ln 2}\text{ , no units,} \tag{2.11}$$

where $\Delta\nu_C$ is the half-width of the absorption line in sec.$^{-1}$ for pure collisional broadening, and $\Delta\nu_D$ is the half-width of the absorption line in sec.$^{-1}$ for pure Doppler broadening. Actually equation 2.11 should contain the natural half-width, $\Delta\nu_N$, and the resonance half-width, $\Delta\nu_R$, in the numerator, but these broadening terms are generally much smaller than $\Delta\nu_C$ for atoms in analytical flames. Qualitatively, the influence of NL on A_T is illustrated in Figure 2.3. As NL increases (for large NL values), the area under the curves in Figure 2.3, that is, A_T, increases linearly with $\sqrt{NL}$, and so I_F will increase linearly with $\sqrt{NL}$.

Part III

Atomic absorption line half-width is large compared to the source line half-width: low atomic concentration.-At small NL values the value of A_T is given by

$$A_T = \int_0^{\Delta\nu_L\sqrt{\pi}/2\sqrt{\ln 2}} [1 - \exp(-k_\nu L)]d\nu = \int_0^{\Delta\nu_L\sqrt{\pi}/2\sqrt{\ln 2}} k_\nu L d\nu =$$

$$\frac{k^\circ L\Delta\nu_L\sqrt{\pi}}{2\sqrt{\ln 2}} \tag{2.12}$$

where the integration is taken over the source line half-width (triangular distribution), $\Delta\nu_L$, rather than the absorption line half-width. The final portion of equation

2.12, the area in Figure 2.4, results by multiplying the peak atomic absorption coefficient times the path length times the triangular half-width of the source line, that is, absorption can only occur over the excitation source line half-width because there is no other incident radiation within the absorption line. This can be qualitatively seen by referring to Figure 2.4. As NL increases (for small NL values), the area (A_T) under the emission line profile increases approximately linearly with NL. This is only true if the source line half-width is considerably less, for example, ten-fold, than the absorption line half-width.

The product of $I^{\circ} A_T$ ($I^{\circ} A_T$ is evaluated because I° for a line source depends upon $\Delta\nu_L$) is given by

$$I^{\circ} A_T = k^{\circ} L I_L = \frac{2\sqrt{\ln 2}\,\lambda^2_{\,o}\, g_u\, N L A_t\, I_L}{8\pi^{3/2}\,\Delta\nu_D\, g_l}, \tag{2.13}$$

where $I^{\circ} = I_L 2\sqrt{\ln 2}/\sqrt{\pi}\,\Delta\nu_L$. The final portion of equation 2.13 results by substituting for k° from equation 2.8.

Atomic absorption line half-width is large compared to the source line half-width: high atomic concentration.- At high NL values, the value of A_T can be found by evaluating the first portion of equation 2.12, that is, if NL is large, then

Fig. 2.4.-Representation of variation of total absorption of radiation from a narrow line source with atomic concentration.

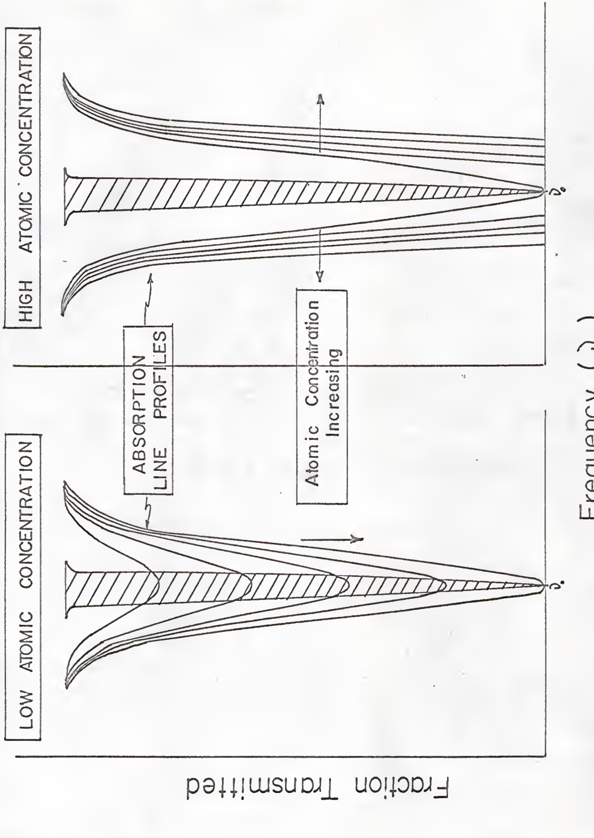
LOW ATOMIC CONCENTRATION
HIGH ATOMIC CONCENTRATION
ABSORPTION LINE PROFILES
Atomic Concentration Increasing
ν_0
ν_0
Frequency (ν)
Fraction Transmitted

$$A_T = \int_0^{\Delta\nu_L\sqrt{\pi}/2\sqrt{\ln 2}} [1 - \exp(-k_\nu L)]d\nu = \int_0^{\Delta\nu_L\sqrt{\pi}/2\sqrt{\ln 2}} d\nu \quad , \qquad (2.14)$$

where the second expression is only true for large values of $k_\nu L$. If the excitation source line half-width is narrow compared to the absorption line half-width, then $k_\nu L$ will be large over the entire source line half-width, and the second portion of equation 2.14 is justified. Therefore, for these conditions, A_T is given by

$$A_T = \frac{\Delta\nu_L\sqrt{\pi}}{2\sqrt{\ln 2}} \quad , \qquad (2.15)$$

and the product $I^\circ A_T$ is given by

$$I^\circ A_T = I_L \qquad (2.16)$$

and so in this case I_F will depend only on I_L and will be independent of NL. Qualitatively, the influence of NL on the value of A_T is illustrated in Figure 2.4. For large NL values, essentially complete absorption occurs at the absorption line peak, that is, over the entire source line profile, and so more radiation can be absorbed only if the source line half-width widens. Thus, A_T and I_F are expected to be constant as NL increases.

Evaluation of Integrated Intensity Expressions for Specific Cases

Refer to Table 2.1 for the integrated intensity expressions (equations 2.17-2.24) for resonance, stepwise-

TABLE 2.1

INTENSITY EXPRESSIONS FOR AN ISOLATED ATOMIC FLUORESCENCE LINE

Resonance Fluorescence Expressions

Atomic Absorption Line Half-Width Much Narrower than the Source Line Half-Width

Low NL $$I_F = I^{\circ} f_X \Omega_a \Phi_T f_Z \frac{\lambda_o^{\,2} g_u NL A_t}{32\pi^2 g_1} \qquad (2.17)$$

High NL $$I_F = I^{\circ} f_X \frac{\Omega_a}{4\pi} \Phi_T f_Z \sqrt{\frac{\lambda_o^{\,2} \Delta\nu_D \, a \, NL A_t g_u}{4 \pi \ln 2 \; g_1}} \qquad (2.18)$$

Atomic Absorption Line Half-Width Much Wider than Source Line Half-Width

Low NL $$I_F = \frac{2\sqrt{\ln 2}}{32\pi^{5/2}} I_L f_X \Omega_a \Phi_T f_Z \frac{\lambda_o^{\,2} g_u NL A_t}{g_1 \Delta\nu_D} \qquad (2.19)$$

High NL $$I_F = I_L f_X \frac{\Omega_a}{4\pi} \Phi_T f_Z \qquad (2.20)$$

Table 2.1 (Cont'd)

Stepwise-Line and Direct-Line Fluorescence

Atomic Absorption Line Half-Width Much Narrower than Source Line Half-Width

Low NL $$I_F = \frac{\Omega_a}{32\pi^2} f_Z f_Y \Phi_T \sum_j I_j^\circ f_{X_j} \frac{\lambda_{o_j}^2 g_{u_j} NL A_{t_j}}{g_{1_j}} \qquad (2.21)$$

High NL $$I_F = \frac{\Omega_a}{4\pi} f_Z f_Y \Phi_T \sum_j I_j^\circ f_{X_j} \sqrt{\frac{\lambda_{o_j}^2 \Delta\nu_{D_j} a_j NL A_{t_j} g_{u_j}}{4 \pi \ln 2 \; g_{1_j}}} \qquad (2.22)$$

Atomic Absorption Line Half-Width Much Narrower than Source Line Half-Width

Low NL $$I_F = \frac{2\sqrt{\ln 2}}{32 \pi^{5/2}} \Omega_a f_Z f_Y \Phi_T \sum_j I_{L_j} f_{X_j} \frac{\lambda_{o_j}^2 g_{u_j} NL A_{t_j}}{g_{1_j} \Delta\nu_{D_j}} \qquad (2.23)$$

High NL $$I_F = \frac{\Omega_a}{4\pi} f_Z f_Y \Phi_T \sum_j I_{L_j} f_{X_j} \qquad (2.24)$$

line, and direct-line fluorescence. These expressions result by substituting the proper expressions into equations 2.4 or 2.5 for $I^{o}A_{T}$. It should be noted that the stepwise-line expression gives the resonance expressions if it is remembered that f_{Y} is unity for resonance absorption-fluorescence and that in general only one transition is involved in resonance fluorescence. Also, it should be noted that if more than one fluorescence line is being considered, the total integrated fluorescence intensity of all lines is merely a summation of specific expressionf of the type given in Table 2.1, that is, $\sum_{i} I_{F_i}$, where the summation is over i fluorescence lines.

Discussion of Equations

From the equations in Table 2.1 it can be noted that as long as NL is low, the integrated fluorescence intensity of a spectral line should vary linearly with atomic concentration for the cases of a wide or a narrow absorption line half-width compared to the source line half-width. This linear correlation is of great analytical interest. For most atoms, the total number of atoms in all electronic energy levels per cm.^{3} of flame gases will be approximately the same as the number per cm.^{3} in the ground energy level, that is, N, unless the atom has one or more very low lying excited energy levels. If the compound introduced into the flame is completely dissociated, if the metal atom is not appreciably ionized, and if the metal atom has little tendency to form compounds with flame gas products, or if these phenomena do not vary greatly with concentration of metal atoms introduced into the flame gases, then I_F will also be linear with the solution concentration of metal introduced into the flame gases. The variation of atomic concentration of a metal with solution concentration of a metal and the dependence of these concentrations on aspiration characteristics, flame temperature and type, and gas and solution flow rates have been considered in several theses and papers (17,22,29) and will not be considered here. This chapter concerns only the variation if I_F with atomic concentration and so could apply to methods of sample atomization other than flames.

From the equations in Table 2.1, it is apparent that I_F can be increased by increasing the path length, L, over which radiation is absorbed. However, it should be pointed out that the measuring device may not register a greater signal unless simultaneously the solid angle over which the fluorescence is viewed is also increased. It can also be noted that the value of I_F is linear with the transition probability, A_t, for low NL values. For high NL values I_F is linear with $\sqrt{A_t}$ if the absorption line half-width is small compared to the excitation source line half-width, and is independent of A_t if the excitation source line half-width is narrow compared to the absorption line half-width. In fact, if NL is high and if the source line half-width is narrow compared to the absorption line half-width, I_F depends only on the intensity of the line source, the solid angle of absorption, the power efficiency, and the two fraction transmitted factors, f_X and f_Z; furthermore, I_F is independent of the factors affecting the shape of the absorption line.

The variation of I_F with wavelength of the absorption line (for resonance absorption-fluorescence) can be determined by use of the expressions $c = \lambda_o \nu_o$ and $(d\lambda/d\nu) = \lambda^2/c$. Using the equations for resonance fluorescence in Table 2.1, it can be shown that I_F is independent of λ_o for wide source line half-widths at low NL and for narrow source line half-widths at high NL; it is dependent on $\sqrt{\lambda_o}$ for wide source line half-widths at high NL; and it is dependent on λ_o^{-1} for narrow source line half-widths at low NL. The variation of I_F with absorption line wavelength is more complex for stepwise- or direct-line fluorescence and must be considered for specific cases.

To compare the value of I_F resulting from excitation by a wide line or continuous source with the I_F resulting from a line source, only the products $I^\circ A_T$ for a wide line source and $\sqrt{\pi}\, I_L A_T / 2\sqrt{\ln 2}\, \Delta\nu_L$ for a narrow line source must be considered because all other parameters in the I_F expression for a given spectral line and a given NL must necessarily be the same. Because $\sqrt{\pi}/2\sqrt{\ln 2}$ is essentially unity, only $I^{\circ} A_T$ for a continuous source must be compared with $I_L A_T / \Delta\nu_L$ for a line source. For a low value of NL, the ratio of these products is given approximately by $I^{\circ} \Delta\nu_D / I_L$, where I° has units of watts cm.$^{-2}$ ster.$^{-1}$ sec.; $\Delta\nu_D$ has units of sec.$^{-1}$; and I_L has units of watts cm.$^{-2}$ ster.$^{-1}$. Because I° is usually given in units cm.$^{-2}$ ster.$^{-1}$ mμ^{-1}, the relative intensity of fluorescence when using a continuous or wide line source to a line source is given by $I^{\circ} \Delta\lambda_D / I_L$, where I° has units of watts cm.$^{-2}$ ster.$^{-1}$ mμ^{-1} and $\Delta\lambda_D$ is the Doppler half-width in mμ. A continuous source such as the xenon 150 watt arc lamp has about the same value of I° as I_L for an intense electrodeless discharge tube, for example, Zn, and so the relative intensity is given by just $\Delta\lambda_D$ which is generally about 0.001 to 0.01 mμ. Therefore, if I° is about the same as I_L in absolute value, a line source will give approximately $1/\Delta\lambda_D$ ($\Delta\lambda_D$ has units of mμ) greater fluorescence intensity, that is, often two or three orders of magnitude greater I_F with a line source (see Chapter III).

The values of I_F and N at the intersection of low and high concentration asymptotes (31) can be found by equating the I_F equations for low and high atomic concentrations. Assuming the extrapolation is from very low and very high NL values, the intersection of fluorescence intensity I_{F_i} for resonance fluorescence excited by a continuous source is given by

$$I_{F_i} = \frac{I^{\circ} f_X \Omega_a \ f_Z \ \Delta\nu_D a}{2\pi\sqrt{\ln 2}} \quad , \tag{2.25}$$

and for a line source, I_{F_i} is given by equation 2.25 except I° is replaced by $I_L \ 2 \ \ \ln 2/ \ \ \pi \ \Delta\nu_L$. The value of N_i (the intersection point atomic concentration) for resonance fluorescence excited by a continuous source is given by

$$N_i = \frac{16\pi \ \Delta\nu_D \ g_1 \ a}{\sqrt{\ln 2} \ A_t \ L\lambda_o^{2} \ g_u} = \frac{60a \ \Delta\nu_D \ g_1}{A_t \ L\lambda_o^{2} \ g_u} \quad , \tag{2.26}$$

and if excited by a line source, N_i is given by

$$N_i = \frac{4\pi^{3/2} \ \Delta\nu_D \ g_1}{\sqrt{\ln 2} \ A_t \ L\lambda_o^{2} \ g_u} = \frac{27\Delta\nu_D \ g_1}{A_t \ L\lambda^{2}{}_{o} \ g_u} \quad . \tag{2.27}$$

Note the absence of the aparameter in equation 2.27.

Similar equations can be derived for stepwise- and direct-line fluorescence as well as for multiplet fluorescence lines. The value of I_{F_i} for resonance fluorescence is independent of the flame path length, L, the transition probability, A_t, and the wavelength of absorption, λ_o.

The values of f_X, f_Y, and f_Z (see Appendix II) approach unity as the entire flame cell (assuming a homogeneous flame) is illuminated by exciting radiation and all of the fluorescence radiation is measured. If only a portion of the flame cell is within the solid angle of excitation (see Figure 2.2) and only a portion of the fluorescence radiation is within the solid angle of the monochromator (see Figure 2.2), then f_X and f_Z can be appreciably less than unity and in fact will approach zero for high atomic concentrations of the absorbing atoms. In fact at large values of N, the growth curve of I_F versus N can curve back toward the abcissa. The general shapes of growth curves are shown in Figure 2.5. These shapes have been verified experimentally. Of course, absorbing particles other than the absorbing atoms of interest will also affect the value of I_F, and perhaps the growth curve shape if the absorbing particles vary in concentration as the absorbing atom concentration varies.

Fig. 2.5.-Some possible growth curve shapes:
A. Absorption line half-width much less than source line half-width.
B. Absorption line half-width much greater than source line half-width.

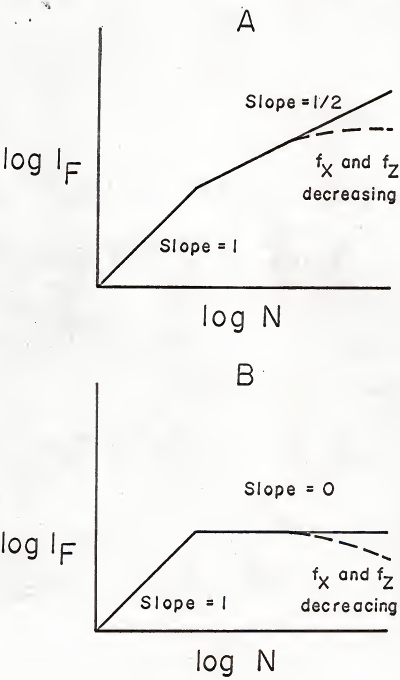
A
Slope = 1/2
log I_F
f_X and f_Z
decreasing
Slope = 1
log N
B
Slope = 0
log I_F
f_X and f_Z
decreacing
Slope = 1
log N

CHAPTER III

DERIVATION OF EXPRESSIONS FOR CALCULATION OF THE LIMIT OF DETECTABILITY IN ATOMIC FLUORESCENCE FLAME SPECTROMETRY

The theoretical treatment of the limiting detectable atomic concentration in atomic emission and atomic absorption flame spectrometry has been given by Winefordner and Vickers (29,30). Their work was made more complete by the additional treatment of the influence of the amplifier-readout noise on the limiting detectable atomic concentration by Winefordner and Veillon (27). The expressions derived by these workers permit the experimenter to calculate the limiting detectable atomic concentration in flame gases of a specified flame-type and experimental system, to optimize certain experimental parameters, for example, the monochromator slit width, with respect to the limiting detectable atomic concentration, and to compare different experimental designs.

Atomic fluorescence flame spectrometry, initially proposed as an analytical method by Winefordner and Vickers (28), has been shown to be a very sensitive method of measurement of several elements (13,25) as well as a very versatile method (21) of analysis. Therefore, a quantitative treatment of the factors influencing the limiting detectable atomic concentration was carried out in order to calculate the limiting detectable atomic concentration for atomic fluorescence flame spectrometry. The treatment is similar to that used by Winefordner and co-workers (27,29, 30). Methods for calculating the optimum monochromator slit width as well as the limiting detectable atomic concentration as a function of type of source of excitation and amplifier-readout system will be given in this chapter. Sample calculations are given for six elements (Zn, Cd, Hg, Cu, Tl, and Na) in three different flames using both narrow line and continuous sources of excitation and A.C. and D.C. amplifier-readout systems.

Theory

The limiting detectable atomic concentration is defined (29,30) as that atomic concentration which results in a signal-to-noise ratio of 2, that is,

$$\left.\frac{i_F}{\overline{\Delta i_T}}\right)_{\text{min.}} = 2 \quad , \qquad (3.1)$$

where i_F is the photoanodic detector signal in amperes due to atomic fluorescence, and $\overline{\Delta i_T}$ is the root-mean-square noise in amperes at the photoanode caused by all noise signals.

For the equations developed below for the fluorescence signal and noise terms, it is necessary only to make the following assumptions: that a flame sample cell (or other cell capable of producing species in the atomic state) is positioned in front of the entrance slit of a monochromator such that the complete cell width is observed (any entrance optical system can be treated by the same approach used by Winefordner and Vickers (29) in the atomic emission paper); that the complete flame cell width is excited by either a narrow line or a continuous source (any optical system between the source of excitation and flame cell can be treated); and that the atomic fluorescence signal results from a single, optically isolated transition. The general case in which there is more than one line that can be excited to produce a fluorescence signal is a simple extension of the expressions given here (see Chapter II and reference (12)).

All terms are defined in Appendix I for convenient reference.

Part I

The fluorescence signal.-The equation for the photoanodic signal in amperes due to atomic fluorescence has the same form as that derived for atomic emission (29) and is given by

$$i_F = \gamma n K T_f W H \Omega_e = n K k_2 W I_F \text{, amperes,} \quad (3.2)$$

where the terms in equation 3.2 are defined as follows:

γ is the photoanodic sensitivity factor, that is, the ratio of the amperes produced at the photoanode to the watts of radiant power reaching the photocathode.

n is the entrance optics factor which accounts for the number of solid angles of atomic fluorescence of value Ω_e which are gathered into the monochromator by means of suitable entrance optics, that is, the effective number of flame images in the solid angle Ω_e viewed by the monochromator.

Ω_e is the solid angle (ster.) viewed by the monochromator.

κ is a factor which accounts for the position of the spectral line peak with respect to the slit function distribution ($\kappa = 1$) when the slit function distribution coincides with the peak of the spectral line)).

T_f is the transmission factor of the spectrometric system.

W is the effective slit width of the monochromator in cm.

H is the effective slit height of the monochromator in cm. (if the slit is fully illuminated, then W and H are equal to slit width and height of the monochromator).

$k_2 = \gamma T_f H \Omega_e$.

I_F is the integrated intensity in watts/cm.^{2} ster. of the atomic fluorescence signal.

Because n and $\mathcal{K}$ can easily be made equal to unity experimentally, they will be assumed to be unity in this chapter. Expressions for I_F at low atomic concentrations considering both narrow line and continuous sources of excitation are evaluated in Chapter II, assuming a D.C. amplifier-readout system; however, if an A.C. amplifier system is used, I_F is merely divided by 2 to account for the fact that half of the exciting light does not reach the monochromator (and therefore the photodetector) due to the mechanical chopper (this assumes that the A.C. signal is produced by the mechanical chopper (half open-half closed)) placed between the source of excitation and the flame (21). Expressions for I_F derived assuming a single resonance transition are given below:

Narrow Line Source with D.C. Readout

$$I_F = \frac{2\sqrt{\ln 2}\; I_L\, \Omega_a\, \Phi_T\, \lambda^2_o\, g_u\, A_t\, NL}{32\pi^{5/2}\, g_1\, \Delta\nu_D} = K_L I_L \Phi_T\, NL\ . \tag{3.3}$$

Narrow Line Source with A.C. Readout

$$I_F = \left(\frac{K_L}{2}\right) I_L\, \Phi_T\, NL\ . \tag{3.4}$$

Continuous Source with D.C. Readout

$$I_F = \frac{\Omega_a\, \lambda^2_o\, g_u\, A_t\, I^{\circ}\, \Phi_T\, NL}{32\pi^2\, g_1} = K_c\, \Phi_T\, I^{\circ}\, NL\ . \tag{3.5}$$

Continuous Source with A.C. Readout

$$I_F = \left(\frac{K_c}{2}\right) I^{\circ} \Phi_T\, NL\ . \tag{3.6}$$

The symbols used in the above intensity expressions are defined as follows:

I_L is the intensity of a narrow line exciting source, in watts/cm.^{2}ster.

I° is the intensity of a continuous exciting source, in watts/cm.^{2}ster.mμ .

Ω_a is the solid angle impinging on the flame cell from the source of excitation, in ster.

Φ_T is the power efficiency for atomic fluorescence, that is, the ratio of watts emitted by atomic fluorescence to watts absorbed by the particles in the flame cell, no units.

λ_o is the wavelength of the center of the line of concern, in cm.

g is the statistical weight of the energy level indicated (u for upper and l for ground energy level), no units.

N is the atomic concentration of the absorbing (and fluorescing) atoms of concern, in atoms/cm.^{3}.

L is the path length of the flame cell which is viewed by the monochromator, in cm.

A_t is the transition probability for the transition (resonance) of concern, in sec.$^{-1}$.

$\Delta\nu_D$ is the Doppler line half-width ($\Delta\nu_D = 7.16 \times 10^{-7} \sqrt{T/M_x}$), in sec.$^{-1}$, where M_x is the atomic weight of the absorbing atom.

$$K_L = \frac{2\sqrt{\ln 2}\ \Omega_a\ \lambda^2_o\ g_u\ A_t}{32\pi^{5/2}\ g_l\ \Delta\nu_D} \ .$$

$$K_c = \frac{\Omega_a\ \lambda^2_o\ g_u\ A_t}{32\pi^2\ g_l} \ .$$

For a complete treatment of I_F and Φ_T, for resonance, stepwise-line, and direct-line fluorescence and for a combination of these refer to Chapter II and the article by McCarthy, Parsons, and Winefordner (12), respectively.

Part II

The total noise expression, $\overline{\Delta i_T}$.-The total root-mean-square photoanodic noise signal, $\overline{\Delta i_T}$ in amperes, is determined by a combination of each type of noise which contributes to the total noise in the fluorescence signal. If the individual noise signals are dependent on the same factors, the noise terms add linearly, and if the component noise signals are independent of each other, they add quadratically. In this treatment, it is necessary to assume all noises are white, that is, equally distributed over all frequencies (7). The general expression for $\overline{\Delta i_T}$ is given below:

$$\overline{\Delta i_T} = \left[\overline{\Delta i_p}^2 + (\overline{\Delta i_c} + \overline{\Delta i})^2 + (\overline{\Delta i_F} + \overline{\Delta i_S} + \overline{\Delta i_R})^2 + \overline{\Delta i_e}^2\right]^{1/2} \ , \tag{3.7}$$

where the symbols are defined as follows:

$\overline{\Delta i_p}$ is the root-mean-square photoanodic noise current, in amperes, due to the shot effect and the Johnson effect on the phototube.

$\overline{\Delta i}_c$ is the root-mean-square photoanodic noise current, in amperes, due to the flicker of the flame background signal.

$\overline{\Delta i}$ is the root-mean-square photoanodic noise current, in amperes, due to the flicker of the thermal emission signal due to the atoms in concern.

$\overline{\Delta i}_F$ is the root-mean-square photoanodic noise current, in amperes, due to the flicker of the atomic fluorescence signal.

$\overline{\Delta i}_S$ is the root-mean-square photoanodic noise current, in amperes, due to the flicker in the signal caused by Rayleigh scattering of incident radiation from salt particles in the flame.

$\overline{\Delta i}_R$ is the root-mean-square photoanodic noise current, in amperes, due to the flicker in the signal caused by both direct reflection and Rayleigh scattering of incident radiation from water droplets in the flame.

$\overline{\Delta i}_e$ is the root-mean-square photoanodic noise current, in amperes, due to the amplifier-readout system employed but referred to the input of the amplifier.

Several of the noise terms can be neglected in the practical case, and the expressions for these terms will be treated in Appendix III for completeness. Because the Johnson noise in the load resistor of the phototube is generally much smaller than the shot effect noise (18), this term will be omitted. Further, at the limit of detection there should, at best, be only a very small signal due to both atomic emission and atomic fluorescence, and neither of these small signals should produce an appreciable noise signal and so will also be neglected. Similarly, at the limit of detection, there is only a very small concentration of the species under consideration being introduced into the flame, and thus there should be only a small noise associated with Rayleigh scattering from salt particles (this may not be quite valid if the solutions are made in a fairly concentrated matrix; however, most samples can be sufficiently diluted, when using the very sensitive method of atomic fluorescence flame spectrometry, that the effect can still generally be made negligible). Therefore, in the practical case equation 3.7 reduces to

$$\overline{\Delta i_T} = (\overline{\Delta i_p}^2 + \overline{\Delta i_c}^2 + \overline{\Delta i_R}^2 + \overline{\Delta i_e}^2)^{1/2} \quad . \qquad (3.8)$$

Part III

The phototube shot noise expression.-The equation for the root-mean-square shot noise, Δi_p, of a phototube has long been known (18) and is given by

$$\Delta i_p = (2e_c \; B \; M \; \Delta f \; i_T)^{1/2} = (\Delta f \; k_1 \; i_T)^{1/2} \; , \qquad (3.9)$$

where the symbols are defined as follows:

e_c is the charge of an electron (1.6×10^{-19} coulombs).

B is the multiplier phototube factor which is related to the gain, G, per dynode by $B = 1 + G^{-1} + G^{-2} + \ldots + G^{-(z-1)}$ (z is the number of dynodes).

M is the total amplification factor (no units) of the photodetector, G^z.

$k_1 = 2e_c B M$.

Δf is the frequency response bandwidth of the amplifier-readout system.

i_T is the total current in amperes at the anode of the phototube.

The above expression is useful for treating both single-stage and multi-stage phototubes. For most any actual experimental case in atomic fluorescence flame spectrometry, i_T can be given by the expression

$$i_T = i_d + i_c + i_R \quad , \tag{3.10}$$

where the symbols are defined as follows:

i_d is the dark current in amperes at the photoanode.

i_c is the photoanodic current in amperes produced by the flame background.

i_R is the photoanodic current in amperes produced by direct reflection and Rayleigh scattering of the incident radiation by water droplets in the flame.

The phototube dark current, i_d, can be measured directly by means of an electrometer with a current readout (see Appendix V). The other currents are given (29) by

$$i_c = \gamma T_f W H \Omega_e I_c s = \gamma T_f W^2 H \Omega_e I_c R_d$$

$$= k_2 W^2 I_c R_d \qquad (3.11)$$

$$i_R)_{cont.} = \gamma T_f W H \Omega_e I_R)_{cont.} = \gamma T_f W^2 H \Omega_e R_d I_R)_{cont.}$$

$$= k_2 W^2 R_d I_R)_{cont.} \qquad (3.12)$$

$$i_R)_{line} = \gamma T_f W H \Omega_e I_R)_{line} = k_2 W I_R)_{line} \qquad (3.13)$$

where terms $I_R)_{line}$ and $I_R)_{cont.}$ are defined in the Reflection section and where s is the spectral band width of the monochromator in mμ, and is given by $s = R_d W + s_c$ (R_d is the reciprocal linear dispersion of the monochromator in mμ/cm., and s_c is the minimum resolving power spectral band width in mμ), and all other terms have been previously defined (also see Appendix I). If the optimum slit width is not too small, that is, ten-fold or more greater than the minimum resolving power slit width, which is usually the case in atomic fluorescence flame spectrometry, then s can be given by $R_d W$.

It should be mentioned that the above equations are given for a D.C. amplifier-readout system; however, the only difference for an A.C. system will be that i_R will be divided by 2 if a mechanical chopper (open half the time) is used. It should also be noted that i_c and $i_R)_{cont.}$ depend on W^2; whereas, $i_R)_{line}$ depends on W.

Part IV

The flame background noise expression.-The equation for the root-mean-square photoanodic noise, $\overline{\Delta i}_c$, due to the flame background signal has been derived by Winefordner and Vickers (29), and is given by

$$\overline{\Delta i}_c = \gamma T_f W^2 H \Omega_e \xi I_c R_d \Delta f = k_2 W^2 R_d \xi I_c \Delta f \quad , \tag{3.14}$$

where ξ is the flame flicker factor, that is, the ratio of the root-mean-square noise fluctuation in the flame background intensity to the intensity of the flame background signal in sec.$^{1/2}$ and all other terms have been defined (see Appendix I). This noise term is the same whether A.C. or D.C. amplifier-readout is used because the signal from the flame background is not chopped when an A.C. system is used. Furthermore, the flame background noise is given by the same equation for atomic emission and atomic absorption as well as for atomic fluorescence flame spectrometry. This noise depends on W^2.

Part V

The reflection and Rayleigh scattering (from water droplets) noise expression.-The expression for $\overline{\Delta i}_R$ has the same form as the flame background noise, $\overline{\Delta i}_c$, when a continuous source of excitation is used, but when a narrow line source of excitation is used, the spectral band width, s, does not enter into the expression, because the line half-width for a narrow line source is much smaller than the usual spectral band width of the monochromator. However, with a continuous source, the spectral band of any monochromator is much narrower than any continuous source. Therefore, separate expressions are given for line and for continuous sources of excitation.

Continuous Source

$$\begin{aligned} \overline{\Delta i_R})_{\text{cont.}} &= \gamma\, T_f\, W\, H\, \Omega_e\, \Gamma_R\, I_R)_{\text{cont.}} \sqrt{\Delta f}\; s \\ &= k_2\, W^2 R_d\, \Gamma_R\, I_R)_{\text{cont.}} \sqrt{\Delta f} \quad . \end{aligned} \tag{3.15}$$

Line Source

$$\begin{aligned} \overline{\Delta i_R})_{\text{line}} &= \gamma\, T_f\, W\, H\, \Omega_e\, \Gamma_R\, I_R)_{\text{line}} \sqrt{\Delta f} \\ &= k_2\, W\, \Gamma_R\, I_R)_{\text{line}} \sqrt{\Delta f} \quad . \end{aligned} \tag{3.16}$$

The parameter Γ_R is the reflection flicker factor, that is, the ratio of the root-mean-square fluctuation in reflection plus Rayleigh scattering signal to the intensity of the reflection plus Rayleigh scattering signal from water droplets in sec.$^{1/2}$, and the parameter I_R is the intensity of radiation reflected and scattered by water droplets and is given by

$$I_R)_{\text{cont.}} = \frac{\rho_R\, I^{\circ}\, \Omega_a}{4\pi} = k_3\, I^{\circ} \ , \tag{3.17}$$

and

$$I_R)_{line} = \frac{\rho_R\ I_L\ \Omega_a}{4\pi} = k_3\ I_L \quad , \tag{3.18}$$

where ρ_R represents the fraction of incident radiation which reaches the monochromator due to reflection and Rayleigh scattering from water droplets (no units), Ω_a is the solid angle over which the flame gases are excited, $k_3 = \rho_R\ \Omega_a/4\pi$, and 4π is the number of solid angles in a sphere. All other terms have already been defined (see Appendix I). Thus, equations 3.15 and 3.16 have the final form,

$$\overline{\Delta i}_R)_{cont.} = \sqrt{\Delta f}\ k_2\ k_3\ W^2\ I^\circ\ R_d\ \Gamma_R \quad , \tag{3.19}$$

and

$$\overline{\Delta i}_R)_{line} = \sqrt{\Delta f}\ k_2\ k_3\ W\ I_L\ \Gamma_R \quad . \tag{3.20}$$

If an A.C. amplifier-readout system is used, both I° and I_L will be divided by 2. Note that $\overline{\Delta i}_R)_{cont.}$ depends on W^2 and $\overline{\Delta i}_R)_{line}$ depends on W.

Part VI

The amplifier-readout noise expression.-The amplifier-readout root-mean-square noise, $\overline{\Delta i}_e$, depends on the total signal measured by the system, on the frequency response bandwidth of the amplifier-readout system in sec.$^{-1}$, and on the readout noise factor, ξ , in sec.$^{+1/2}$, which is the ratio of the amplifier (electrometer) noise (which results in noise at the readout but is referred to the amplifier input) to the total input signal which is effective in producing a signal at the output. There is also a small, constant noise signal associated with any amplifier-readout which is present even when the input is shorted out. Since this term is very small when compared to the other noises when a signal is being measured, it will not be necessary to consider it here. The general amplifier-readout noise expression has been derived by Winefordner and Veillon (27),

$$\overline{\Delta i}_e = \xi\, i_T \sqrt{\Delta f} \quad , \qquad (3.21)$$

where all terms have been defined above (also see Appendix I).

Part VII

The signal-to-noise expressions. The signal-to-noise ratio, $i_F / \overline{\Delta i}_T$, can be calculated for any experimental system using the appropriate values of parameters and using the appropriate combination of the signal and noise terms given above. It should be emphasized that different final expressions will result depending on the type of excitation source -- narrow line or continuous -- and the type of amplifier-readout -- A.C. or D.C. Therefore, four expressions are given for the signal-to-noise ratio (see Table 3.1) which result when measuring resonance radiation of atoms near the limiting detectable atomic concentration in atomic fluorescence flame spectrometry.

TABLE 3.1

DERIVED SIGNAL-TO-NOISE EXPRESSIONS FOR ATOMIC FLUORESCENCE FLAME SPECTROMETRY

Expression When Using a Continuous Source of Excitation with a D.C. Amplifier-Readout

$$\frac{i_F}{\overline{\Delta i_T}} = k_2\ K_c\ W\ I^{\circ}\ \Phi_T\ N\ L \Big/ [\Delta f k_1 (i_d + k_2 W^2 R_d [I_c + k_3 I^{\circ}]) + \Delta f (k_2 W \xi I_c R_d)^2$$

$$+\ \Delta f (k_2 k_3 W^2 R_d I^{\circ}\ \Gamma_R)^2 + \Delta f\ \zeta^2 (i_d + k_2 W^2 R_d [I_c + k_3 I^{\circ}]^2]^{1/2} \qquad (3.22)$$

Expression When Using a Continuous Source of Excitation with an A.C. Amplifier-Readout

$$\frac{i_F}{\overline{\Delta i_T}} = (k_2\ K_c/2)\ W\ I^{\circ}\ \Phi_T\ N\ L \Big/ [\Delta f k_k (i_d + k_2 W^2 R_d [I_c + k_3 I^{\circ}/2]) + \Delta f (k_2 W^2 \xi\ I_c R_d)^2$$

$$+\ \Delta f (k_2 k_3 W^2 R_d I^{\circ}\ \Gamma_R/2)^2 + \Delta f\ \zeta^2 (i_d + k_2 W^2 R_d [I_c + k_3 I^{\circ}/2])^2]^{1/2} \qquad (3.23)$$

Table 3.1 (Cont'd)

Expression When Using a Narrow Line Source of Excitation with a D.C. Amplifier-Readout

$$\frac{i_F}{\overline{\Delta i_T}} = k_2 K_L W I_L \Phi_T N L \Big/ [\Delta f k_1 (i_d + k_2 W [I_c W R_d + k_3 I_L]) + \Delta f (k_2 W^2 \xi I_c R_d)^2$$

$$+ \Delta f (k_2 k_3 W I_L \Gamma_R)^2 + \Delta f \xi^2 (i_d + k_2 W [I_c W R_d + k_3 I_L])^2]^{1/2} \quad (3.24)$$

Expression When Using a Narrow Line Source of Excitation with an A.C. Amplifier-Readout

$$\frac{i_F}{\overline{\Delta i_T}} = (k_2 K_L/2) W I_L \Phi_T N L \Big/ [\Delta f k_1 (i_d + k_2 W [I_c W R_d + k_3 I_L/2]) + \Delta f (k_2 W^2 \xi I_c R_d)^2$$

$$+ \Delta f (k_2 k_3 W I_L \Gamma_R/2)^2 + \Delta f \xi^2 (i_d + k_2 W [I_c W R_d + k_3 I_L/2])^2]^{1/2} \quad (3.25)$$

Part VIII

Calculation of the limiting detectable atomic concentration and the optimum slit width.-Once the appropriate signal-to-noise expression has been determined, the limiting detectable atomic concentration, $N_{min.}$, in atoms/cm.^{3} can be calculated by substituting into equation 3.1 and solving for $N_{min.}$. The equations for $N_{min.}$ are given in Table 3.2 for the four cases presented in Table 3.1.

For any given instrumental system and flame-type and conditions, the monochromator slit width is the only parameter which can be conveniently optimized because all other parameters are generally fixed by the experimental design (the voltage on the phototube can be varied; however, it has been shown (11) to have little effect on the signal-to-noise ratio). An expression for the optimum slit width can be found by differentiating $N_{min.}$ with respect to W and setting the resulting expression equal to zero and solving for W. Unfortunately, the equation for the optimum slit width results in an imperfect quartic. The quartic expressions are not given in this manuscript because in practice it is generally simpler to calculate the value of $N_{min.}$ as a function of slit width and obtain the optimum slit width by graphical means. This procedure is easily applicable to computer technique (see Appendix VIII).

TABLE 3.2

DERIVED EXPRESSIONS FOR $N_{min.}$ FOR ATOMIC FLUORESCENCE SPECTROMETRY

Expression When Using a Continuous Source of Excitation with a D.C. Amplifier-Readout

$$N_{min.} = 2[\Delta f k_1(i_d+k_2W^2R_d[I_c+k_3I^\circ]) + \Delta f(k_2W\xi I_cR_d)^2 + \Delta f(k_2k_3W^2R_d\Gamma_RI^\circ)^2 + \Delta f\xi^2(i_d+k_2W^2R_d[I_c+k_3I^\circ])^2]^{1/2} \Big/ k_2K_cW\, I^\circ \Phi_T\, L \qquad (3.26)$$

Expression When Using a Continuous Source of Excitation with an A.C. Amplifier-Readout

$$N_{min.} = 4[\Delta f k_1(i_d+k_2W^2R_d[I_c+k_3I^\circ/2]) + \Delta f(k_2W^2\xi I_cR_d)^2 + \Delta f(k_2k_3W^2R_d\Gamma_RI^\circ/2)^2 + \Delta f\xi^2(i_d+k_2W^2R_d[I_c+k_3I^\circ/2])^2]^{1/2} \Big/ k_2K_cW\, I^\circ \Phi_T\, L \qquad (3.27)$$

Table 3.2 (Cont'd)

Expression When Using a Line Source of Excitation with a D.C. Amplifier-Readout

$$N_{min.} = 2[\Delta f k_1(i_d+k_2W[I_cWR_d+I_Lk_3])+\Delta f(k_2W^2 \xi I_cR_d)^2+\Delta f(k_2k_3WI_L \Gamma_R)^2$$

$$+ \Delta f \xi^2(i_d+k_2W[I_cWR_d+k_3I_L)^2]^{1/2} \Big/ k_2K_LW I_L \Phi_T L \qquad (3.28)$$

Expression When Using a Line Source of Excitation with an A.C. Amplifier-Readout

$$N_{min.} = 4[\Delta f k_k(i_d+k_2W[I_cR_dW+I_Lk_3/2])+\Delta f(k_2W^2 \xi I_cR_d)^2+\Delta f(k_2k_3W \Gamma_R I_L/2)^2$$

$$+ \Delta f \xi^2(i_d+k_2W[I_cWR_d+k_3I_L/2])^2]^{1/2} \Big/ k_2K_LW I_L \Phi_T L \qquad (3.29)$$

Use of Derived Expressions and Sample Concentrations

The parameters in the above equations fall into three categories -- spectral (A_t, g_u, etc.), apparatus (R_d I°, H, B, M, etc.), and experimental (I_c, ξ, Γ_R, etc.). The spectral and apparatus parameters are generally fixed or are directly measurable. In Appendix V, the values of these parameters are listed for the systems assumed for the sample calculations. Many of the parameters in the $N_{min.}$ expressions were measured on the actual experimental systems assumed for the sample calculations. Adequate values could have been assumed for these parameters, but it was felt that a more complete treatment would involve knowing the value of these parameters for the assumed experimental system.

Sample calculations were made for six elements, namely, Zn, Cd, Hg, Cu, Tl, and Na, considering both line and continuous sources with A.C. and D.C. amplifier-readout systems. A low resolution grating monochromator was used and either a 150 watt continuous xenon arc or electrodeless discharge tubes (narrow line sources). A 1P28 R.C.A. multiplier phototube was used as the photodetector and either a lock-in A.C. amplifier or a D.C. electrometer was used for the amplifier-readout system. Total-consumption aspirator-burners were used for all studies. (See Appendix V for a complete description of the apparatus.) Table 3.3

TABLE 3.3

CALCULATED VALUES OF $N_{MIN.}$ AND $W_{OPT.}$ FOR Zn, Cd, Hg, Cu, Tl, AND Na

Element Symbol	Wave-length (A)	Flame[a]	CONTINUOUS SOURCE[b]				LINE SOURCE[b]			
			A.C.		D.C.		A.C.		D.C.	
			$W_{opt.}$	$N_{min.}$	$W_{opt.}$	$N_{min.}$	$W_{opt.}$	$N_{min.}$	$W_{opt.}$	$N_{min.}$
Zn	2139	1	0.04	1.2×10^{13}	0.04	5.9×10^{12}	0.04	3.6×10^{9}	0.04	1.8×10^{9}
		2	0.45	2.4×10^{11}	0.40	9.2×10^{10}	0.45	4.5×10^{7}	0.45	2.8×10^{7}
		3	0.55	1.1×10^{11}	0.40	7.8×10^{10}	2.00	2.7×10^{7}	2.50	2.6×10^{7}
Cd	2288	1	0.02	1.0×10^{12}	0.02	5.4×10^{11}	0.02	5.6×10^{7}	0.03	5.5×10^{7}
		2	0.15	1.6×10^{10}	0.10	9.8×10^{9}	0.40	9.5×10^{6}	0.75	9.5×10^{6}
		3	0.15	8.8×10^{9}	0.10	6.2×10^{9}	2.5[c]	6.7×10^{6}	2.5[c]	6.7×10^{6}
Hg	2537	1	0.01[d]	4.7×10^{12}	0.01[d]	2.3×10^{12}	0.01[d]	2.1×10^{9}	0.01[d]	1.1×10^{9}
		2	0.09	7.1×10^{10}	0.07	4.4×10^{10}	0.10	6.2×10^{7}	0.12	5.9×10^{7}
		3	0.09	5.9×10^{10}	0.06	4.1×10^{10}	0.65	6.0×10^{7}	0.90	6.0×10^{7}
Cu	3248	1	0.01[d]	3.2×10^{12}	0.01[d]	1.6×10^{12}	0.01[d]	6.9×10^{9}	0.01[d]	3.4×10^{9}
		2	0.04	2.3×10^{10}	0.04	1.3×10^{10}	0.04	6.3×10^{7}	0.04	5.3×10^{7}
		3	0.07	2.2×10^{10}	0.05	1.5×10^{10}	0.15	6.8×10^{7}	0.15	6.6×10^{7}

TABLE 3.3 (Continued)

Element Symbol	Wave-length (A)	Flame[a]	CONTINUOUS SOURCE[b]				LINE SOURCE[b]			
			A.C.		D.C.		A.C.		D.C.	
			$W_{opt.}$	$N_{min.}$	$W_{opt.}$	$N_{min.}$	$W_{opt.}$	$N_{min.}$	$W_{opt.}$	$N_{min.}$
Tl	3776	1	0.01[d]	5.6×10^{12}	0.01[d]	2.8×10^{12}	0.01[d]	3.3×10^{10}	0.01[d]	1.6×10^{10}
		2	0.06	8.2×10^{10}	0.04	5.5×10^{10}	0.10	2.1×10^{8}	0.15	2.1×10^{8}
		3	0.06	8.4×10^{10}	0.04	5.9×10^{10}	0.35	2.7×10^{8}	0.45	2.6×10^{8}
Na	5890	1	0.04	1.9×10^{11}	0.04	9.7×10^{10}	0.04	8.8×10^{8}	0.04	4.4×10^{8}
		2	0.15	4.8×10^{9}	0.15	2.5×10^{9}	0.15	1.7×10^{7}	0.15	9.3×10^{6}
		3	0.25	1.3×10^{9}	0.20	8.7×10^{8}	0.35	3.9×10^{6}	0.35	2.9×10^{6}

[a] Flame 1. Oxyhydrogen (O_2 - 3 l./min.; H_2 - 7 l./min.) viewed at 3 cm. above the burner tip.
Flame 2. Flame 1 viewed at 6 cm. above the burner tip.
Flame 3. Air-Hydrogen (air - 3 l./min.; H_2 - 8 l./min.) viewed at 6 cm. above the burner tip.

[b] The $W_{opt.}$ values are in mm., and $N_{min.}$ values are in atoms/cm.^{3} of flame gases.

[c] There was less than a 10% change in $N_{min.}$ for a 0.01 - 5.00 mm. change in slit width.

[d] This is the approximate value of the minimum resolving power slit width of the monochromator being used for these calculations.

gives the results of the calculations using the graphical procedure described above. A FORTRAN IV program was developed to perform these calculations and is described in Appendix VIII.

Discussion

Much useful information can be obtained from the results of these calculations. To point out the important features of the use of the equations in Tables 3.1 and 3.2, and the calculations made using these equations (see Table 3.3), the discussion will be divided into three parts.

Part I

Comparison of sources and amplifier-readout systems.- It is evident that intense narrow line sources give much better results than continuous sources of excitation when the intensities have comparable absolute magnitudes (see Chapter II), the intensity of a narrow line source has units of watts/cm.^{2} ster. mμ. This result can be easily understood from the fact that the total power from a narrow line source (source such as an electrodeless discharge tube where the source line half-width is generally narrower than the absorption line half-width of atoms in flame) can be absorbed while only a small fraction of the power over a narrow wavelength interval (the absorption line half-width) from a continuous source is absorbed. The amount of radiation absorbed from a continuous source is determined by the line half-width of the absorption line of the atomic species of concern. If $I_L = I^{\circ}$, that is, the absolute magnitude of the intensity of a line source is approximately the same as the absolute magnitude of a continuous source, then from equations 3.3 and 3.5 it can be shown that the line source will give approximately $1/\Delta\lambda_D$, ($\Delta\lambda_D$ is the Doppler half-width of the absorption line in mμ) greater fluorescence intensity (see Chapter II), and therefore a line source will generally give a lower value of $N_{min.}$ Increasing the intensity of a source of excitation will lower $N_{min.}$ unless the major source of noise is due to reflection and Rayleigh scattering from water droplets. Unfortunately, when calculations are made for the oxyhydrogen flame at a height of 6 cm. above the burner tip, that is, where the best results for this flame are normally obtained experimentally, the reflection noise term contributes significantly to the total noise term; however, the reflection noise from a chamber-type aspirator-burner (or a total-consumption aspirator-burner with the addition of organic solvents) has been shown (21) to reduce this noise by as much as 95 per cent. Thus, the use of more intense continuous sources may possibly be a useful means of obtaining low limits of detection for many elements with a single source of excitation.

It can be seen from Table 3.3 that the $N_{min.}$ obtained when using an A.C. amplifier-readout system is from two-fold smaller to about equal to the $N_{min.}$ obtained for a D.C. amplifier-readout system. It must be remembered, however, that these data were calculated under the assumption of a $\Delta f = 1.0$ sec.$^{-1}$ for both the A.C. and D.C. systems. The Δf of an amplifier-readout system is often determined by the time constant of the readout system; this time constant is usually fixed by a resistance-capacitance (RC) network on the input of the readout, and is just the resistance, R_o, in ohms times the capacitance, C_o, in farads. The value of Δf is then given by $\Delta f = 1/R_oC_o$. The normal time constant for most readout systems is on the order of 1 - 0.001 sec. A.C. amplifiers often have tuned circuits and built-in RC networks on their outputs; whereas, many D.C. amplifiers do not. Thus, it is not always true that any A.C. amplifier system is superior to any D.C. amplifier system. The addition of a simple RC circuit to the output of a D.C. system will often result in a response similar to that in an A.C. system for equivalent Δf's (assuming thermal emission of the atoms in concern is not appreciable). It should be stressed that A.C. amplifier-readout systems do not respond to all of the photodetector signals, that is, an A.C. amplifier-readout system responds only to the photodetector signal which is modulated at the frequency of the chopper (actually the A.C. amplifier lets through all frequencies which are between the frequency of modulation $\pm \Delta f/2$). The A.C. amplifier-readout system does not respond to constant signals, that is, D.C. signals. In some cases an A.C. amplifier-readout system results in the same noise signal as a D.C. amplifier-readout system having the same value of Δf, for example, the flame background noise.

Part II

The optimum slit width and flame.-The optimum slit width, $W_{opt.}$, is most readily determined, theoretically, by graphical means, that is, determining the minimum of a $N_{min.}$ is W curve. Several representative $N_{min.}$ versus W curves are illustrated in Figures 3.1, 3.2, and 3.3. These curves are also used to indicate the influence of source type, source intensity, and flame background intensity.

In Figure 3.1, three elements are compared in a slightly fuel rich oxyhydrogen flame viewed at 6 cm. above the tip of the burner when excited with a 150 watt xenon arc (continuous source), and under these conditions the slit width is a relatively important parameter. The optimum slit width, $W_{opt.}$, is obtained when the flame background noise, the reflection noise, or a combination of both just balances the phototube shot noise. The background and reflection noises depend on W^2 and the fluorescence signal depends on W; this accounts for the linear positive slope

Fig. 3.1.-Typical $N_{min.}$ versus monochromator slit width curves for Cd, Cu, and Na when excited by a continuous source.

Key to Figure: (Data from Flame 4 of Table 3.3)

A. Cd -- A.C.; B. Cd -- D.C.;

C. Cu -- A.C.; D. Cu -- D.C.;

E. Na -- A.C.; and F. Na -- D.C.

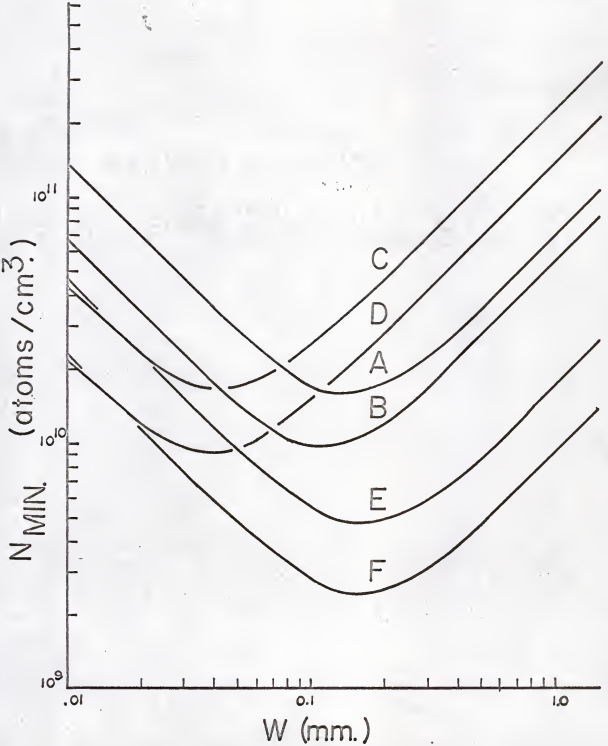
$N_{MIN.}$ (atoms/cm^3.)
10^{11}
10^{10}
10^{9}
.01
0.1
1.0
W (mm.)
C
D
A
B
E
F

Fig. 3.2.-Typical $N_{min.}$ versus monochromator slit width curves for Cd, Cu, and Na when excited by a narrow line source.

Key to Figure: See Figure 3.1.

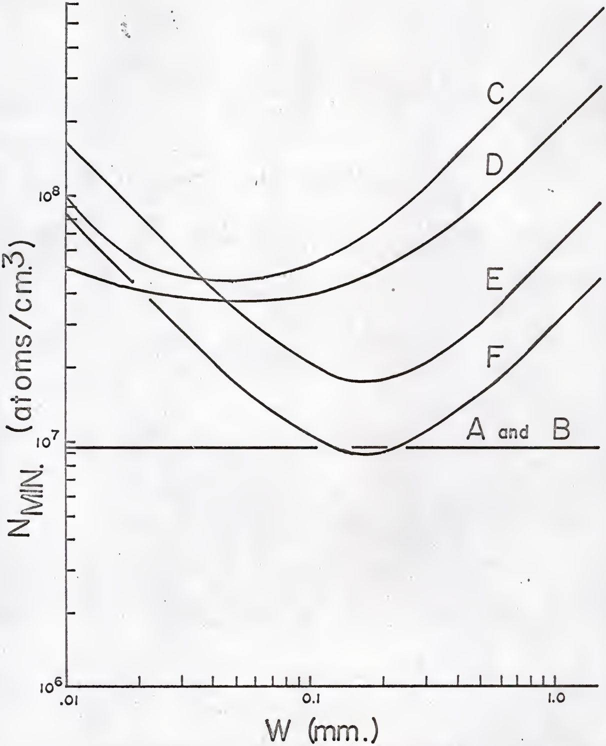
C
D
E
F
A and B
$N_{MIN.}$ (atoms/cm.^{3})
10^8
10^7
10^6
.01
0.1
1.0
W (mm.)

Fig. 3.3.-Typical variation of $N_{min.}$ versus monochromator slit width curves with variation in flame background intensity.

Key to Figure: (Data from Na -- D.C.)

A. Flame 2, Table 3.3; B. Flame 4, Table 3.3; and C. Flame 6, Table 3.3.

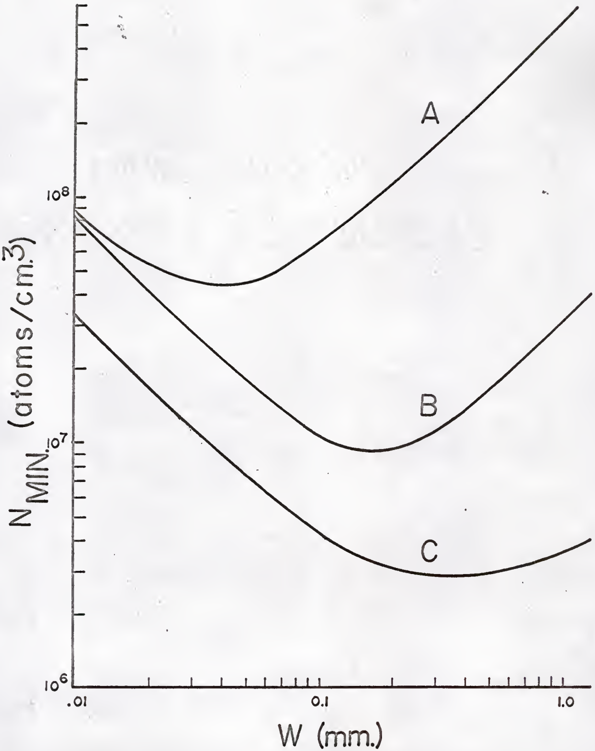
$N_{MIN.}$ (atoms/cm.^{3})
10^8
10^7
10^6
.01
0.1
1.0
W (mm.)
A
B
C

for W's greater than $W_{opt.}$. The shot noise depends upon the total current passing through the phototube, i_T, which contains a constant current, i_d. At small slit widths, that is, W's $\lesssim$ 0.05 mm., the shot noise -- which is determined primarily by i_d -- is the most important noise term and so this results in the $N_{min.}$ versus W curves having a negative slope at small W's.

When the A.C. amplifier-readout is compared to a similar D.C. system, only a very small shift to higher $W_{opt.}$'s is observed besides somewhat higher limiting detectable atomic concentrations (see Figure 3.1).

In Figure 3.2, curves of $N_{min.}$ versus W are given for three elements using the same flame and experimental conditions used in Figure 3.1 (except that narrow line sources of excitation are used). It is readily seen that there is a lesser dependence of $N_{min.}$ on slit width when narrow line sources are used, because the reflection noise term is dependent, in this case, on W rather than W^2. An essentially straight line for Cd results because the intensity of the electrodeless discharge tube is about two orders of magnitude greater than the other sources (see Appendix V), and the reflection noise signal completely dominates the total noise term. This means that when an intense, narrow line source, for example, 10^{-1} watt/cm.^{2} ster. is used, there will probably be little need to optimize the slit width. It further means that the limiting detectable atomic concentration could not be reduced by increasing the source intensity but could be further reduced only by reducing the reflection noise. This can be accomplished (21) either by the use of chamber-type aspirator-burners (the use of which would also lower the flame background somewhat due to their laminar nature) or by using organic solvents with total-consumption aspirator-burners. For example, the limiting detectable atomic concentration for Cd could be lowered by about two orders of magnitude, to about 10^5 atoms/cm.^{3}, if the reflection noise were essentially eliminated without increasing the flame background.

In Figure 3.3, $N_{min.}$ versus W curves are given for Na in three flames (see Table 3.3) using a D.C. amplifier-readout and excited with a line source. These curves illustrate that if the flame background is decreased, the limiting detectable atomic concentration is lowered, because the noise due to the flame background is almost always one of the more significant terms in the total noise expression at $N_{min.}$. It should also be noted that the lower the flame background, the less significant is the variation in W on the value of $N_{min.}$. As the flame background decreases, the reflection noise has a more significant contribution to the total noise near the limiting detectable atomic concentration, and therefore in the limiting case of negligible flame background, $N_{min.}$ is essentially independent of W (refer to curves A and B in Figure 3.2).

It should be mentioned that in none of the sample calculations in this chapter did the amplifier-readout noise contribute significantly to the total noise, and therefore $\overline{\Delta i_e}$ could be removed from the equations in Tables 3.1 and 3.2 without loss of accuracy. However, $\overline{\Delta i_e}$ could become significant if the amplifier-readout system was especially noisy.

If the flames are considered purely from the standpoint of limiting detectable atomic concentration (rather than necessarily the limiting detectable solution concentration), then one simple rule can be followed, namely, use the flame with the lowest flame background noise to obtain the lowest value of $N_{min.}$. However, if compound formation involving the element of concern is significant, then factors which are outside the scope of this paper must be considered, and the flame which results in the lowest amount of compound formation in conjunction with the lowest possible flame background should be used.

Part III

Methods of lowering the limiting detectable atomic concentration in atomic fluorescence flame spectrometry.- From the expressions in Table 3.2, it is evident that there are several parameters which can be varied in order to lower the limiting detectable atomic concentration. The monochromator slit width has already been discussed in some detail and so will not be treated here.

It can be seen from Table 3.2 that the path length, L, and the power efficiency, Φ_T, are both inversely related to $N_{min.}$. If L is increased by use of larger burners or slot-type burners, the solid angle, Ω_e, over which radiation enters the monochromator must also be increased in order to decrease $N_{min.}$. Because Ω_e is generally fixed for any particular monochromator, any increase in L (except to fill the solid angle Ω_e) would have to involve a rearrangement of entrance optics which might well result in no decrease in $N_{min.}$. The Φ_T factor, on the other hand, can be increased by the appropriate choice of flame gases. This has been shown by Alkemade (1) and has been used effectively in practice (21). For a complete discussion of Φ_T refer to the paper by McCarthy, Parsons, and Winefordner (12).

The intensity of the source of excitation can be increased up to a point to decrease the limiting detectable atomic concentration. Because all of the noise terms except the flame background involve this intensity, increasing the excitation source intensity value will only lower the limiting detectable atomic concentration until the noise terms which are dependent on intensity of the source become the dominant factors in the total noise. This is true whether a narrow line source or a continuous source of excitation is used. Similarly, lowering the intensity of the flame background will lower the limiting detectable atomic concentration until the flame flicker noise ceases to be significant factor of the total noise (also see Chapter IV).

Of the other experimental parameters, n -- the number of solid angles gathered into the monochromator -- can also be increased to decrease the limiting detectable atomic concentration, and any decrease of R_d, the reciprocal linear dispersion should also decrease $N_{min.}$; however, this usually results also in a decrease in T_f and Ω_e which would probably counterbalance the effect of R_d on $N_{min.}$.

Finally, each noise term decreases as the square root of Δf, and this is a factor that can usually be decreased greatly by proper choice of the amplifier-readout system; however, a decrease in Δf usually is accompanied by an increase in the time of analysis. Thus, an optimum value of Δf would be the smallest possible value that is consistent with the amount of solution available, the cost per analysis, and the time limitations for obtaining results.

In the actual experimental case, after the basic apparatus and optical setup have been decided upon, the optimum slit width and the flame type and composition are then the only real variables (the flame conditions determine the factors which influence sample flow rate, aspiration efficiency, etc.). The optimization of W is relatively straightforward for any particular flame type, whether determined experimentally or calculated for the given flame. However, the optimization of the flame type and conditions must be done experimentally and usually empirically because compound formation in the flame is one of the most important and the least elucidated parameter in determining the limiting detectable atomic concentration in terms of solution concentration (see Appendix VII). The treatment of this subject is beyond the realm of this manuscript, but it should be stated that any empirical optimization is best done using statistical experimental design techniques.

CHAPTER IV

THEORETICAL COMPARISON OF ATOMIC FLUORESCENCE, ATOMIC EMISSION, AND ATOMIC ABSORPTION FLAME SPECTROMETRY

The derivation of expressions for the signal-to-noise ratio at the limit of detectability in Chapter III, in addition to those derived for atomic emission and atomic absorption flame spectrometry by Winefordner and co-workers (27,29,30) has made it possible to compare directly the calculated limiting detectable atomic concentrations of elements (atoms/cm.^{3}) for these flame spectrometric methods under identical experimental conditions. This is extremely useful because much information of practical significance can be obtained regarding the complementary nature of these methods.

In this chapter the calculated limits of detectability of six elements -- Zn, Cd, Hg, Cu, Tl, and Na -- measured for eight different flame conditions using atomic emission, atomic absorption, and atomic fluorescence flame spectrometry are compared.

Theory and Calculations

For the sake of simplicity, only the resonance transitions for the elements of concern have been compared. All of the expressions used in this chapter have been derived and are either given in Chapter III or Table 4.1 along with references. A list of symbols and their definitions is given in Appendix I. The equations are given in the final form which is useful for calculation, and the reader is referred to the appropriate references for complete derivations and discussion of the expressions. All of the data needed for calculating limiting detectable atomic concentrations are either compiled from existing data or measured in this laboratory. The experimental parameters are discussed and tabulated in Appendix V, as well as a description of the apparatus used to measure them. FORTRAN IV programs were designed to perform all of the calculations and are discussed in Appendix VIII.

Results

In Table 4.2 the calculated values of limiting detectable atomic concentrations, $N_{min.}$ and the optimum monochromator slit width, $W_{opt.}$, for the atomic fluorescence, atomic emission, and atomic absorption flame spectrometric determinations of Zn, Cd, Hg, Cu, Tl, and Na atomized into eight different flames (assumed to be in thermal equilibrium) are given. The $W_{opt.}$ values were not given for atomic absorption flame spectrometry because $N_{min.}$ does not vary significantly with W over the slit widths normally

TABLE 4.1

EQUATIONS NEEDED FOR THIS CHAPTER

Atomic Emission Flame Spectrometry

4.1^{a} $N_{min.} = \dfrac{3.8\text{x}10^{34}\ g_1\ e^{E_u/kT}}{\nu_o\ g_u\ A_t\ LW\ k_2}(\overline{\Delta i}_p{}^2+\overline{\Delta i}_c{}^2+\overline{\Delta i}_e{}^2)$ reference (27)

4.2 $\overline{\Delta i}_p = [k_1\Delta f(i_d+k_2I_cW[R_dW+s_c]))]^{1/2}$ reference (29)

4.3 $\overline{\Delta i}_c = [\Delta f(k_2I_c\ \xi\ W)^2(R_dW+s_c)^2]^{1/2}$ reference (29)

4.4 $\overline{\Delta i}_e = [\zeta^2\Delta f(i_d+k_2I_cW[R_dW+s_c])^2]^{1/2}$ reference (27)

4.5^{b} $N_i = \dfrac{60\ a\ \Delta\nu_D\ g_1}{A_tL\ \lambda_o{}^2\ g_u}$ reference (31)

Table 4.1 (Cont'd)

Atomic Absorption Flame Spectrometry

4.6 $N_{min.} = \frac{53.5\ \Delta\nu_D\ g_l}{L\ \lambda_o^2\ g_u\ A_t} \chi \sqrt{\Delta f}$ reference (30)

4.7 $\overline{\Delta i}_p = [\Delta f\ k_1 k_2 W(I_A^{\circ} + I_c R_d W)]^{1/2}$ reference (30)

4.8 $\overline{\Delta i}^{o} = \sqrt{\Delta f}\ k_2\ \chi\ I_A^{\circ}\ W/2.0$ reference (30)

4.9 $\overline{\Delta i}_e = \sqrt{\Delta f}\ \zeta\ k_2\ I_A^{\circ}\ W/2.0$ reference (27)

---

[a] $W_{opt.}$ is obtained by the graphical method described in Chapter III.

[b] The same expression for N_i is obtained by both atomic emission and atomic fluorescence flame spectrometry when a continuous source of excitation is used (see Chapter II).

TABLE 4.2

CALCULATED VALUES OF W(OPT.) AND N(MIN.) FOR THE RESONANCE LINES OF Zn, Cd, Hg, Cu, Tl, AND Na AS A FUNCTION OF FLAME TYPE FOR ATOMIC FLUORESCENCE, ATOMIC EMISSION, AND ATOMIC ABSORPTION FLAME SPECTROMETRY

			FLUORESCENCE[b]				EMISSION[b]		ABSORPTION[b]
			Continuous		Line				
Element	Wave-length(A)	Flame[a]	$W_{opt.}$	$N_{min.}$	$W_{opt.}$	$N_{min.}$	$W_{opt.}$	$N_{min.}$	$N_{min.}$
Zn	2139	1	0.01	$4.2x10^{12}$	0.10	$7.1x10^{8}$	0.02	$3.6x10^{12}$	$2.9x10^{9}$
		2	0.04	$1.2x10^{13}$	0.04	$3.6x10^{9}$	0.02	$1.5x10^{12}$	$5.4x10^{9}$
		3	0.40	$1.6x10^{11}$	1.00	$5.8x10^{7}$	1.00	$8.0x10^{22}$	$1.3x10^{9}$
		4	0.40	$9.2x10^{10}$	0.45	$2.8x10^{7}$	0.45	$2.9x10^{18}$	$1.4x10^{9}$
		5	0.18	$1.3x10^{12}$	0.25	$9.9x10^{8}$	0.20	$1.2x10^{13}$	$5.1x10^{9}$
		6	0.40	$7.8x10^{10}$	2.50	$2.6x10^{7}$	1.50	$2.7x10^{27}$[c]	$1.1x10^{9}$
		7	0.20	$1.3x10^{11}$	0.20	$5.0x10^{7}$	0.20	$3.0x10^{10}$	$5.7x10^{9}$
		8	0.20	$2.0x10^{10}$	0.20	$6.5x10^{6}$	0.20	$4.8x10^{14}$	$1.6x10^{9}$

TABLE 4.2 (Continued)

			FLUORESCENCE[b]				EMISSION[b]		ABSORPTION[b]
			Continuous		Line				
Element	Wave-Length(A)	Flame[a]	$W_{opt.}$	$N_{min.}$	$W_{opt.}$	$N_{min.}$	$W_{opt.}$	$N_{min.}$	$N_{min.}$
Cd	2288	1	0.04	$9.6\text{x}10^{10}$	0.15	$1.8\text{x}10^{7}$	0.04	$3.1\text{x}10^{11}$	$2.9\text{x}10^{9}$
		2	0.02	$5.4\text{x}10^{11}$	0.03	$5.5\text{x}10^{7}$	0.04	$1.6\text{x}10^{11}$	$5.2\text{x}10^{9}$
		3	0.10	$6.3\text{x}10^{9}$	2.5[d]	$7.6\text{x}10^{6}$	0.45	$9.6\text{x}10^{20}$	$1.2\text{x}10^{9}$
		4	0.10	$9.8\text{x}10^{9}$	0.75	$9.5\text{x}10^{6}$	0.15	$7.4\text{x}10^{16}$	$1.4\text{x}10^{9}$
		5	0.05	$1.6\text{x}10^{11}$	2.5[d]	$4.3\text{x}10^{8}$	0.08	$7.6\text{x}10^{11}$	$5.0\text{x}10^{9}$
		6	0.10	$6.1\text{x}10^{9}$	2.5[d]	$6.7\text{x}10^{6}$	0.75	$1.5\text{x}10^{25}$	$1.1\text{x}10^{9}$
		7	0.08	$1.2\text{x}10^{11}$	2.5[d]	$1.2\text{x}10^{7}$	0.08	$3.1\text{x}10^{9}$	$5.6\text{x}10^{9}$
		8	0.07	$1.0\text{x}10^{10}$	2.5[d]	$9.3\text{x}10^{5}$	0.07	$2.5\text{x}10^{13}$	$1.6\text{x}10^{9}$
Hg	2537	1	0.03	$1.2\text{x}10^{12}$	0.03	$2.5\text{x}10^{8}$	0.03	$8.8\text{x}10^{10}$	$3.6\text{x}10^{9}$
		2	0.01[e]	$2.3\text{x}10^{12}$	0.01[e]	$1.1\text{x}10^{9}$	0.03	$3.7\text{x}10^{10}$	$9.5\text{x}10^{9}$
		3	0.06	$6.4\text{x}10^{10}$	0.40	$1.0\text{x}10^{8}$	0.28	$1.9\text{x}10^{19}$	$2.3\text{x}10^{9}$
		4	0.07	$4.4\text{x}10^{10}$	0.12	$5.9\text{x}10^{7}$	0.10	$3.8\text{x}10^{15}$	$2.5\text{x}10^{9}$
		5	0.03	$6.0\text{x}10^{11}$	0.08	$2.1\text{x}10^{9}$	0.04	$2.1\text{x}10^{11}$	$9.2\text{x}10^{9}$
		6	0.06	$4.1\text{x}10^{10}$	0.90	$6.0\text{x}10^{7}$	0.45	$1.2\text{x}10^{23}$	$2.1\text{x}10^{9}$
		7	0.04	$5.6\text{x}10^{10}$	0.04	$6.0\text{x}10^{7}$	0.04	$1.6\text{x}10^{9}$	$1.0\text{x}10^{10}$
		8	0.04	$7.9\text{x}10^{9}$	0.04	$8.9\text{x}10^{6}$	0.04	$4.6\text{x}10^{12}$	$2.8\text{x}10^{9}$

TABLE 4.2 (Continued)

Element	Wave-length(A)	Flame[a]	FLUORESCENCE[b]				EMISSION[b]		ABSORPTION[b]
			Continuous		Line				
			$W_{opt.}$	$N_{min.}$	$W_{opt.}$	$N_{min.}$	$W_{opt.}$	$N_{min.}$	$N_{min.}$
Cu	3248	1	0.01^e	$1.7x10^{12}$	0.01^e	$2.0x10^9$	0.01^e	$3.5x10^9$	$1.4x10^{10}$
		2	0.01^e	$1.1x10^{12}$	0.01^e	$2.5x10^9$	0.01^e	$3.1x10^9$	$2.9x10^{10}$
		3	0.04	$7.0x10^{11}$	0.11	$4.1x10^8$	0.09	$4.2x10^{15}$	$6.8x10^9$
		4	0.04	$9.1x10^9$	0.04	$3.8x10^7$	0.04	$5.7x10^{12}$	$7.5x10^9$
		5	0.01^e	$5.5x10^{11}$	0.03	$2.0x10^{10}$	0.02	$5.1x10^9$	$2.7x10^{10}$
		6	0.05	$1.1x10^{10}$	0.15	$4.8x10^7$	0.15	$3.5x10^{18}$	$6.1x10^9$
		7	0.01^e	$3.8x10^{10}$	0.01^e	$1.0x10^8$	0.01^e	$4.7x10^8$	$2.8x10^{10}$
		8	0.01^e	$4.6x10^9$	0.01^e	$1.1x10^7$	0.01^e	$7.5x10^{11}$	$8.0x10^9$
Tl	3776	1	0.03	$7.4x10^{12}$	0.03	$2.2x10^{10}$	0.03	$1.4x10^8$	$2.2x10^{10}$
		2	0.01^e	$5.9x10^{12}$	0.01^e	$3.4x10^{10}$	0.03	$9.6x10^7$	$2.8x10^{10}$
		3	0.04	$2.7x10^{11}$	0.35	$6.2x10^8$	0.25	$3.9x10^{13}$	$5.9x10^9$
		4	0.04	$1.2x10^{11}$	0.15	$4.4x10^8$	0.10	$1.8x10^{11}$	$1.1x10^{10}$
		5	0.01^e	$4.7x10^{12}$	0.06	$1.2x10^{11}$	0.03	$3.0x10^8$	$4.2x10^{10}$
		6	0.04	$1.2x10^{10}$	0.45	$5.4x10^8$	0.30	$7.7x10^{15}$	$1.3x10^{10}$
		7	0.03	$1.2x10^{11}$	0.03	$7.9x10^8$	0.03	$1.2x10^7$	$4.4x10^{10}$
		8	0.03	$1.8x10^{10}$	0.03	$1.1x10^8$	0.03	$1.6x10^9$	$1.2x10^{10}$

TABLE 4.2 (Continued)

			FLUORESCENCE[b]				EMISSION[b]		ABSORPTION[b]
			Continuous		Line				
Element	Wave-length(A)	Flame[a]	$W_{opt.}$	$N_{min.}$	$W_{opt.}$	$N_{min.}$	$W_{opt.}$	$N_{min.}$	$N_{min.}$
Na	5890	1	0.09	$2.8x10^{10}$	0.09	$1.3x10^{8}$	0.09	$1.9x10^{6}$	$9.0x10^{9}$
		2	0.04	$9.7x10^{10}$	0.04	$4.4x10^{8}$	0.10	$1.2x10^{6}$	$9.0x10^{9}$
		3	0.20	$1.6x10^{9}$	0.40	$5.5x10^{6}$	0.40	$2.5x10^{9}$	$2.1x10^{9}$
		4	0.15	$2.5x10^{9}$	0.15	$9.3x10^{6}$	0.15	$1.1x10^{8}$	$2.4x10^{9}$
		5	0.03	$3.0x10^{10}$	0.25	$7.7x10^{8}$	0.10	$2.8x10^{6}$	$8.8x10^{9}$
		6	0.20	$8.7x10^{8}$	0.35	$2.9x10^{6}$	1.00	$4.5x10^{10}$	$1.9x10^{9}$
		7	0.10	$1.4x10^{9}$	0.10	$7.0x10^{6}$	0.10	$3.9x10^{5}$	$9.7x10^{9}$
		8	0.10	$1.9x10^{8}$	0.10	$8.2x10^{5}$	0.10	$5.6x10^{6}$	$2.7x10^{9}$

[a] Flame 1. Oxyhydrogen (O_2 - 3 l./min.; H_2 5 l./min.) viewed at 3 cm. above the burner tip.
Flame 2. Oxyhydrogen (O_2 - 3 l./min.; H_2 7 l./min.) viewed at 3 cm. above the burner tip.
Flame 3. Flame 1 viewed at 6 cm. above the burner tip.
Flame 4. Flame 2 viewed at 6 cm. above the burner tip.
Flame 5. Air-hydrogen (air - 3 l./min.; H_2 - 6 l./min.) viewed at 3 cm. above the burner tip.
Flame 6. Flame 5 viewed at 6 cm. above the burner tip.
Flame 7. Argon-hydrogen-entrained air (argon - 3 l./min.; H_2 - 8 l./min.) viewed at 3 cm. above the burner tip.
Flame 8. Flame 7 viewed at 6 cm. above the burner tip.

[b] $W_{opt.}$ values are in mm., and $N_{min.}$ values are in atoms/cm.^{3}.

[c] This is the maximum number that the computer will calculate.

[d] $N_{min.}$ did not vary significantly with W under these conditions.

[e] This is the minimum resolving power slit width on the monochromator.

available, that is, most any slit width greater than the minimum resolving power slit width will give essentially identical results. The atomic fluorescence data are given for both narrow-line and continuous sources of excitation. In Figures 4.1, 4.2, and 4.3, typical calculated $N_{min.}$ versus W curves for the three methods are given.

In Table 4.3 the calculated ranges of near-linearity for the atomic fluorescence and atomic emission flame spectrometric measurement of the above elements in each flame are given. The calculated range of near-linearity is measured from the limit of detectability ($N_{min.}$) to the point of intersection (N_i) of the low and high atomic concentration asymptotes. Winefordner, Vickers, and Remington (31) derived an expression for N_i for atomic emission flame spectrometry. A similar approach is used in Chapter II to derive the expressions for N_i for atomic fluorescence; the expression for atomic fluorescence is identical to the one derived for atomic emission flame spectrometry when using a continuous source of excitation.

Figures 4.4, 4.5, 4.6, 4.7, and 4.8 give typical r.m.s. noise versus W curves for the most significant noises as well as the total r.m.s. noise term for various atoms measured by the three methods. These curves should be typical for the measurement of most lines of any atom using atomic fluorescence, atomic emission, and atomic

Fig. 4.1.-Curves of $N_{min.}$ versus monochromator slit width for atomic fluorescence flame spectrometry using a continuous source with five flame types.

Key to Figure: Data from Hg -- D.C.; Flames listed in Table 4.2.

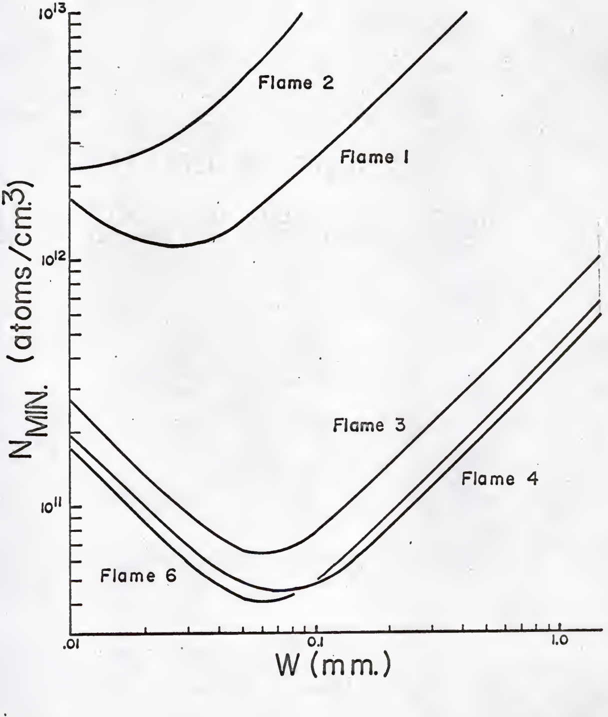
10^{13}
10^{12}
10^{11}
$N_{MIN.}$ (atoms/cm.^{3})
Flame 2
Flame 1
Flame 3
Flame 4
Flame 6
.01
0.1
1.0
W (mm.)

Fig. 4.2.-Typical curves of $N_{min.}$ versus monochromator slit width for atomic fluorescence flame spectrometry using a narrow line source with four flame types.

Key to Figure: Data from Hg -- D.C.; Flames listed in Table 4.2.

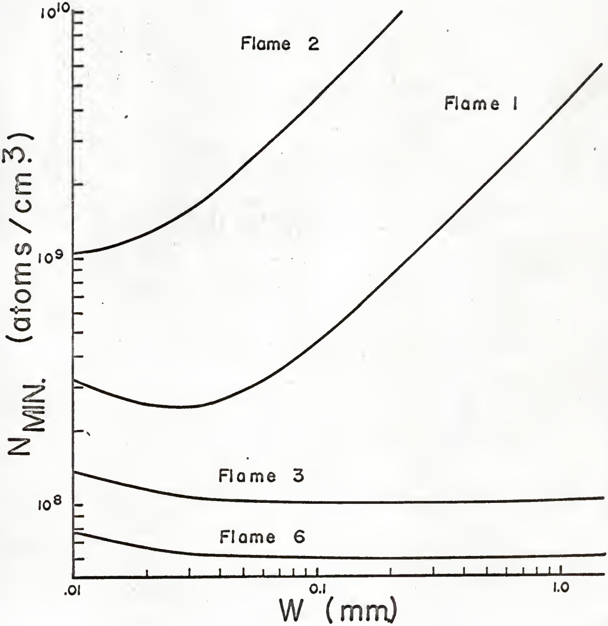
10^{10}
10^{9}
10^{8}
$N_{MIN.}$ (atoms/cm^3)
Flame 2
Flame 1
Flame 3
Flame 6
.01
0.1
1.0
W (mm)

Fig. 4.3.-Typical curves of $N_{min.}$ versus monochromator slit width for atomic emission and atomic absorption flame spectrometry with four flame types.

Key to Figure: Data from Na -- D.C. (for emission) and Na -- A.C. (for absorption); Flames listed in Table 4.2.

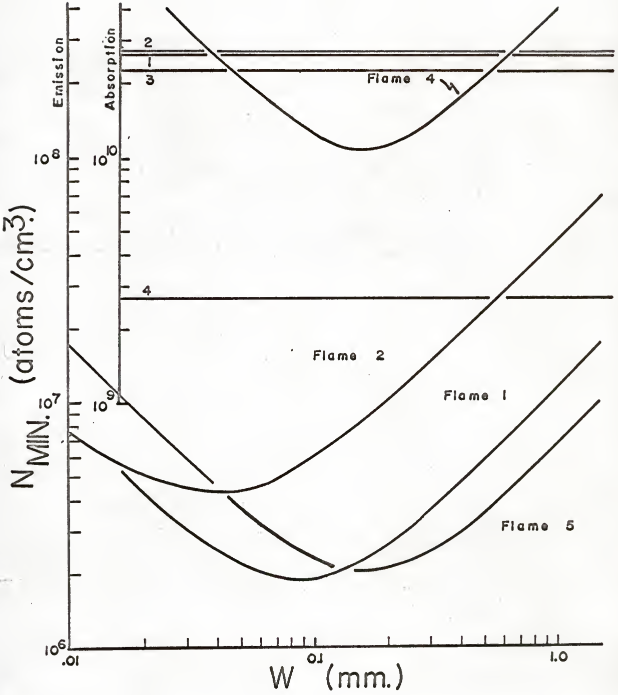
Emission
Absorption
2
1
3
Flame 4
4
Flame 2
Flame 1
Flame 5
10^8
10^{10}
10^7
10^9
10^6
$N_{MIN.}$ (atoms/cm^3)
.01
0.1
1.0
W (mm.)

TABLE 4.3

APPROXIMATE RANGE OF NEAR-LINEARITY OF ANALYTICAL GROWTH CURVES FOR OPTIMUM OXYHYDROGEN OR AIR-HYDROGEN FLAMES

Element	Flame[a]	FLUORESCENCE RANGE[b] Continuous	FLUORESCENCE RANGE[b] Line	EMISSION RANGE[b]
Zn	2			c
	6	$7.8\text{x}10^{10}$ — $4\text{x}10^{11}$	$2.6\text{x}10^{7}$ — $2\text{x}10^{11}$	
Cd	2			$1.6\text{x}10^{11}$ — $7\text{x}10^{11}$
	6	$6.1\text{x}10^{9}$ — $3\text{x}10^{11}$	$6.7\text{x}10^{6}$ — $1\text{x}10^{11}$	
Hg	2			$3.7\text{x}10^{10}$ — $9\text{x}10^{11}$
	4		$5.9\text{x}10^{7}$ — $3\text{x}10^{11}$	
	6	$4.1\text{x}10^{10}$ — $5\text{x}10^{11}$		
Cu	2			$3.1\text{x}10^{9}$ — $6\text{x}10^{11}$
	4	$9.1\text{x}10^{9}$ — $3\text{x}10^{11}$	$3.8\text{x}10^{7}$ — $1\text{x}10^{11}$	
Tl	2			$9.6\text{x}10^{7}$ — $8\text{x}10^{11}$
	4		$4.4\text{x}10^{8}$ — $2\text{x}10^{11}$	
	6	$1.2\text{x}10^{10}$ — $5\text{x}10^{11}$		
Na	2			$1.2\text{x}10^{6}$ — $1\text{x}10^{12}$
	6	$8.7\text{x}10^{8}$ — $3\text{x}10^{12}$	$2.9\text{x}10^{6}$ — $1\text{x}10^{12}$	

[a] The flame types are listed in Table 4.2.
[b] The range values are in atoms/cm.^{3}.
[c] The limit of detection is on the high concentration segment of the analytical growth curve.

Fig. 4.4.-Typical r.m.s. noise versus monochromator slit width curves for atomic fluorescence flame spectrometry using a continuous source.

Key to Figure: (Data from Zn -- D.C.; Flame 4, Table 4.2) A. total noise; B. phototube shot noise; C. reflection and scattering (from water droplets) noise; D. flame background noise; and E. amplifier-readout noise.

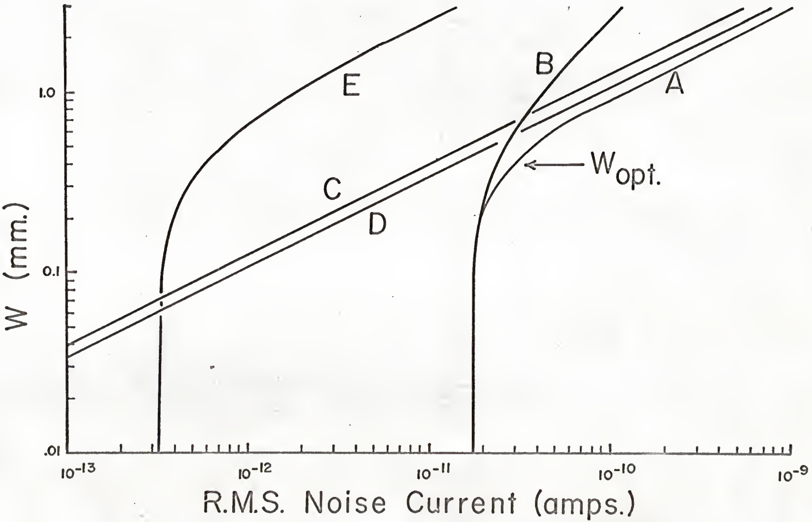
W (mm.)
1.0
0.1
.01
10^{-13}
10^{-12}
10^{-11}
10^{-10}
10^{-9}
R.M.S. Noise Current (amps.)
A
B
C
D
E
$W_{opt.}$

Fig. 4.5.-Typical r.m.s. noise versus monochromator slit width curves for atomic fluorescence flame spectrometry using a normal intensity narrow line source.

Key to Figure: See Figure 4.4.

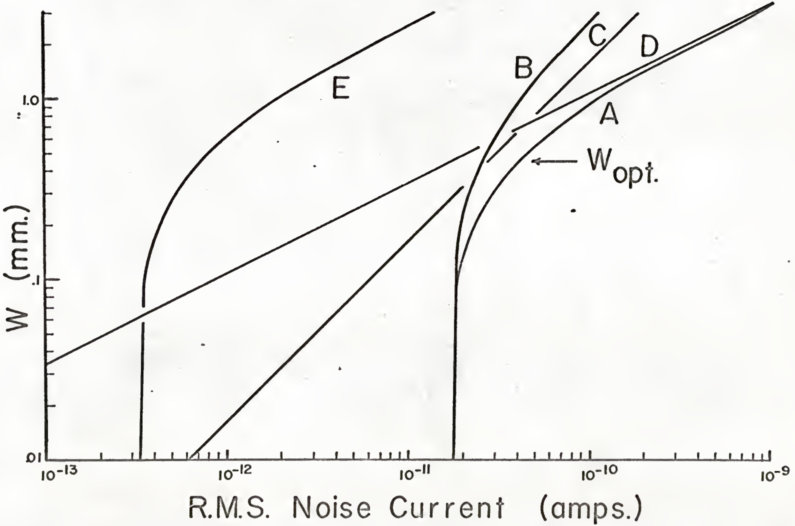
W (mm.)
1.0
.1
.01
10^-13
10^-12
10^-11
10^-10
10^-9
R.M.S. Noise Current (amps.)
A
B
C
D
E
W_opt.

Fig. 4.6.-Typical r.m.s. noise versus monochromator slit width curves for atomic fluorescence flame spectrometry using a very high intensity narrow line source.

Key to Figure: (Data from Cd -- D.C.). Noises are listed in Figure 4.4.

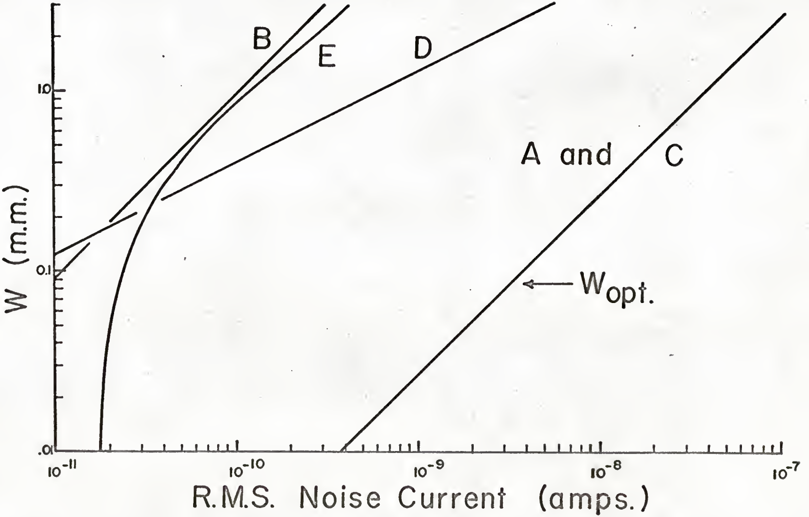
B
E
D
A and C
Wopt.
W (m.m.)
1.0
0.1
.01
10^-11
10^-10
10^-9
10^-8
10^-7
R.M.S. Noise Current (amps.)

Fig. 4.7.-Typical r.m.s. noise versus monochromator slit width curves for atomic emission flame spectrometry.

Key to Figure: (Data from Na -- D.C.; Flame 2, Table 4.2)

A. total noise; B. phototube shot noise; C. flame background noise; D. amplifier-readout noise.

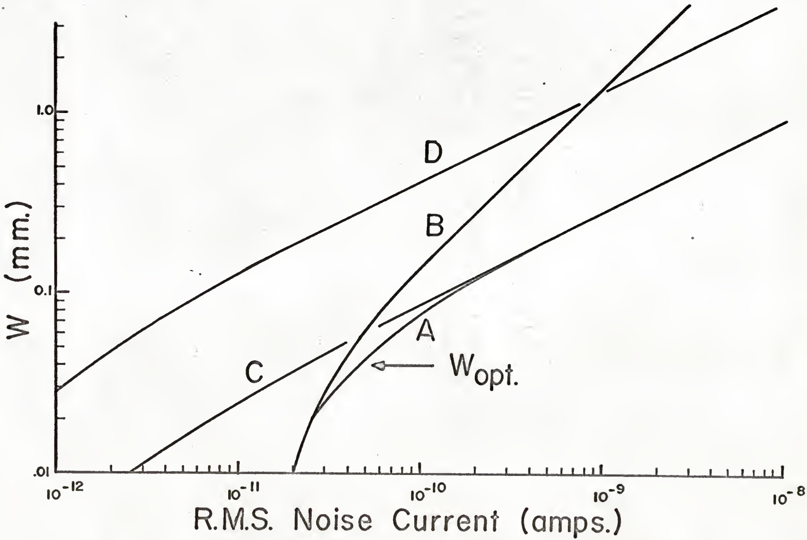
W (mm.)
1.0
0.1
.01
D
B
A
C
W$_{opt.}$
10^{-12}
10^{-11}
10^{-10}
10^{-9}
10^{-8}
R.M.S. Noise Current (amps.)

Fig. 4.8.-Typical r.m.s. noise versus monochromator slit width curves for atomic absorption flame spectrometry.

Key to Figure: (Data from Zn -- A.C.; Flame 2, Table 4.2)

A. total noise; B. phototube shot noise; C. flame background noise; D. source noise; and E. amplifier-readout noise.

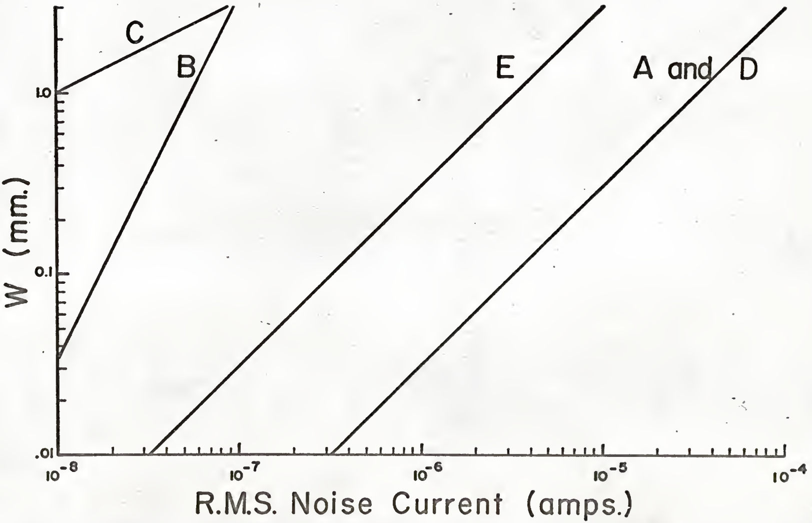
C
B
E
A and D
1.0
0.1
.01
W (mm.)
10^{-8}
10^{-7}
10^{-6}
10^{-5}
10^{-4}
R.M.S. Noise Current (amps.)

absorption flame spectrometry and using most of the commercially available experimental equipment and the usual experimental conditions.

Discussion

Part I. Comparison of Calculated $W_{opt.}$ and $N_{min.}$ Values for Atomic Fluorescence, Atomic Emission, and Atomic Absorption Flame Spectrometry as a Function of Flame Type and Conditions

Elements by atomic absorption flame spectrometry.- In atomic absorption flame spectrometry, the value of $N_{min.}$ varies only slightly from element to element and from flame type to flame type and so will be discussed separately in this section. The limiting detectable atomic concentration for nearly all resonance lines of all elements and experimental conditions (other than path length) varies only about an order of magnitude which indicates that the most important factors in determining the limit of detection for an element determined by atomic absorption flame spectrometry involve introduction of the sample into the flame cell and atomization of the sample once in the flame cell; these factors are not necessarily the most significant ones in the other two methods of analysis as is indicated by the relatively large variation of $N_{min.}$ from element to element and from flame type to flame type (see Table 4.2).

In other words, the amount of compound formation and ionization is probably always more important than the spectral and instrumental parameters in atomic absorption flame spectrometry.

Several conclusions can be made, however, about the limit of detectability in atomic absorption flame spectrometry. If it is assumed that an atom, such as zinc, is present primarily in the atomic form in most flames (3), then the atomic concentration and the solution concentration can be directly compared. It can be seen from the results in Table 4.2 that the limiting detectable atomic concentration obtained by atomic absorption flame spectrometry is about two orders of magnitude greater than obtained by atomic fluorescence flame spectrometry when using identical experimental conditions (see Appendix V). The best experimental limiting detectable solution concentrations obtained for the Zn 2139 Å line by these two methods are 0.1 ppb (parts per billion) for atomic fluorescence (13), and 5 ppb for atomic absorption (19) which is certainly consistent with the calculated results. However, it should be noted that somewhat different experimental conditions than were used here, for example, L = 10 cm. rather than 1.0 or 3.0 cm. and/or a multipass optical system, would account for somewhat lower limiting detectable atomic concentration in atomic absorption flame spectrometry than would be calculated by the data used in this dissertation.

Zinc by atomic fluorescence and atomic emission flame spectrometry.-Zinc is difficult to determine by atomic emission flame spectrometry because its resonance line, 2139 Å, has an excitation energy of 5.79 ev. In fact, there is simply not enough energy available in most analytical flames (which are approximately in thermal equilibrium) to excite zinc appreciably. In addition, the response of many multiplier phototubes at this wavelength is low. However, despite the low sensitivity of many multiplier phototubes at wavelengths below 2500 Å, calculations of limiting detectable atomic concentration for atoms measured by atomic fluorescence flame spectrometry predict very small values for Zn when an intense, narrow line source of excitation is used. A comparison of the ratio of calculated values of $N_{min.}$ for the Zn 2139 Å line with the ratio of experimentally obtained limiting detectable solution concentrations for a variety of experimental conditions gives excellent agreement.

All other elements in Table 4.2 by atomic fluorescences and atomic emission flame spectrometry.-These elements all behave more or less in the same fashion as Zn, except that they are all more easily excited than Zn. All of the best values of $N_{min.}$ for atomic fluorescence flame spectrometry predicted from theory (the argon-hydrogen-entrained air flame is not discussed because of the uncertainty of the data used in the calculations) result for either the slightly fuel rich oxyhydrogen (flame 4) or the air-hydrogen (flame 6) flames (viewed at 6 cm. above the tip of the burner -- see Table 4.2), because these flames have the smallest flame background noises (see Part II of this section). The values for $N_{min.}$ in atomic emission flame spectrometry for these elements decrease roughly an order of magnitude for a decrease of 1.0 eV. in its excitation energy, and without exception the hottest flame (flame 2 for the flames which the data are most accurate, flame 7 if the argon-hydrogen-entrained air flame is included) gives the lowest limit of detection for all of the elements by atomic emission flame spectrometry (also, see Appendix VI). These observations indicate the large dependence on flame temperature of the limit of detectability in atomic emission flame spectrometry. It should be pointed out that nearly identical results are predicted for Na measured by atomic emission and atomic fluorescence flame spectrometry(when a narrow line source of excitation is used).

Optimum monochromator slit width.-There is a general trend in the calculated values of $W_{opt.}$ for both atomic fluorescence and atomic emission flame spectrometry. This trend follows the flame background noise, that is, ξI_c. A decrease in flame background intensity I_c and/or a decrease in the flame flicker factor ξ will result in an increase in $W_{opt.}$. Generally, it is easier to decrease the value of I_c by the proper choice of a flame; whereas, the value of ξ will generally not vary over three-fold for most properly adjusted flames. For example, in a given flame it is possible to decrease I_c by several orders of magnitude by making the measurements above the luminous portion of the flame gases, and yet the value of ξ will not vary significantly for these two regions of observation. This situation has been used to advantage for the high sensitivity determination of Zn, Cd, etc., in the ppb concentration range in atomic fluorescence flame spectrometry (13). Further examples of this are readily seen in Table 4.2. The sensitivity of $N_{min.}$ with variation in W, that is, the rapidity with which $N_{min.}$ increases with a change in W away from $W_{opt.}$, also decreases with decreasing flame background noise when a narrow line source is used in atomic fluorescence flame spectrometry. There is a greater sensitivity of $N_{min.}$ with W when a continuous source is used in atomic fluorescence flame spectrometry. The variation of $N_{min.}$ with W for atomic emission, atomic fluorescence, and atomic absorption flame spectrometry is shown in Figures 4.1, 4.2, and 4.3, and is discussed in detail for atomic fluorescence flame spectrometry in Chapter III.

Part II. The Calculated Range of Near-Linearity for Atomic Fluorescence and Atomic Emission Flame Spectrometry

An estimate of the range of near-linearity can be determined by calculating the limit of detectability ($N_{min.}$) and the atomic concentration (N_i) corresponding to the intersection point between the low and high concentration asymptotic portions of the analytical growth curve. This range is certainly not the full range of usefulness in a practical experimental case; it is merely the range over which the signal is approximately linear with N, the atomic concentration (this does not imply that the signal is linear with solution concentration). Above the intersection point, N_i, the signal is proportional to either some function of N, for example, $\sqrt{N}$ in atomic emission flame spectrometry and in atomic fluorescence flame spectrometry when using a wide line or continuous source of excitation, or it is independent of N in the case of atomic fluorescence flame spectrometry when using a narrow line source of excitation. In an actual experimental situation, the range of usefulness will always be at least as large and possibly (except in the case of atomic fluorescence flame spectrometry when a narrow line source is used) as much as several orders of magnitude larger than the calculated range of near-linearity. In Table 4.3 the range of near-linearity for the six elements investigated with the best (oxyhydrogen or air-hydrogen) flame type for each is given. The range predicted for atomic fluorescence flame spectrometry for both continuous and narrow line sources of excitation and for atomic emission flame spectrometry can only be extended for a particular line of a particular element by lowering $N_{min.}$ because N_i is essentially fixed by the spectral parameters (see Table 4.1).

It should be pointed out that there is no direct means of estimating the range of near-linearity in atomic absorption flame spectrometry. A range could be estimated by using the value of $N_{min.}$ at the low concentration end and the value of $N_{max.}$ at the upper concentration end ($N_{max.}$ is that concentration which gives a transmitted signal, i_t, which can just be read over the total noise, for example, $i_t/\Delta i_T = 2$). However, the error at the upper end is just as great as the error at the lower end, and so this range is not directly comparable to the ranges for the atomic emission and atomic fluorescence methods. Generally, the useful range of analytical curves in atomic absorption flame spectrometry is about two orders of magnitude.

Part III. Variation and Comparison of r.m.s. Noise Terms with Monochromator Slit Width in Atomic Fluorescence, Atomic Emission, and Atomic Absorption Flame Spectrometry

In Figures 4.4, 4.5, 4.6, 4.7, and 4.8 the variation of the specific r.m.s. noise terms and the total r.m.s.

noise term, $\overline{\Delta i_T}$, for all three flame spectrometric methods is illustrated. An arrow indicates $W_{opt.}$ when an optimum value is present. These results are typical for most lines of most atoms measured by the specified techniques.

Atomic fluorescence flame spectrometry.-When a continuous source of excitation is used in atomic fluorescence flame spectrometry, a combination of the flame background, phototube, and reflection plus Rayleigh scattering (from water droplets) noise terms usually dominate the total noise term at $W_{opt.}$. This is shown in Figure 4.4. If the intensity of the continuous source were increased, the reflection noise would quickly become the dominate noise, and $W_{opt.}$ would decrease in value because the reflection noise varies as W^2. This would also result in a decrease in $N_{min.}$. However, $N_{min.}$ can not be decreased by further increase in the intensity of the source, unless the factors causing the noise due to reflection can be reduced without causing a simultaneous increase in the other noise terms. It should be noted that the amplifier-readout noise term is insignificant in this case as well as all other cases discussed below.

When using a normal intensity narrow line source for atomic fluorescence flame spectrometry, the reflection, flame background, and phototube noises determine $W_{opt.}$ (see Figure 4.5), and when using a high intensity narrow line source for atomic fluorescence flame spectrometry, the reflection noise alone determines $W_{opt.}$ (see Figure 4.6). It should be noted that in the latter case there is little variation of $N_{min.}$ with W (see Figure 4.2).

Thus, it can be seen that in atomic fluorescence the total noise can be decreased, and therefore $N_{min.}$ can be decreased by decreasing the phototube, flame background, and/or the reflection noises. The only ways to decrease the phototube noise are to cool the phototube or to use an amplifier-readout system with smaller Δf; otherwise, this noise is fixed by the various currents that pass through the phototube. The effect of decreasing the flame background noise can be illustrated by comparing the $N_{min.}$ and $W_{opt.}$ values in Table 4.2 (also see Figure 3.3) and noting that the best flames for analysis in terms of $N_{min.}$ values are those with the smallest flame backgrounds, and therefore the smallest flame background noises. The flame background noise, $\overline{\Delta i}_c$, can be decreased by decreasing ξ, the flame flicker factor, I_c, the flame background intensity, and Δf of the amplifier-readout system (see Chapter III). The reflection noise is essentially a result of reflection and scattering of incident light by unevaporated water droplets present in the flame. This can be decreased by using either a chamber-type aspirator-burner or using organic solvents in a total-consumption aspirator-burner (21). However, the former method will decrease the total amount of solution reaching the flame, and the latter will increase the flame background noise. The reflection noise, $\overline{\Delta i_R}$, can also be decreased by decreasing Δf of the amplifier-readout system.

Atomic emission flame spectrometry.-The total noise in atomic emission flame spectrometry is dominated by the flame background noise and the phototube noise at $W_{opt.}$ (see Figure 4.7). Unfortunately, any decrease in the flame background is usually accompanied by a decrease in the temperature of the flame, the most important factor in determining the intensity of the emission signal. Thus, in atomic emission flame spectrometry, the temperature of the flame is of greater importance than the flame background noise. The phototube and flame background noises can, of course, be decreased by any of the methods already discussed.

Atomic absorption flame spectrometry.-It is readily seen from Figure 4.8 that the source noise completely dominates the total noise term in atomic absorption flame spectrometry for the experimental conditions selected (see Appendix V). The source noise, $\overline{\Delta i}^{\circ}$, can be decreased by decreasing Δf of the amplifier-readout system, the intensity of the source of excitation, I_A°, and the source flicker factor χ. However, the value of $N_{min.}$ is independent of I_A°. This accounts for the lack of dependence of $N_{min.}$ on W. If the source intensity were decreased by four to five orders of magnitude, then the phototube and flame background noise would become significant; however, the resulting intensity would be so small that it would be difficult experimentally to obtain an accurate zero absorbance or a 100 per cent transmittance reading on the available amplifier-readout systems. Thus, the noises and their variation with W for atomic absorption flame spectrometry are only of academic interest for the experimental conditions studied in this paper as well as for most practical atomic absorption flame spectrometric studies.

Part IV. Comparison of Experimental Designs in Atomic Fluorescence, Atomic Emission, and Atomic Absorption Flame Spectrometry

Sources of excitation.-An increase in the intensity of the source of excitation (continuous or narrow line) in atomic fluorescence flame spectrometry results in a decrease in $N_{min.}$ until the reflection noise dominates the total noise term (see Figure 4.6). However, most narrow line sources available are not intense enough to cause the reflection noise to be the dominating noise term. This indicates that research should be carried out on intense narrow line sources. The only source measured for this paper with sufficient intensity to give a reflection noise that was the dominate noise was the Cd electrodeless discharge tube; it was more intense by nearly two orders of magnitude than the electrodeless discharge tubes of the other elements studied. It should be emphasized that the sources must be intense over the absorption line half-width of the element of concern; therefore, self-reversed lamps, no matter how intense, are of little use in atomic fluorescence flame spectrometry (as well as for atomic absorption flame spectrometry). The 150 watt continuous source used in this study was about an order of magnitude too low in intensity to cause the reflection noise to be the dominating noise term; therefore, the limit of detectability could be lowered by using a more intense continuous source of excitation (at least up to the point where the reflection noise becomes the dominate noise term). It should also be pointed out that in atomic fluorescence flame spectrometry, if more intense sources are used, then flames with larger flame backgrounds can be used, and the same $N_{min.}$ can be obtained in both cases. This means that lower values of limiting detectable solution concentrations should be obtainable for those elements which tend toward compound formation because higher flame temperatures can be used to decrease the compound equilibria.

Because the flame itself is the source of excitation in atomic emission flame spectrometry, the temperature of the flame is the most important single factor in determining $N_{min.}$. The limit of detectability decreases with increasing flame temperature until ionization of the element under consideration becomes significant; thus, if the appropriate information is available about the various equilibria in the flame, an optimum flame temperature could be calculated. This information, unfortunately, is usually not available.

In atomic absorption flame spectrometry, the intensity of the source is not usually an important parameter. Therefore, if the intensity is not too low or too high for the phototube-amplifier-readout system to handle, there is no need to consider it as a parameter. However, the width of the source line must be small in relation to the absorption half-width of the element of concern to obtain the lowest values of $N_{min.}$ (see Table 4.1). This is the reason that most sources must be operated at currents as small as possible and still give an intensity high enough to be observable by the phototube-amplifier-readout system. Hollow-cathode discharge tubes have had great success in atomic absorption flame spectrometry because they usually have intensities in the proper range and yet have narrow emission line profiles. It should be remembered that a definite warmup time is required for hollow-cathode discharge tubes when using a single-beam instrument.

Flame sample cells and entrance optics.-In atomic fluorescence and atomic absorption flame spectrometry, the flame cell simply is a means of providing atoms in the ground energy level which are available for absorption of incident radiation. If the theoretical aspects are considered alone, it would seem that the lower the flame background intensity, the lower $N_{min.}$; however, when the practical aspects are considered, the importance of compound formation may well outweigh flame noise considerations in choosing a flame for a cell. This is especially true in atomic absorption flame spectrometry where the flame noise is not an important parameter, in determining $N_{min.}$.

In the case of atomic emission flame spectrometry, the flame is the source of excitation as well as the means of providing atoms. This indicates that the temperature of the flame is a more important parameter than the magnitude of the flame background intensity. This is clearly seen from the results of the calculations presented in Table 4.3. This has certain advantages in that theory predicts for many elements (unless ionization is the most significant factor) that the best working conditions for obtaining the lowest detectable solution concentration are essentially the same as for obtaining the lowest detectable atomic concentration.

In atomic emission flame spectrometry $N_{min.}$ will be lowered by focusing multiple images of the flame on the entrance slit of the monochromator; in atomic absorption and atomic fluorescence flame spectrometry, $N_{min.}$ will be lowered by multiple passes of the exciting radiation through the flame cell. Many such systems have been described in the literature, and these are reviewed in the books by Herrmann and Alkemade (8) and Mavrodineanu and Boiteux (14). The response of all three flame spectrometric methods is directly proportional to the path length, L, of the flame cell; however, only in atomic absorption flame spectrometry is the increase of L a convenient method of decreasing $N_{min.}$. This is usually done by the use of slot-type chamber burners which have the disadvantage of much lower aspiration efficiencies than total-consumption aspirator-burners.

Monochromators and detection systems.-When a continuous source of excitation is used in atomic fluorescence flame spectrometry and in atomic emission flame spectrometry, the monochromator should have as good a resolution as possible in conjunction with high Ω_e and T_f values, because any impurity or substance in the sample matrix is capable of being excited; therefore, if the wavelength of the impurity is close to the wavelength of interest, the only way to avoid error is to resolve the two lines or to use a physical separation step prior to measurement.

When a narrow line source is used in atomic fluorescence flame spectrometry, the monochromator should have T_f and Ω_e values as large as possible. This is because any impurities present in the flame will not be excited by the narrow line source (unless the same impurity is present in the source of excitation), and thermal emission is usually negligible under the best flame conditions for atomic fluorescence, that is, above the luminous portion of the flame.

Atomic absorption flame spectrometry is not affected greatly by the type of monochromator, for example, very little change in the value of $N_{min.}$ and variation in the shape of the $N_{min.}$ versus W curve. Thus, the choice of monochromator should be determined by practical considerations, that is, space, cost, other possible uses, etc. The double-beam system should also be considered. The double-beam system in atomic absorption flame spectrometry compensates for drift in source intensity and so avoids the time spent in waiting for the source to warm up. A double-beam system would also be advantageous in atomic fluorescence flame spectrometry for the same reason.

The choice of phototube and blaze angle of the grating is dependent upon the wavelengths of the elements which are to be analyzed, and the reader is referred to the books by Herrmann and Alkemade (8) and Mavroudineanu and Boiteux (14) for a more complete discussion of these topics. However, it should be noted that the voltage impressed on the phototube has little effect on the signal-to-noise ratio, and therefore on the value of $N_{min.}$, for any of the flame spectrometric methods (11).

The choice of an amplifier-readout system is left up to personal preference because of the large number of available systems. However, there are several guidelines which can be followed. In the case of atomic absorption flame spectrometry, when an A.C. system is used, some of the thermal emission will generally be observed by the system. The constant thermal emission signal can be eliminated by use of an A.C. amplifier, and the noises can be minimized by use of a tuned A.C. amplifier of very narrow frequency response band width (Δf). If thermal emission is not compensated for when using a wide band A.C. or a D.C. amplifier, this will lead to lack of linearity of absorbance with N.

In atomic emission and atomic fluorescence flame spectrometry there is no great change in $N_{min.}$ with either a D.C. or an A.C. system providing Δf is made small enough. The value of Δf can be decreased by the addition of an RC circuit as was discussed in Chapter III.

APPENDICES

APPENDIX I

SYMBOLS AND DEFINITIONS OF TERMS USED

a = the classical damping constant = $(\ln 2)^{1/2} \Delta\nu_C \Delta\nu_D$ (no units).

$A_{eff.}$ = the limiting area in the monochromator optical system, cm.^{2}.

A_t = the transition probability, sec.$^{-1}$.

A_T = the total absorption factor, that is, the fraction of incident radiation absorbed, sec.$^{-1}$.

b = the distance over which fluorescence radiation must travel before leaving the flame cell, cm. (see Figure 2.2).

B = characteristic phototube factor = $1 + G^{-1} + G^{-2} + \ldots G^{-(z-1)}$, no units.

c = the speed of light, cm./sec.

C = solution concentration, moles/l.

C_o = capacitance of an RC circuit, farads.

d = distance over which incident radiation must travel in the flame cell before the fluorescence it produces is observed by the monochromator, cm. (see Figure 2.2).

e_c = the charge of an electron, 1.6×10^{-19} coulombs.

E_ν = the frequency distribution of the incident radiation, ergs cm.$^{-2}$ ster.$^{-1}$ sec.

E_u = the energy required to excite an energy level, eV.

f_X = absorption factor for area X of Figure 2.2 (no units).

f_Y = absorption factor for area Y of Figure 2.2 (no units).

f_Z = absorption factor for area Z of Figure 2.2 (no units).

F = the focal length of the collimating lens (or mirror) in the monochromator, cm.

G = the gain per stage of the multiplier phototube (no units).

g_j = statistical weight of state j (no units).

h = Planck's constant, 6.624×10^{-27} ergs sec.

H = effective slit height of monochromator, cm.

i = photoanodic current due to the intensity of thermal atomic emission, amps.

$\overline{\Delta i}$ = r.m.s. noise due to the fluctuation of the intensity of thermal atomic emission, amps.

I = the intensity of thermal atomic emission, watts/cm.^{2}ster.

I_A = the intensity absorbed by a resonance line, watts/cm.^{2}.

i_c = photoanodic current due to the intensity of the flame background, amps.

$\overline{\Delta i}_c$ = r.m.s. noise due to the fluctuation of the intensity of the flame background, amps.

I_c = intensity of flame background, watts/cm.^{2}ster.$^{-2}$ mμ.

i_d = photoanodic dark current, amps.

$\overline{\Delta i}_e$ = r.m.s. noise of the amplifier-readout system referred to the amplifier input, amps.

i_F = photoanodic current due to the intensity of atomic fluorescence, amps.

$\overline{\Delta i}_F$ = r.m.s. noise due to the fluctuation in the intensity of atomic fluorescence, amps.

I_F = intensity of atomic fluorescence, watts/cm.^{2} ster.

$\overline{\Delta i}_J$ = r.m.s. noise on phototube due to Johnson noise, amps.

I_L = intensity of narrow line source of excitation in atomic fluorescence flame spectrometry, watts/cm.^{2} ster.

$\overline{\Delta i}_p$ = photoanodic noise due to shot and Johnson r.m.s. noise current, amps.

i_R = photoanodic current due to the intensity of reflection and Rayleigh scattering of incident light by water droplets, amps.

$\overline{\Delta i}_R$ = r.m.s. noise due to the fluctuation of the intensity of the reflection and Rayleigh scattering of incident light by water droplets, amps.

I_R = intensity of reflection and Rayleigh scattering of incident light by water droplets, watts/cm.^{2}ster.

i_s = photoanodic current due to the intensity of a standard light source, amps.

I_s = intensity of a standard light source, watts/cm.^{2} ster. mμ.

i_S = photoanodic current due to the intensity of Rayleigh scattering of incident radiation by salt particles, amps.

I_S = intensity of Rayleigh scattering of incident radiation by salt particles, watts/cm.^{2}ster. mμ .

$\overline{\Delta i_S}$ = r.m.s. noise due to fluctuation of the intensity of Rayleigh scattering by salt particles, amps.

i_t = photoanodic current of transmitted radiation in atomic absorption flame spectrometry, amps.

i_T = total photoanodic current due to all sources, amps.

$\overline{\Delta i_T}$ = total r.m.s. photoanodic noise due to all sources, amps.

$I\nu_t$ = the intensity transmitted through the flame of average length L at frequency ν , watts/cm.^{2}ster.

i_o = photoanodic current of incident radiation in atomic absorption flame spectrometry, amps.

I° = the intensity of continuous (or wide line) source of excitation, watts/cm.^{2}ster. mμ .

I°_A = the intensity of the source in atomic absorption flame spectrometry, watts/cm.^{2}ster.

I°_ν = the intensity of the exciting radiation as a function for frequency, watts/cm.^{2}ster. mμ .

j = energy state symbol (no units).

k = Boltzmann constant, 8.618×10^{-5} eV./°K.

k = the average atomic absorption coefficient for a line over all frequencies and all atoms, cm.$^{-1}$.

k_ν = the atomic absorption coefficient, $cm.^{-1}$.

k° = the atomic absorption coefficient at the absorption line center for a purely Doppler broadened line, $cm.^{-1}$.

$k_1 = 2\ e_c\ B\ M.$

$k_2 = \gamma\ T_f\ H\,\Omega_e$.

$k_3 = \rho_R\,\Omega_a/4\pi$.

$$K_c = \frac{\Omega_a \lambda^2{}_o\ g_u\ A_t}{32\pi^2\ g_l} .$$

$$K_L = \frac{2\sqrt{\ln 2}}{32\pi^{5/2}} \times \frac{\Omega_a \lambda^2{}_o\ g_u\ A_t}{g_l\ \Delta\nu_D} .$$

l = the path length over which a fluorescence signal emanates in the direction of the monochromator, cm. (see Figure 2.2).

L = path length of the flame cell, cm.

M = amplification factor of multiplier phototube, G^z, no units.

M_x = molecular weight of species x, atomic mass units.

n = number of solid angles, Ω_e, which enter the monochromator, ster.

n_T/n_{298} = the expansion factor of hot flame gases (no units).

N = the atomic concentration of atoms in the flame, $atoms/cm.^3$.

N_i = the atomic concentration corresponding to the point of intersection of the low and high concentration segments of the analytical growth curve in atomic fluorescence and atomic emission flame spectrometry, atoms/cm.^{3}.

$N_{min.}$ = the minimum detectable atomic concentration of atoms in the flame, atoms/cm.^{3}.

Q = the flow rate of unburned gases in the flame, cm./sec.

R = the gas constant, ergs/mole °K.

R_o = resistance of RC circuit, ohms.

R_d = reciprocal linear dispersion of the monochromator, mμ/cm.

S = a factor related to the total absorption of a purely Doppler broadened line by equation II.14.

s = the spectral band width of the monochromator, mμ.

s_c = the minimum resolving spectral band width of the monochromator, mμ.

T = the flame temperature, °K.

T_L = the temperature of the phototube load resistor, °K.

W = the effective slit width of the monochromator, cm.

$W_{opt.}$ = the optimum slit width of monochromator, cm.

X, Y, and Z = areas of the flame cell, cm.^{2} (see Figure 2.2).

z = the number of dynodes in the multiplier phototube (no units).

α = the ratio of the emission line half-width to the absorption line half-width (no units).

β = the fraction of the sample species in the atomic form (no units).

δ = a correction factor to account for damping as well as Doppler broadening (no units).

Δf = the frequency response band width of the amplifier-readout system, sec.$^{-1}$.

ϵ = the aspiration efficiency of solution introduction into a burner (no units).

γ = photoanodic sensitivity of photodetector, amps. at anode per watt of radiant power at photocathode, amps./watt.

Γ_F = atomic fluorescence flicker factor, $\Delta I_F/I_F$, sec.$^{1/2}$.

Γ_R = reflection and Rayleigh scattering of incident radiation by water droplets flicker factor, $\Delta I_R/I_R$, sec.$^{1/2}$.

Γ_S = Rayleigh scattering of incident radiation by salt particles flicker factor, $\Delta I_S/I_S$, sec.$^{1/2}$.

K = slit function parameter (no units).

λ_o = peak wavelength of line of concern, cm.

$\Delta\lambda_D$ = the half-width of the absorption line for pure Doppler broadening, mμ .

ν_f = the frequency of the atomic fluorescence radiation, sec.$^{-1}$.

ν_a = the frequency of the atomic absorption, sec.$^{-1}$.

ν_o = the frequency of the line center of a transition, sec.$^{-1}$.

$\Delta \nu_C$ = the half-width of the absorption line for pure collisional broadening, sec.$^{-1}$.

$\Delta\nu_D$ = the half-width of the absorption line for pure Doppler broadening, sec.$^{-1}$.

$\Delta\nu_L$ = the half-width of the emission line, sec.$^{-1}$.

$\Delta\nu_N$ = the half-width of the absorption line for natural broadening, sec.$^{-1}$.

$\Delta\nu_R$ = the half-width of the absorption line for resonance broadening, sec.$^{-1}$.

Ω_a = the solid angle of exciting radiation from the source and incident on the flame cell, ster.

Ω_e = the solid angle collected by the monochromator, ster.

ϕ = the quantum efficiency for atomic fluorescence (no units).

Φ = the solution flow rate into a burner, ml./min.

Φ_T = the power efficiency for atomic fluorescence (no units).

π = 3.1416 (no units).

ρ = correction factor to account for hyperfine structure of the source and absorption line (no units).

ρ_R = fraction of incident radiation reaching monochromator (no units).

ξ = flame background flicker factor, $\Delta I_c/I_c$, sec.$^{1/2}$.

ψ = thermal emission flicker factor, $\Delta I/I$, sec.$^{1/2}$.

χ = the source flicker factor, $\Delta I_A^\circ/I_A^\circ$, sec.$^{1/2}$.

ζ = amplifier-readout noise factor, sec.$^{1/2}$.

APPENDIX II

EVALUATION OF f_X, f_Y, f_Z, AND THE TOTAL ABSORPTION, A_T

Part I. f_X,f_Y, and f_Z

Consider a container with absorbing and emitting atoms at all points. Radiation emitted at any point within the container and in the plus x direction will be decreased by the absorption factor $\exp(-\overline{k}x)$, where $\overline{k}$ is the average atomic absorption coefficient for the line over all frequencies and all atoms, and x is the path length over which the fluorescence radiation must travel. If the container is l cm. (see Figure 2.2) long in the plus x direction, then the absorption factor is $\exp(-\overline{k}l)$ for radiation emitted from the left side of the container in the plus x direction, and the absorption factor is 1.0 for radiation emitted from the right side, that is, no absorption occurs. Thus, the average absorption factor, f_Y, for radiation emitted at any point in the plus x direction must be

$$f_Y = \frac{1 + \exp(-kl)}{2} \quad , \qquad \text{(II.1)}$$

This same equation results by considering radiation emitted from each infinitesmal point and then taking the average. Kolb and Streed (10) used the more general approach and obtained the same result.

The decrease in intensity of any column of radiation passing through an absorbing medium of length x is given by the absorption factor of $\exp(-\bar{k}x)$, and so f_X and f_Z are given by

$$f_X = \exp(-\bar{k}d) \quad , \tag{II.2}$$

and

$$f_Z = \exp(-\bar{k}b) \quad . \tag{II.3}$$

Mitchell and Zemansky (15) have evaluated a parameter called the "absorption" $A\alpha$, which is related to $\exp(-\bar{k}x)$ by

$$\exp(-\bar{k}x) = 1 - A\alpha \quad . \tag{II.4}$$

The "absorption," $A\alpha$, is defined by

$$A\alpha = \frac{\int_0^\infty E_\nu \exp(-k_\nu x)\,d\nu}{\int_0^\infty E_\nu\, d\nu} \quad , \tag{II.5}$$

where E_ν is the frequency distribution of the incident radiation. Now if it is assumed that the frequency distribution is Gaussian, that is, $E_\nu = k^\circ \exp(-\nu^2)$ and if the emitting and absorbing layers are fairly thin, then the following series (15) results for $\exp(-\bar{k}x)$

$$\exp(-\bar{k}x) = 1 - \frac{k^\circ x}{\sqrt{1 + \alpha^2}} + \frac{(k^\circ x)^2}{2!\sqrt{1 + \alpha^2}} - \frac{(k^\circ x)^3}{3!\sqrt{1 + \alpha^2}} + \dots \frac{(-1)^{n+1}(k^\circ x)^{n-1}}{(n - 1)!\sqrt{1 + \alpha^2}} \tag{II.6}$$

where α is the ratio of the emission line half-width to the absorption line half-width. Because the emitting and absorbing atoms in a flame cell are under identical conditions, α is unity, and so

$$\exp(-\bar{k}x) = 1 - \frac{k^{\circ}x}{\sqrt{2}} + \frac{(k^{\circ}x)^2}{2!\sqrt{3}} - \frac{(k^{\circ}x)^3}{3!\sqrt{4}} + \ldots \frac{(-1)^{n+1}(k^{\circ}x)^{n-1}}{(n-1)!\sqrt{n}} . \qquad \text{(II.7)}$$

If the spectral lines are also broadened by damping factors, then

$$\exp(-\bar{k}x) = 1 - \frac{k^{\circ}\delta x}{\sqrt{2}} + \frac{(k^{\circ}\delta x)^2}{2!\sqrt{3}} - \frac{(k^{\circ}\delta x)^3}{3!\sqrt{4}} + \ldots \frac{(-1)^{n+1}(k^{\circ}\delta x)^{n-1}}{(n-1)!\sqrt{n}} \qquad \text{(II.8)}$$

where δ is a correction factor to account also for damping as well as Doppler broadening.

The absorption factors f_X, f_Y, and f_Z are therefore given by the following expressions:

$$f_X = 1 - \frac{k^{\circ}\delta d}{\sqrt{2}} + \frac{(k^{\circ}\delta d)^2}{2!\sqrt{3}} - \frac{(k^{\circ}\delta d)^3}{3!\sqrt{4}} + \ldots \frac{(-1)^{n+1}(k^{\circ}\delta d)^{n-1}}{(n-1)!\sqrt{n}} \qquad \text{(II.9)}$$

$$f_Y = 1 - \frac{k^{\circ}\delta l}{\sqrt{2}} + \frac{(k^{\circ}\delta l)^2}{2!\sqrt{3}} - \frac{(k^{\circ}\delta l)^3}{3!\sqrt{4}} + \ldots \frac{(-1)^{n+1}(k^{\circ}\delta l)^{n-1}}{(n-1)!\sqrt{n}} \qquad \text{(II.10)}$$

$$f_Z = 1 - \frac{k^\circ \delta b}{\sqrt{2}} + \frac{(k^\circ \delta b)^2}{2!\sqrt{3}} - \frac{(k^\circ \delta b)^3}{3!\sqrt{4}}$$

$$+ \ldots \frac{(-1)^{n+1}(k^\circ \delta b)^{n-1}}{(n-1)!\sqrt{n}} . \quad \text{(II.11)}$$

If the atomic lines are broadened primarily by the Doppler effect, the $\delta = 1.0$. If $k^\circ \delta x$ (x is d,b, or l) is 10^{-3}, 10^{-2}, 10^{-1}, 1, and 10, the above series converge (to three significant figures) in 1,2,3,5, and 30 terms, respectively.

Part II. A_T

The total absorption, A_T, is defined by equation 2.3, namely

$$A_T = \int_0^\infty [1-\exp(-k_\nu L)]d\nu \quad . \quad \text{(II.12)}$$

Mitchell and Zemansky (15) define the S for pure Doppler broadening by

$$S = \frac{2\sqrt{\ln 2}}{\sqrt{\pi}\,\Delta\nu_d\, k^\circ L} \int_0^\infty [1 - \exp(-k^\circ L\, e^{-\nu^2})]d\nu \quad . \quad \text{(II.13)}$$

Therefore, A_T is related to S (for pure Doppler broadening) by

$$A_T = \frac{\sqrt{\pi}\,\Delta\nu_D\, k^\circ L}{2\sqrt{\ln 2}} S \quad . \quad \text{(II.14)}$$

If the absorption line is narrow compared to the source line half-width and if the absorption line is broadened primarily by Doppler broadening, then the following expression (15) results

$$A_T = \frac{\sqrt{\pi}\,\Delta\nu_D\,k^{\circ}L}{2\sqrt{\ln 2}}\left[1 - \frac{k^{\circ}L}{2!\sqrt{2}} + \frac{(k^{\circ}L)^2}{3!\sqrt{3}} - \ldots \frac{(-1)^{n+1}(k^{\circ}L)^{n-1}}{n!\sqrt{n}}\right], \qquad (II.15)$$

which reduces to equation 2.7 for small values of $k^{\circ}L$.

If the absorption line is wide compared to the source line half-width, the S will approach unity (15) and $\Delta\nu_D$ is the half-width of the emission line, $\Delta\nu_L$, and so A_T is given approximately by

$$A_T = \frac{\pi\,k^{\circ}L\,\Delta\nu_L}{2\sqrt{\ln 2}} \quad . \qquad (II.16)$$

APPENDIX III

NOISE TERMS WHICH DO NOT GENERALLY CONTRIBUTE TO THE TOTAL NOISE IN ATOMIC FLUORESCENCE FLAME SPECTROMETRY

Johnson Noise, $\overline{\Delta i}_J$. The Johnson noise is a small thermal noise caused by heating of the load resistor across the phototube and is given (18) by

$$\overline{\Delta i}_J = \left[\frac{4\ k\ T_L\ \Delta f}{R_L}\right]^{1/2} \qquad \text{(III.1)}$$

where k is the Boltzmannconstant, T_L is the temperature of the load resistor, R_L. This term adds quadratically with the shot noise term (refer to equation 3.9).

Atomic Emission Noise, $\overline{\Delta i}$. The atomic emission noise is caused by the fluctuation in the thermal emission of atoms in the flame. This noise has the same form as the flame background flicker noise, that is,

$$\overline{\Delta i} = k_2\, \psi\ I\ W \sqrt{\Delta f} \quad , \qquad \text{(III.2)}$$

where ψ is the atomic emission flicker factor in sec.$^{+1/2}$, which should be identical to ξ for atoms in a flame in thermal equilibrium, and I is the intensity of thermal emission in watts/cm.^{2} ster. If the atomic line of a given element happens to be on a molecular band of the same element, the noise due to flicker in the band emission will be given by expression III.2 multiplied by the spectral band width, s (of course I will then be the band intensity with units of watts/cm.^{2} ster. mμ). This noise, however, will generally be negligible even at atomic concentrations considerably greater than the limiting detectable atomic concentrations.

Atomic Fluorescence Noise, $\overline{\Delta i}_F$. This noise has the same form as the atomic emission noise (refer to equation III.2), namely,

$$\overline{\Delta i}_F = k_2 \Gamma_F I_F W \sqrt{\Delta f} \quad , \qquad \text{(III.3)}$$

where Γ_F is the atomic fluorescence flicker factor, that is, the ratio of the r.m.s. noise fluctuation in the atomic fluorescence intensity to the intensity of atomic fluorescence, in sec.$^{1/2}$.

Rayleigh Scattering of Incident Light from Salt Particles Noise, $\overline{\Delta i}_S$. This term is also similar to the atomic emission noise factor and therefore is given by

$$\overline{\Delta i}_S = k_2 \Gamma_S I_S W \sqrt{\Delta f} \quad , \qquad \text{(III.4)}$$

where Γ_S is the scattering flicker factor, that is, the ratio of the r.m.s. noise fluctuation in the incident intensity scattered by salt particles to the incident intensity scattered by salt particles, sec.$^{1/2}$, and I_S is the intensity of scattered radiation which depends upon the type of source used and is given by

$$I_S)_{cont.} = k_3 I^{\circ} R_d W , \qquad \text{(III.5)}$$

and

$$I_S)_{line} = k_3 I_L , \qquad \text{(III.6)}$$

for continuous and narrow line sources, respectively.

A MORE ACCURATE EXPRESSION FOR i_T

In equation 3.9 for the shot noise current, $\overline{\Delta i_p}$, and in equation 3.21 for the electrometer noise current, $\overline{\Delta i_e}$, the total current, i_T, in amperes at the photoanode appears. It was assumed in the body of the paper, that the photoanodic current, i, due to the intensity of emission from the atoms in concern, the photoanodic current, i_s, due to the intensity of Rayleigh scattering by salt particles, and the photoanodic current, i_F, due to the intensity of atomic fluorescence were all negligible. These assumptions are generally valid (see text of Chapter III), but for completeness a more accurate expression for i_T will be given, namely

$$i_T = i_d + i_c + i_R + i + i_S + i_F , \qquad \text{(III.7)}$$

where

$$i = k_2 I W , \qquad \text{(III.8)}$$

and

$$i_S = k_2 I_S W , \qquad \text{(III.9)}$$

and i_F is given by equation 3.2. Of course, I_S, depends on the type of source used (see equations III.5 and III.6).

APPENDIX IV

SPECTRAL CONSTANTS

The spectral constants needed for the calculations performed in this dissertation were all taken in modified form from N.B.S. tables. The modifications were made so that the proper form of the spectral parameters for calculation would result. The g_u and E_u values were calculated from Moore's "Atomic Energy Levels" (16). The g values are simply given by 2J + 1, where J is the multiplicity of the energy level of concern, and E_u is found by conversion of the energy level from cm.$^{-1}$ to eV. The g_l values were either the ground energy g value or were obtained from a weighted average (4:1) of the ground energy level and values taken from a dissertation by Boumans (2). The A_t values were taken from Corliss and Bozman (4), whose g_uA_t values were simply divided by g_u. The A_t values have units of sec.$^{-1}$, the wavelengths are expressed in Å, E_u in eV., and the g values are unitless. The symbols of the elements are in capital letters due to the restrictions of the computer output. The spectral parameters are tabulated in Table IV.1.

TABLE IV.1

VALUES OF ATOMIC SPECTRAL CONSTANTS

FOR SOME ANALYTICALLY IMPORTANT LINES OF SIXTY ELEMENTS

ELEMENT	LINE	G(1)	G(2)	A(T)	E(U)
AG	3281	4.0	2.0	0.82	3.78
AG	3383	2.0	2.0	0.56	3.66
AG	5209	4.0	2.0	3.75	6.04
AL	3093	6.0	2.8	0.91	4.02
AL	3962	2.0	2.8	0.65	3.14
AS	1937	4.0	4.2	0.88	6.40
AS	2349	2.0	4.2	3.00	6.58
AU	2428	2.0	2.0	0.90	5.10
AU	2676	2.0	2.0	0.55	4.63
AU	3123	4.0	2.0	0.48	5.10
B	2497	2.0	2.0	3.50	4.96
B	2498	2.0	2.0	7.00	4.96
BA	5535	3.0	1.0	0.67	2.24
BE	2349	3.0	1.0	0.97	5.28
BE	4573	5.0	1.0	1.10	7.99
BE	8254	1.0	1.0	1.80	6.77
BI	2231	6.0	4.0	0.12	5.55
BI	2898	2.0	4.0	6.00	5.69
BI	3068	2.0	4.0	3.50	4.03
C	2479	3.0	1.0	6.33	7.68
CA	4227	3.0	1.0	0.33	2.93
CA	6122	3.0	1.0	0.40	3.91
CD	2288	3.0	1.0	4.00	5.42
CD	3261	3.0	1.0	0.00	3.80
CD	3466	3.0	1.0	3.70	7.37
CO	2407	12.0	13.0	2.08	5.15
CO	3454	12.0	13.0	2.17	4.02
CR	3579	9.0	7.0	0.92	3.46
CR	3605	7.0	7.0	0.74	3.44
CR	4254	9.0	7.0	0.22	2.91
CS	4555	4.0	2.0	0.35	2.72
CS	6723	4.0	2.0	0.80	3.23
CS	8521	4.0	2.0	0.32	1.45
CU	3248	2.0	4.0	2.05	3.81
EU	4594	10.0	8.0	0.67	2.70
EU	4661	6.0	8.0	0.77	2.66
FE	2483	11.0	12.0	3.09	4.99
FE	2719	7.0	12.0	1.86	4.56
FE	3720	11.0	12.0	0.23	3.33

TABLE IV.1(CONTINUED)

ELEMENT	LINE	G(1)	G(2)	A(T)	E(U)
GA	2874	4.0	2.8	1.48	4.31
GA	4172	2.0	2.8	1.00	3.07
GD	3783	9.0	9.0	2.00	3.40
GD	4226	15.0	9.0	1.20	3.15
GE	2652	5.0	2.4	5.20	4.85
GE	3039	3.0	2.4	8.00	4.96
HF	2890	3.0	7.2	0.67	4.29
HF	2941	5.0	7.2	0.84	4.21
HG	2537	3.0	1.0	1.17	4.89
HG	4358	3.0	1.0	8.70	7.93
IN	3039	4.0	2.5	1.78	4.08
IN	4511	2.0	2.5	1.10	3.02
IR	2503	12.0	4.0	0.92	4.95
IR	3221	8.0	4.0	0.55	4.20
K	7665	4.0	2.0	0.40	1.61
K	7699	2.0	2.0	0.39	1.61
LA	3574	4.0	5.2	0.65	3.47
LI	6104	4.0	2.0	3.25	1.85
LI	6708	2.0	2.0	0.60	1.85
LU	4519	4.0	2.0	0.05	2.74
LU	3312	4.0	2.0	0.35	3.74
MG	2852	3.0	1.0	3.13	4.34
MG	3838	7.0	1.0	5.57	5.94
MN	2795	8.0	6.0	1.04	4.43
MN	4031	8.0	6.0	0.18	3.07
MO	3133	9.0	7.0	1.09	3.96
MO	3903	5.0	7.0	0.42	3.18
NA	5890	4.0	2.0	0.45	2.10
NA	5896	2.0	2.0	0.45	2.10
NA	8183	4.0	2.0	1.10	3.62
NA	8195	6.0	2.0	1.45	3.62
NB	4059	12.0	7.6	0.65	3.18
NB	4168	2.0	7.6	0.55	2.97
NI	2320	11.0	11.4	1.00	5.34
NI	3525	5.0	11.4	0.90	3.54
NI	3619	7.0	11.4	1.07	3.85
OS	2637	9.0	12.2	1.22	4.70
OS	3059	9.0	12.2	0.82	4.05
P	2536	4.0	4.0	9.25	7.21

TABLE IV.1 (CONTINUED)

ELEMENT	LINE	G(1)	G(2)	A(T)	E(U)
P	2553	2.0	4.0	1.50	7.17
PB	2170	3.0	1.2	0.23	5.71
PB	4058	3.0	1.2	3.06	4.37
PD	2448	3.0	1.0	0.28	5.06
PD	2476	3.0	1.0	0.37	5.00
PD	3405	9.0	1.0	1.33	4.45
PD	3635	5.0	1.0	1.24	4.22
PT	2659	9.0	8.0	0.91	4.66
PT	3065	5.0	8.0	0.52	4.04
RB	4202	4.0	2.0	0.24	2.95
RB	4216	2.0	2.0	0.24	2.94
RB	7800	4.0	2.0	0.75	1.59
RE	3460	8.0	6.0	0.85	3.58
RE	4889	8.0	6.0	0.00	2.53
RH	3435	12.0	13.6	0.34	3.61
RH	3692	8.0	13.6	0.35	3.36
RU	3499	13.0	15.8	0.32	3.54
RU	3728	11.0	15.8	0.42	3.32
SB	2176	4.0	4.0	0.62	5.70
SB	2311	2.0	4.0	0.75	5.36
SB	2529	2.0	4.0	8.00	6.12
SB	2598	4.0	4.0	6.00	5.83
SC	3907	6.0	5.2	2.00	3.17
SC	4020	4.0	5.2	2.50	3.08
SE	1960	3.0	5.6	3.33	6.32
SE	2075	5.0	5.6	0.11	5.97
SI	2516	5.0	2.6	2.60	4.95
SI	2524	1.0	2.6	8.40	4.92
SM	4297	15.0	17.0	1.40	3.38
SN	2840	5.0	2.0	4.20	4.79
SN	2863	3.0	2.0	1.77	4.33
SR	4607	3.0	1.0	0.28	2.69
TA	2647	4.0	7.8	2.05	4.68
TA	2661	6.0	7.8	4.17	5.35
TE	2143	3.0	5.3	1.93	5.78
TE	2386	3.0	5.3	2.73	5.78
TH	3719	7.0	3.0	0.16	3.33
TH	3803	5.0	3.0	0.19	3.26
TI	3654	11.0	8.2	0.56	3.41

TABLE IV.1 (CONTINUED)

ELEMENT	LINE	G(1)	G(2)	A(T)	E(U)
TI	3949	3.0	8.2	1.13	3.14
TL	2768	4.0	2.1	1.02	4.48
TL	3776	2.0	2.1	0.50	3.28
TL	5350	2.0	2.1	1.05	3.28
TM	4094	10.0	8.0	0.52	3.03
U	3871	13.0	5.0	0.42	3.20
V	3183	8.0	8.8	4.38	3.93
V	4385	10.0	8.8	0.58	3.11
W	4009	9.0	4.1	0.20	3.46
W	4295	5.0	4.1	0.11	3.25
Y	3621	4.0	5.2	1.55	3.49
Y	4077	6.0	5.2	0.72	3.04
Y	4102	4.0	5.2	1.28	3.09
YB	3464	3.0	1.0	0.24	3.58
YB	3988	3.0	1.0	0.53	3.11
ZN	2139	3.0	1.0	6.33	5.79
ZN	3345	7.0	1.0	4.00	7.78
ZN	4811	3.0	1.0	7.00	6.65
ZR	3520	7.0	8.2	0.71	3.52

APPENDIX V

PROCEDURES USED TO OBTAIN THE EXPERIMENTAL PARAMETERS NEEDED FOR ALL CALCULATIONS

All of the experimental parameters, as well as many apparatus parameters, have been either directly measured or calculated from experimentally measured parameters. The methods of measurement and the equations used for these calculations are discussed below, and the values of the parameters are tabulated in Table V.1. The spectral parameters are tabulated in Appendix IV.

All experimental parameters (used for calculating all of the theoretical values presented in the text) were measured on a Czerny-Turner grating monochromator with a 3000 Å blazed grating (No. 4-8400, American Instrument Co., Silver Spring, Md.) using an R.C.A. 1P28 multiplier-phototube and either a D.C. electrometer-power supply (No. 26-770, Jarrell-Ash Co., Waltham, Mass.) or a lock-in A.C. amplifier (No. JB-4, Princeton Applied Research Corp., Princeton, N.J.) for amplification of the signal produced by the photodetector. The sources of excitation used for atomic fluorescence flame spectrometry, when narrow line sources of excitation were required, were electrodeless discharge tubes (Ophthos Instrument Co., Rockville, Md.) which were placed in a 3/4 wave resonant cavity (Ophthos

TABLE V.1

DATA USED FOR CALCULATIONS IN TEXT

A. APPARATUS PARAMETERS

1. Parameters Independent of Wavelength.

Symbol	Value	
EM	2.86×10^6 ,	no units
i_d	3.3×10^{-10} ,	amps.
f	1.0	$sec.^{-1}$
R_d	33.0	mμ/cm.
T_f	0.5	no units
H	1.0	cm.
Ω_e	0.037	ster.
Ω_a	0.071	ster.

2. Parameters Dependent on Wavelength.

Element	Wavelength(Å)	I_L(watts/cm.^{2} ster.)
Zn	2139	2.9×10^{-3}
Cd	2288	1.9×10^{-1}
Hg	2537	4.5×10^{-3}
Cu	3248	4.2×10^{-3}
Tl	3776	1.4×10^{-3}
Na	5890	8.9×10^{-3}

TABLE V.1 (Continued)

B. PARAMETERS MEASURED EXPERIMENTALLY

1. Parameters Independent of Wavelength.

Symbol	Flame[a]	Value
Γ_R (sec.$^{\frac{1}{2}}$)	1	0.35
	2	0.38
	3	0.35
	4	0.35
	5	0.37
	6	0.43
	7	0.36
	8	0.25
ξ (sec.$^{\frac{1}{2}}$)	1	0.040
	2	0.021
	3	0.060
	4	0.060
	5	0.030
	6	0.070
	7	0.020
	8	0.059
L (cm.)	1	1.0
	2	1.0
	3	3.0
	4	3.0
	5	1.0
	6	3.0
	7	1.0
	8	3.0
T (^{o}K)	1	2336
	2	2405
	3	1195
	4	1479
	5	2205
	6	1003
	7	2750
	8	1900

TABLE V.1 (Continued)

2. Parameters Dependent on Wavelength.

Element Wavelength (Å)		An 2139	Cd 2288	Hg 2537	Cu 3248	Tl 3776	Na 5890
Symbol	Flame						
Φ_T (no units)	1	1.4×10^{-3}	1.0×10^{-2}	1.1×10^{-3}	7.0×10^{-4}	1.0×10^{-4}	6.5×10^{-3}
	2	3.1×10^{-3}	5.5×10^{-3}	1.5×10^{-3}	4.8×10^{-3}	5.6×10^{-6}	5.0×10^{-3}
	3	2.8×10^{-3}	1.8×10^{-2}	2.2×10^{-3}	1.2×10^{-3}	5.0×10^{-4}	1.3×10^{-2}
	4	6.3×10^{-3}	1.1×10^{-2}	3.0×10^{-3}	9.7×10^{-3}	1.1×10^{-3}	1.3×10^{-2}
	5	2.8×10^{-3}	5.0×10^{-3}	1.7×10^{-3}	3.0×10^{-3}	5.7×10^{-4}	1.3×10^{-2}
	6	5.5×10^{-3}	1.8×10^{-2}	3.4×10^{-3}	5.9×10^{-3}	9.7×10^{-4}	2.6×10^{-2}
	7	2.8×10^{-2}	5.0×10^{-2}	1.7×10^{-2}	3.0×10^{-2}	5.7×10^{-3}	1.3×10^{-1}
	8	5.5×10^{-2}	1.8×10^{-1}	3.4×10^{-2}	5.9×10^{-2}	9.7×10^{-3}	2.6×10^{-1}
$\Delta\nu_D$ (sec.$^{-1}$).	1	3.3×10^{9}	2.3×10^{9}	1.1×10^{9}	2.0×10^{9}	1.0×10^{9}	3.7×10^{9}
	2	6.1×10^{9}	4.3×10^{9}	2.9×10^{9}	4.1×10^{9}	2.0×10^{9}	3.7×10^{9}
	3	4.3×10^{9}	3.1×10^{9}	2.1×10^{9}	2.9×10^{9}	0.8×10^{9}	2.6×10^{9}
	4	4.8×10^{9}	3.4×10^{9}	2.3×10^{9}	3.2×10^{9}	1.5×10^{9}	2.9×10^{9}
	5	5.8×10^{9}	4.1×10^{9}	2.8×10^{9}	3.9×10^{9}	1.9×10^{9}	3.6×10^{9}
	6	3.9×10^{9}	2.8×10^{9}	1.9×10^{9}	2.6×10^{9}	1.7×10^{9}	2.4×10^{9}
	7	6.5×10^{9}	4.6×10^{9}	3.1×10^{9}	4.4×10^{9}	2.1×10^{9}	4.0×10^{9}
	8	5.4×10^{9}	3.9×10^{9}	2.6×10^{9}	3.6×10^{9}	1.7×10^{9}	3.3×10^{9}

TABLE V.1 (Continued)

[a] The conditions for the flames are as follows:

Flame 1. Oxyhydrogen (O_2 - 3 L/min.; H_2 - 5 1./min.) viewed at 3 cm. above the burner tip.
Flame 2. Oxyhydrogen (O_2 - 3 1./min.; H_2 - 7 1./min.) viewed at 3 cm. above the burner tip.
Flame 3. Flame 1 viewed at 6 cm. above the burner tip.
Flame 4. Flame 2 viewed at 6 cm. above the burner tip.
Flame 5. Air-hydrogen (air - 3 1./min.; H_2 - 6 1./min.) viewed at 3 cm. above the burner tip.
Flame 6. Flame 5 viewed at 6 cm. above the burner tip.
Flame 7. Argon-hydrogen-entrained air (argon - 3 1./min.; H_2 - 8 1./min.) viewed at 3 cm. above the burner tip.
Flame 8. Flame 7 viewed at 6 cm. above the burner tip.

Instrument Co.) and powered by a microwave power generator (No. PGM10X-1, Raytheon Co., Manchester, N.H.) with a reflected power meter (No. 725.3, Microwave Devices, Inc., Farmington, Conn.). A 150 watt xenon arc (No. 416-992, American Instrument Co.) was used for the atomic fluorescence flame spectrometric studies requiring a continuous source. In Figure V.1 the entrance optics assumed for each of the methods of analysis is given.

Phototube characteristics. The values of γ, the photoanodic sensitivity of the photodetector (amps. at the anode per watt of radiant power at the photocathode), can be determined by measuring the photodetector and current resulting when using a standard intensity source (measurements are made as a function of wavelength at the desired phototube voltage), and calculating γ from a modified form of equation 3.13,

$$\gamma = \frac{i_s}{T_f \; W \; H \; \Omega_e \; I_s} \tag{V.1}$$

where i_s is the photoanodic current due to the intensity of the standard source, I_s, and the other terms have been defined (see Appendix I). The results of these measurements and calculations are presented in Figure V.2 for a multiplier phototube at 900 volts. Since the phototube voltage is not a significant parameter, 900 volts were used for all measurements and calculations.

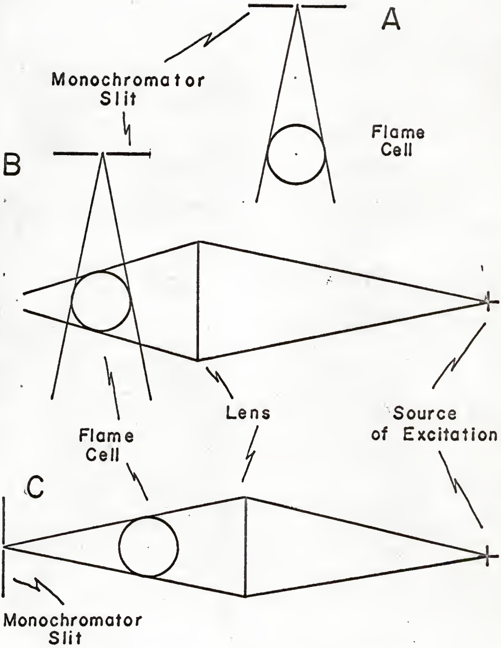

Fig. V.1.-Schematic diagrams of entrance optics assumed for atomic emission (A), atomic fluorescence (B), and atomic absorption (C) flame spectrometry.

Fig. V.2.-Measured γ versus wavelength curve at 900 volts on the phototube.

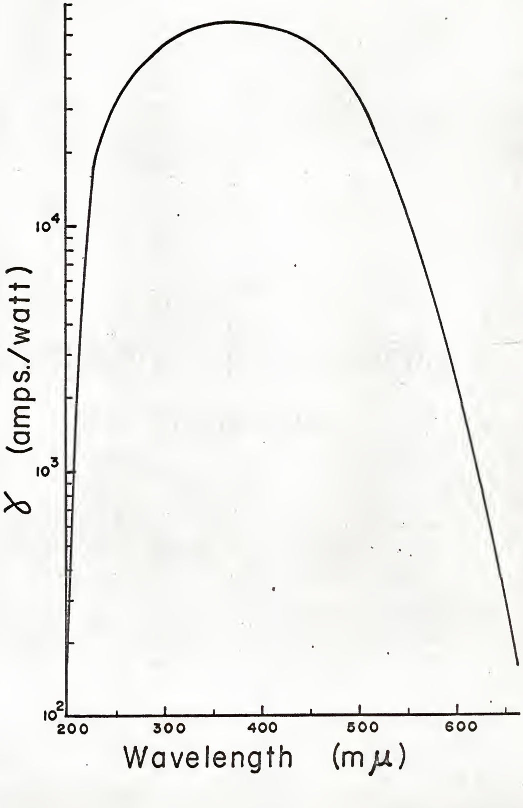
γ (amps./watt)
10⁴
10³
10²
200
300
400
500
600
Wavelength (mμ)

The dark current of the phototube can be measured directly and was found to be 3.3×10^{-10} amps. at 900 volts on the phototube.

The product of B, the characteristic phototube factor (see Appendix I), and M, the amplification factor of the phototube, can be calculated from equation 3.9

$$BM = \frac{\Delta i_p{}^2}{2e_c \; \Delta f \; i_d} \tag{V.2}$$

by measuring the root-mean-square (r.m.s.) photoanodic noise due to the dark current signal of the phototube. This noise is obtained by measuring the peak-to-peak noise and dividing by $2\sqrt{2}$ (29). The value of BM was calculated to be 2.86×10^6 (no units) for 900 volts on the phototube.

Monochromator. All of the monochromator parameters can be directly measured and the only parameter which might cause difficulty is Ω_e, the solid angle (ster.) collected by the monochromator. This is given by

$$\Omega_e = \frac{A_{eff.}}{F^2} \quad , \tag{V.3}$$

where F is the focal length of the collimating mirror (or lens), and $A_{eff.}$ is the limiting optical area of the monochromator (this is usually the effective (illuminated) area of the collimating mirror (or lens) or the grating (or prism)). In the monochromator used in this study, the grating determined the value of $A_{eff.}$, and Ω_e was found to be 3.7×10^{-2} ster. The value of Ω_a, the solid angle (ster.) incident on the flame cell from the source of excitation (see Figure V.1), is determined by the lens placed in front of the source of excitation and is calculated by an equation of the same form as V.3. The value of Ω_a for the lens used in this study was 7.1×10^{-2} ster.

Flame Parameters. The intensity of the flame background, I_c (watts/cm.^{2}ster.mμ) can be calculated by an equation of the same form as 3.12

$$I_c = \frac{i_c}{T_f W^2 H \, \Omega_e R_d} \qquad (V.3a)$$

by measuring the photoanodic current, i_c, as a function of wavelength for the various flame types which were studied. The results of the I_c calculations are presented in Figures V.3 and V.4.

The flicker factor for the flame background, ξ , was calculated by measuring the r.m.s. photoanodic noise current due to the flame background signal (the procedure for measuring the r.m.s. noise was discussed in this Appendix, page 144). The calculated phototube noise, $\overline{\Delta i}_p$, is then subtracted from the measured value (this is a quadratic subtraction). The value $\overline{\Delta i}_p$ is calculated from equation V.4, namely

$$\overline{\Delta i}_p = [\Delta f \; k_1(i_d + i_c)]^{1/2} \qquad (V.4)$$

Fig. V.3.-Measured flame background intensity versus wavelength curves for oxy-hydrogen and air-hydrogen flames as a function of flame gas composition and height above the burner tip.

Key to Figure: Curve numbers correspond to

flames in Table V.1.

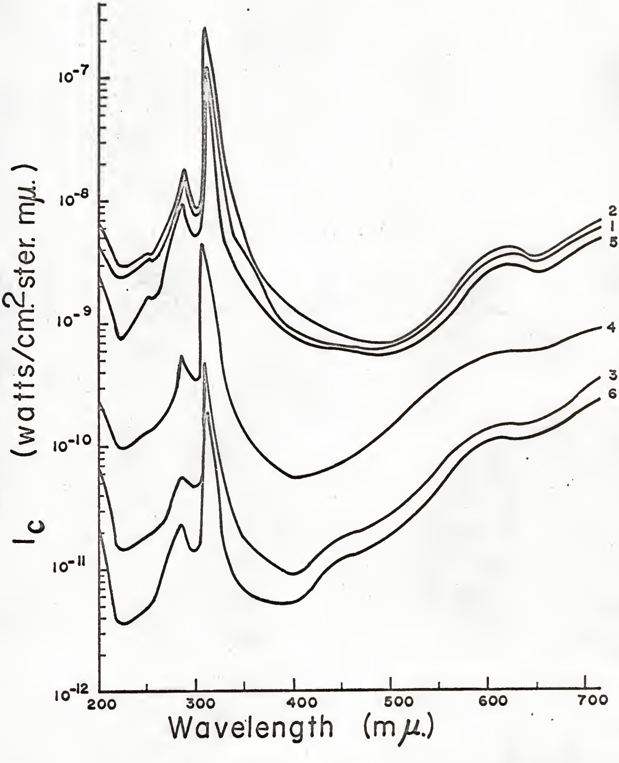
I_c (watts/cm.^{2}ster. mμ.)
10^{-7}
10^{-8}
10^{-9}
10^{-10}
10^{-11}
10^{-12}
200
300
400
500
600
700
Wavelength (mμ.)
2
1
5
4
3
6

Fig. V.4.-Measured flame background intensity versus wavelength curves for the argon-hydrogen-entrained air flame as a function of the height above the burner tip.

Key to Figure: Curve numbers correspond to flames in Table V.1.

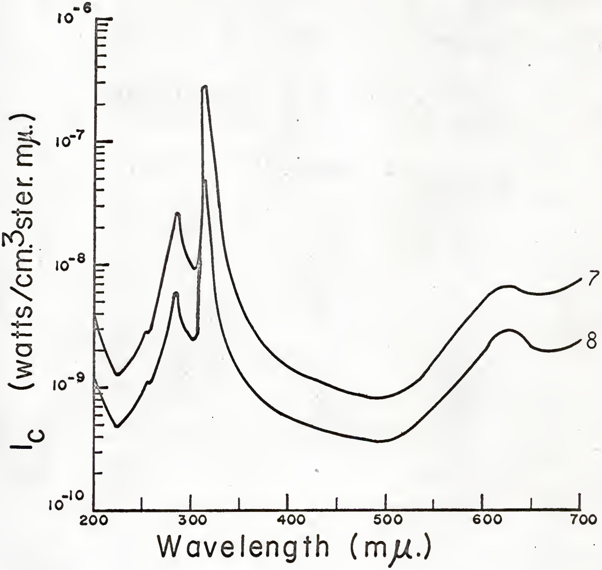
10^{-6}
10^{-7}
10^{-8}
10^{-9}
10^{-10}
I_c (watts/cm.^{3}ster. mμ.)
200
300
400
500
600
700
Wavelength (mμ.)
7
8

where i_d and i_c are measured values. The resulting r.m.s. noise due solely to flame flicker is divided by the photoanodic current due to the intensity of the flame background, i_c; the final equation is thus

$$\xi = \Delta i_c/i_c \quad . \qquad (V.5)$$

This value turns out to be constant with wavelength as woud be expected. See Table V.1 for the results for the flames used in this study.

The flame temperatures for the oxyhydrogen flames were calculated by means of the empirical equation developed by Winefordner and co-workers (24). (Also, see Appendix VII for a method of determining the aspiration efficiency, an important parameter in calculating the flame temperature by this method.)

The temperatures of the air-hydrogen and argon-hydrogen-entrained air flames were estimated by comparing the ratio of the logarithms of the photoanodic signal current due to the intensity of the flame background of Flame 2 (Table V.1) to the photoanodic signal current due to the intensity of the unknown flame with the ratio of the logarithms of the photoanodic signal currents due to the intensity of the flame background of Flame 2 (Table V.1) to that of Flame 1 (Table V.1). These ratios were then compared to the ratios of the various temperatures involved, and the unknown temperature was calculated, that is

$$\frac{\log R_{i_S}}{\log R_{i_U}} = \frac{R_{T_S}}{R_{T_U}} \quad , \qquad (V.6)$$

$$R_{T_U} = \frac{T_S}{T_U} \quad , \qquad (V.7)$$

and

$$T_U = \frac{T_S \log R_{i_S}}{R_{T_S} \log R_{i_U}} \quad , \qquad (V.8)$$

where R_i stands for the ratio of the currents; R_T, the ratio of the temperatures, and the subscripts denote standard values, S, or one standard and one unknown value, U. This method of estimation involves the assumption that the emissivity for all of the flames studied is constant with wavelength. It is felt that this assumption is valid because the combustion reactions are the same for all of these flames. A range of temperatures of about ± 50°K was obtained using this method.

Sources of Excitation. Again, the intensity of the sources of excitation can be calculated by an equation of the same form as equation V.1 for the narrow line sources and V.3 for the continuous source. The current due to the intensity of the source is measured and the appropriate equation is solved for the intensity at the appropriate wavelength. The data for the line sources are presented in Table V.1 and for the 150 watt xenon arc in Figure V.5.

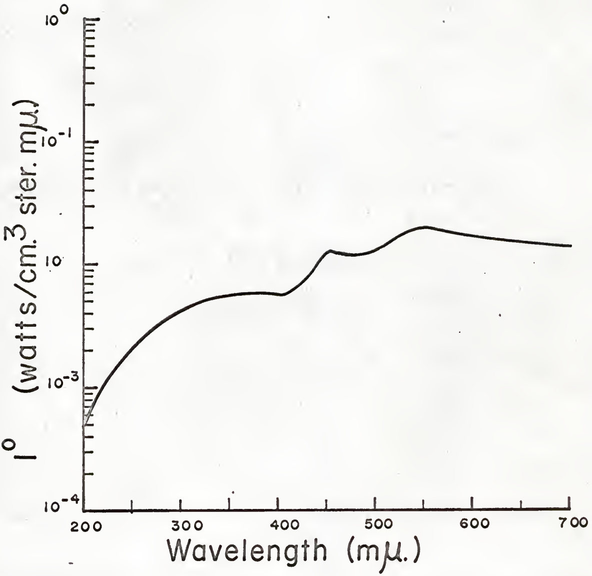

Fig. V.5.-Measured intensity versus wavelength curve for 150 watt xenon arc.

The fraction of light reflected from water droplets, ρ_R, can be calculated simply by taking the ratio of the current due to the intensity of the source of excitation to the current due to the reflected light. The latter term is obtained by subtracting the current due to the flame background and dark current from the total current which is obtained when the light from the source of excitation is striking the water droplets in the flame of concern. The results of ρ_R as a function of wavelength and flame type are presented in Figure V.6.

The calculation of Γ_R, the reflection of incident light plus Rayleigh scattering from water droplet flicker factor, is somewhat more difficult in that the final noise and signal which are used in calculating Γ_R must be obtained by taking the differences of relatively large numbers, that is, the signals and noises due to the flame background and phototube shot noise must be subtracted (the signals subtract linearily, and the noises subtract quadratically) from the measured values; therefore, the accuracy for this value is probably less than that of any other measured parameter. The measured values are $\overline{\Delta i_T}$ and i_T, which consist of

$$\overline{\Delta i_T} = (\overline{\Delta i_p}^2 + \overline{\Delta i_c}^2 + \overline{\Delta i_R}^2)^{1/2} \quad , \qquad (V.9)$$

Fig. V.6.-Measured fraction of incident radiation reflected and scattered by water droplets in the flame versus wavelength curves.

Key to Figure: Curve numbers correspond to flames listed in Table V.1.

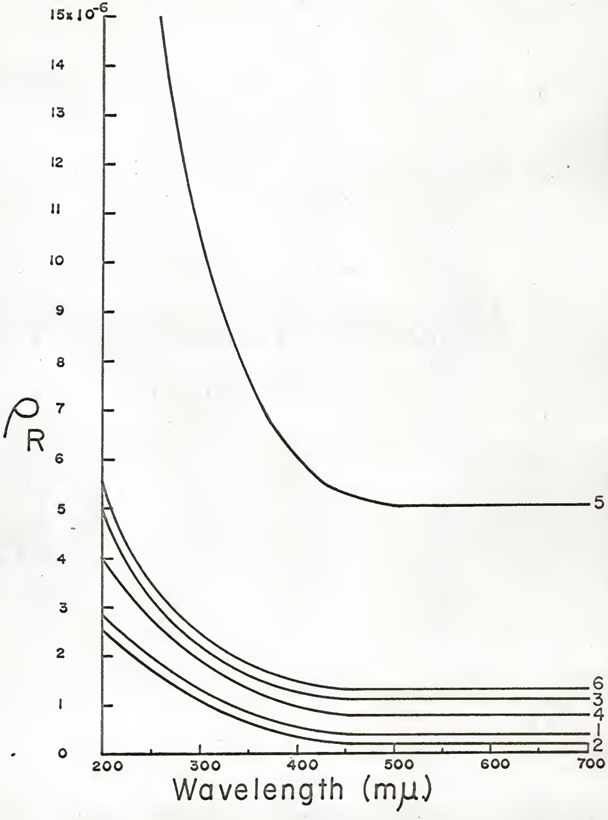
15x10⁻⁶
14
13
12
11
10
9
8
7
6
5
4
3
2
1
0
ρ_R
200
300
400
500
600
700
Wavelength (mμ)
5
6
3
4
1
2

and

$$i_T = i_d + i_c + i_R \quad . \qquad (V.10)$$

The square of the phototube shot noise is given by

$$\overline{\Delta i}_p^{\,2} = 2e_c BM\Delta f i_T \quad , \qquad (V.11)$$

and the flame background noise is calculated as previously discussed; thus, $\overline{\Delta i}_R$ is calculated by equation V.9. The measurement of i_R has already been discussed, and so

$$\Gamma_R = \overline{\Delta i}_R / i_R \quad . \qquad (V.12)$$

The results of Γ_R for the flame types considered are presented in Table V.1.

Calculated and Measured Spectral Parameters. The Doppler half-widths, $\Delta\nu_D$, were calculated by the well known equation (15),

$$\Delta\nu_D = 7.16 \times 10^{-7} \nu_o \sqrt{T/M_x} \qquad (V.13)$$

using the temperatures calculated and estimated as described above.

The power efficiencies, Φ_T, were measured according to Alkemade's method (1). This consisted of measuring the intensity of the species of interest due to atomic fluorescence and dividing by the difference in I_o and I_t when the same system was used for atomic absorption measurements. These data are tabulated in Table V.1 for the elements in each flame type used in this study.

Parameters Which Were Given Assumed Values. The only parameters which were not experimentally measured and were given assumed values were ξ , the ratio of the r.m.s. noise due to the amplifier-readout system referred to the amplifier input signal; a, the damping (broadening) factor; and I_A°, the intensity of the source of radiation in atomic absorption. The validity of the assumed values will now be discussed. A well-regulated amplifier-readout system should not, and generally does not, have more than about 0.1 per cent r.m.s. noise compared with the amplified signal; therefore, ξ was set equal to 0.001 for all calculations. The ξ term is only important for calculating the amplifier-readout r.m.s. noise which is ultimately of negligible significance compared to the total noise term of any flame spectrometric method. A few values of the a parameter have been measured by Hofmann and Kohn (9) and Alkemade (1) for atoms in analytical flames. Their values ranged from 0.2 - 2.0 in most cases; therefore, an a value of unity was used for calculating the upper limit of the range of near-linearity for atomic emission and atomic absorption flame spectrometry. For this purpose only the order of magnitude of a is important. The intensity of an average hollow cathode discharge tube (8.9×10^{-4} watts/cm.^{2} ster.) was assumed for the calculations of the r.m.s. noise terms in atomic absorption flame spectrometry (5). It should be noted that for the examples used in this manuscript the source noise completely dominates the total noise term in atomic absorption flame spectrometry (see the discussion in Part II of Chapter IV), and so I_A° does not appear in the final expression for $N_{min.}$.

APPENDIX VI

CALCULATED VALUES OF $N_{MIN.}$ AND $W_{OPT.}$ FOR ANALYTICALLY USEFUL LINES OF SIXTY ELEMENTS UNDER SIX FLAME CONDITIONS IN ATOMIC EMISSION AND ATOMIC ABSORPTION FLAME SPECTROMETRY

The values of $N_{min.}$ and $W_{opt.}$ for atomic emission flame spectrometry and $N_{min.}$ for atomic absorption flame spectrometry obtained for 136 spectral lines of 60 elements when viewed under six different flame conditions are tabulated in Table VI.1. The limiting detectable atomic concentration, $N_{min.}$, and the optimum monochromator slit width, $W_{opt.}$, for atomic emission flame spectrometry were calculated using equation 4.1 in conjunction with the graphical method described in Chapter III. The $N_{min.}$ values for atomic absorption were calculated using equation 4.15. Due to the computer print-out all values of the form 1.00×10^{10} are printed in the form 1.00E10, and all letters are capitalized.

The key to the flame conditions is as follows:

Flame 1. Oxyhydrogen (O_2 - 3, l./min.; H_2 - 5, l./min.) viewed at 3 cm. above the burner tip.

Flame 2. Oxyhydrogen (O_2 - 3, l./min.; H_2 - 7, l./min.) viewed at 3 cm. above the burner tip.

Flame 3. Air-hydrogen (air - 3, l./min.; H_2 - 6, l./min.) viewed at 3 cm. above the burner tip.

Flame 4. Flame 3 viewed at 6 cm. above the burner tip.

Flame 5. Argon-hydrogen-entrained air (argon - 3, l./min.; H_2 - 8, l./min.) viewed at 3 cm. above the burner tip.

Flame 6. Flame 5 viewed at 6 cm. above the burner tip.

TABLE VI.1

CALCULATED VALUES FOR THE MINIMUM ATOMIC CONCENTRATION AT THE OPTIMUM SLIT WIDTH FOR SOME ANALYTICALLY IMPORTANT LINES OF SIXTY ELEMENTS UNDER SEVERAL FLAME TYPES AND CONDITIONS FOR ATOMIC EMISSION AND ATOMIC ABSORPTION FLAME SPECTROMETRY

			ATOMIC EMISSION		ATOMIC ABSORPTION
ELEMENT	LINE	TYPE	W(OPT) MM.	N(MIN) ATOMS/CC.	N(MIN) ATOMS/CC.
AG	3281	1	0.01	1.68E 09	9.23E 09
		2	0.01	1.61E 09	9.37E 09
		3	0.02	2.52E 09	8.97E 09
		4	0.20	1.24E 18	2.02E 09
		5	0.01	1.05E 08	1.00E 10
		6	0.01	2.85E 10	2.78E 09
AG	3383	1	0.01	1.62E 09	2.47E 10
		2	0.01	1.25E 09	2.50E 10
		3	0.02	3.01E 09	2.40E 10
		4	0.25	6.18E 17	5.39E 09
		5	0.02	1.09E 08	2.68E 10
		6	0.02	2.37E 10	7.41E 09
AG	5209	1	0.06	1.29E 13	5.04E 08
		2	0.09	4.80E 12	5.12E 08
		3	0.08	6.50E 13	4.90E 08
		4	0.01	2.96E 27	1.10E 08
		5	0.08	1.29E 11	5.47E 08
		6	0.07	3.34E 15	1.52E 08
AL	3093	1	0.01	2.31E 10	1.85E 10
		2	0.01	8.45E 09	1.88E 10
		3	0.01	3.85E 10	1.80E 10
		4	0.25	1.17E 19	4.05E 09
		5	0.01	2.08E 09	2.01E 10
		6	0.01	1.35E 12	5.57E 09
AL	3962	1	0.04	5.87E 07	3.70E 10
		2	0.04	3.85E 07	3.76E 10
		3	0.04	1.33E 08	3.60E 10
		4	0.35	1.67E 15	8.09E 09
		5	0.04	5.90E 06	4.02E 10
		6	0.03	6.51E 08	1.11E 10

TABLE VII (CONTINUED)

			ATOMIC EMISSION		ATOMIC ABSORPTION
ELEMENT	LINE	TYPE	W(OPT) MM.	N(MIN) ATOMS/CC.	N(MIN) ATOMS/CC.
AS	1937	1	0.35	9.07E 15	1.05E 11
		2	0.40	3.75E 15	1.07E 11
		3	0.50	4.45E 16	1.02E 11
		4	0.01	2.96E 27	2.30E 10
		5	0.55	5.75E 13	1.14E 11
		6	0.45	3.19E 18	3.17E 10
AS	2349	1	0.03	1.89E 14	8.00E 09
		2	0.04	6.57E 13	8.11E 09
		3	0.06	6.95E 14	7.77E 09
		4	0.01	2.96E 27	1.75E 09
		5	0.07	7.47E 11	8.68E 09
		6	0.06	5.79E 16	2.40E 09
AU	2428	1	0.03	8.87E 11	3.07E 10
		2	0.04	3.69E 11	3.12E 10
		3	0.05	2.15E 12	2.98E 10
		4	0.60	4.55E 24	6.71E 09
		5	0.06	1.17E 10	3.33E 10
		6	0.05	5.04E 13	9.24E 09
AU	2676	1	0.02	1.69E 11	3.75E 10
		2	0.03	7.66E 10	3.81E 10
		3	0.03	4.50E 11	3.65E 10
		4	0.30	5.12E 22	8.20E 09
		5	0.03	4.73E 09	4.07E 10
		6	0.03	6.67E 12	1.13E 10
AU	3123	1	0.01	1.50E 13	1.35E 10
		2	0.01	6.55E 12	1.37E 10
		3	0.01	9.30E 12	1.31E 10
		4	0.06	2.65E 25	2.96E 09
		5	0.01	2.86E 11	1.47E 10
		6	0.01	5.35E 14	4.07E 09

TABLE VI.1 (CONTINUED)

			ATOMIC EMISSION		ATOMIC ABSORPTION
ELEMENT	LINE	TYPE	W(OPT) MM.	N(MIN) ATOMS/CC.	N(MIN) ATOMS/CC.
B	2497	1	0.03	1.21E 11	3.10E 10
		2	0.04	4.99E 10	3.15E 10
		3	0.05	3.10E 11	3.01E 10
		4	0.55	2.58E 23	6.77E 09
		5	0.05	1.94E 09	3.36E 10
		6	0.04	6.32E 12	9.32E 09
B	2498	1	0.03	6.06E 10	1.55E 10
		2	0.04	2.50E 10	1.57E 10
		3	0.05	1.55E 11	1.50E 10
		4	0.55	1.29E 23	3.38E 09
		5	0.05	9.73E 08	1.68E 10
		6	0.04	3.16E 12	4.65E 09
BA	5535	1	0.02	2.41E 06	1.39E 09
		2	0.03	1.49E 06	1.41E 09
		3	0.03	3.59E 06	1.35E 09
		4	0.30	1.25E 11	3.04E 08
		5	0.09	1.13E 05	1.51E 09
		6	0.08	2.37E 06	4.18E 08
BE	2349	1	0.03	6.29E 11	4.91E 10
		2	0.04	2.64E 11	4.98E 10
		3	0.06	1.58E 12	4.77E 10
		4	0.65	1.16E 25	1.07E 10
		5	0.07	6.31E 09	5.32E 10
		6	0.06	4.39E 13	1.47E 10
BE	4573	1	0.04	1.56E 17	3.52E 09
		2	0.06	4.36E 16	3.57E 09
		3	0.06	1.37E 18	3.42E 09
		4	0.01	2.96E 27	7.68E 08
		5	0.05	3.87E 14	3.82E 09
		6	0.05	3.97E 20	1.06E 09

TABLE VI.1(CONTINUED)

			ATOMIC EMISSION		ATOMIC ABSORPTION
ELEMENT	LINE	TYPE	W(OPT) MM.	N(MIN) ATOMS/CC.	N(MIN) ATOMS/CC.
BE	8254	1	0.30	1.46E 17	1.83E 09
		2	0.35	4.89E 16	1.85E 09
		3	0.40	8.01E 17	1.78E 09
		4	0.01	2.96E 27	3.99E 08
		5	0.40	8.03E 14	1.98E 09
		6	0.30	9.37E 19	5.50E 08
BI	2231	1	0.04	4.32E 13	1.92E 11
		2	0.06	1.73E 13	1.95E 11
		3	0.09	1.03E 14	1.87E 11
		4	0.01	2.96E 27	4.20E 10
		5	0.09	3.76E 11	2.09E 11
		6	0.08	3.93E 15	5.78E 10
BI	2898	1	0.01	4.71E 12	1.97E 09
		2	0.01	1.74E 12	2.00E 09
		3	0.01	1.79E 13	1.92E 09
		4	0.10	1.59E 27	4.31E 08
		5	0.01	5.65E 10	2.14E 09
		6	0.02	5.47E 14	5.93E 08
BI	3068	1	0.01	1.73E 10	7.60E 09
		2	0.01	8.87E 09	7.71E 09
		3	0.01	2.92E 10	7.39E 09
		4	0.08	4.61E 19	1.66E 09
		5	0.01	7.47E 08	8.25E 09
		6	0.01	3.44E 11	2.29E 09
C	2479	1	0.03	1.59E 16	5.54E 09
		2	0.04	4.64E 15	5.62E 09
		3	0.05	8.76E 16	5.38E 09
		4	0.01	2.96E 27	1.21E 09
		5	0.05	3.23E 13	6.01E 09
		6	0.05	1.81E 19	1.67E 09

TABLE VI.1 (CONTINUED)

			ATOMIC EMISSION		ATOMIC ABSORPTION
ELEMENT	LINE	TYPE	W(OPT) MM.	N(MIN) ATOMS/CC.	N(MIN) ATOMS/CC.
CA	4227	1	0.04	8.29E 06	1.17E 10
		2	0.06	4.83E 06	1.19E 10
		3	0.04	2.37E 07	1.14E 10
		4	0.30	8.65E 13	2.56E 09
		5	0.05	1.09E 06	1.27E 10
		6	0.04	8.17E 07	3.53E 09
CA	6122	1	0.04	7.28E 09	3.19E 09
		2	0.06	3.71E 09	3.23E 09
		3	0.07	1.54E 10	3.10E 09
		4	0.20	7.65E 19	6.96E 08
		5	0.05	4.31E 08	3.46E 09
		6	0.04	2.06E 11	9.58E 08
CD	2288	1	0.04	3.13E 11	3.64E 09
		2	0.04	1.56E 11	3.70E 09
		3	0.08	7.69E 11	3.54E 09
		4	0.75	1.55E 25	7.96E 08
		5	0.08	3.13E 09	3.95E 09
		6	0.07	2.45E 13	1.10E 09
CD	3261	1	0.01	4.18E 11	1.68E 12
		2	0.01	3.61E 11	1.70E 12
		3	0.02	5.77E 11	1.63E 12
		4	0.15	3.47E 20	3.67E 11
		5	0.01	3.89E 10	1.82E 12
		6	0.01	6.48E 12	5.05E 11
CD	3466	1	0.02	1.97E 15	3.06E 08
		2	0.02	6.75E 14	3.11E 08
		3	0.02	1.10E 16	2.97E 08
		4	0.01	2.96E 27	6.69E 07
		5	0.02	6.67E 12	3.32E 08
		6	0.02	1.86E 18	9.20E 07

TABLE VI.1 (CONTINUED)

			ATOMIC EMISSION		ATOMIC ABSORPTION
ELEMENT	LINE	TYPE	W(OPT) MM.	N(MIN) ATOMS/CC.	N(MIN) ATOMS/CC.
CO	2407	1	0.03	5.45E 11	2.70E 10
		2	0.04	2.26E 11	2.74E 10
		3	0.06	1.35E 12	2.63E 10
		4	0.65	3.92E 24	5.90E 09
		5	0.06	6.71E 09	2.93E 10
		6	0.06	3.03E 13	8.12E 09
CO	3454	1	0.02	2.39E 09	8.77E 09
		2	0.02	1.32E 09	8.89E 09
		3	0.02	4.98E 09	8.52E 09
		4	0.30	1.02E 19	1.91E 09
		5	0.02	9.91E 07	9.51E 09
		6	0.02	4.96E 10	2.64E 09
CR	3579	1	0.02	2.04E 08	1.42E 10
		2	0.02	1.21E 08	1.44E 10
		3	0.03	3.83E 08	1.38E 10
		4	0.30	2.35E 16	3.10E 09
		5	0.03	1.28E 07	1.54E 10
		6	0.03	2.30E 09	4.27E 09
CR	3605	1	0.02	3.44E 08	2.22E 10
		2	0.02	1.98E 08	2.25E 10
		3	0.03	4.27E 08	2.16E 10
		4	0.30	3.24E 16	4.85E 09
		5	0.03	1.79E 07	2.41E 10
		6	0.03	3.07E 09	6.68E 09
CR	4254	1	0.04	2.87E 07	3.54E 10
		2	0.05	1.88E 07	3.59E 10
		3	0.05	6.15E 07	3.44E 10
		4	0.30	2.42E 14	7.73E 09
		5	0.05	3.54E 06	3.84E 10
		6	0.04	2.55E 08	1.06E 10

TABLEVI.1 (CONTINUED)

			ATOMIC EMISSION		ATOMIC ABSORPTION
ELEMENT	LINE	TYPE	W(OPT) MM.	N(MIN) ATOMS/CC.	N(MIN) ATOMS/CC.
CS	4555	1	0.05	4.74E 06	7.28E 09
		2	0.05	3.28E 06	7.39E 09
		3	0.06	9.60E 06	7.08E 09
		4	0.25	1.53E 13	1.59E 09
		5	0.05	6.95E 05	7.90E 09
		6	0.05	3.25E 07	2.19E 09
CS	6723	1	0.30	1.45E 10	9.91E 08
		2	0.40	8.15E 09	1.01E 09
		3	0.40	3.08E 10	9.63E 08
		4	4.00	6.16E 17	2.16E 08
		5	1.00	4.20E 08	1.08E 09
		6	1.00	5.03E 10	2.98E 08
CS	8521	1	0.30	1.33E 07	1.22E 09
		2	0.35	1.01E 07	1.23E 09
		3	0.40	1.62E 07	1.18E 09
		4	3.50	5.04E 09	2.66E 08
		5	1.00	1.32E 06	1.32E 09
		6	0.90	7.19E 06	3.66E 08
CU	3248	1	0.01	3.49E 09	1.98E 10
		2	0.01	3.10E 09	2.01E 10
		3	0.02	5.11E 09	1.93E 10
		4	0.15	3.46E 18	4.33E 09
		5	0.01	4.70E 08	2.15E 10
		6	0.01	7.46E 10	5.96E 09
EU	4594	1	0.05	3.67E 06	5.55E 09
		2	0.06	2.39E 06	5.63E 09
		3	0.06	7.40E 06	5.39E 09
		4	0.25	1.09E 13	1.21E 09
		5	0.05	5.21E 05	6.02E 09
		6	0.05	2.46E 07	1.67E 09

TABLEVI.1 (CONTINUED)

			ATOMIC EMISSION		ATOMIC ABSORPTION
ELEMENT	LINE	TYPE	W(OPT) MM.	N(MIN) ATOMS/CC.	N(MIN) ATOMS/CC.
EU	4661	1	0.05	4.59E 06	7.70E 09
		2	0.06	3.01E 06	7.82E 09
		3	0.06	9.15E 06	7.49E 09
		4	0.25	1.05E 13	1.68E 09
		5	0.06	6.72E 05	8.36E 09
		6	0.05	2.94E 07	2.32E 09
FE	2483	1	0.03	1.69E 11	1.71E 10
		2	0.04	7.21E 10	1.74E 10
		3	0.05	4.46E 11	1.67E 10
		4	0.55	4.48E 23	3.74E 09
		5	0.06	1.93E 09	1.86E 10
		6	0.04	9.33E 12	5.15E 09
FE	2719	1	0.02	6.66E 10	3.41E 10
		2	0.02	3.13E 10	3.46E 10
		3	0.03	1.88E 11	3.31E 10
		4	0.30	1.25E 22	7.44E 09
		5	0.02	2.28E 09	3.70E 10
		6	0.02	2.89E 12	1.02E 10
FE	3720	1	0.03	4.50E 08	6.85E 10
		2	0.03	3.06E 08	6.95E 10
		3	0.03	9.48E 08	6.65E 10
		4	0.30	3.07E 16	1.50E 10
		5	0.03	3.52E 07	7.43E 10
		6	0.03	4.95E 09	2.06E 10
GA	2874	1	0.01	1.93E 10	1.33E 10
		2	0.01	8.83E 09	1.34E 10
		3	0.01	5.00E 10	1.29E 10
		4	0.20	4.30E 20	2.89E 09
		5	0.01	8.09E 08	1.44E 10
		6	0.01	5.76E 11	3.98E 09

TABLE VII (CONTINUED)

			ATOMIC EMISSION		ATOMIC ABSORPTION
ELEMENT	LINE	TYPE	W(OPT) MM.	N(MIN) ATOMS/CC.	N(MIN) ATOMS/CC.
GA	4172	1	0.01	1.06E 08	1.28E 10
		2	0.02	6.32E 07	1.30E 10
		3	0.02	2.18E 08	1.25E 10
		4	0.30	5.58E 14	2.80E 09
		5	0.04	2.82E 06	1.39E 10
		6	0.04	2.63E 08	3.86E 09
GD	3783	1	0.01	2.83E 08	4.09E 09
		2	0.01	1.73E 08	4.15E 09
		3	0.01	5.93E 08	3.97E 09
		4	0.30	7.40E 15	8.93E 08
		5	0.03	4.70E 06	4.44E 09
		6	0.03	8.14E 08	1.23E 09
GD	4226	1	0.04	1.33E 07	2.93E 09
		2	0.05	8.41E 06	2.98E 09
		3	0.05	3.05E 07	2.85E 09
		4	0.30	5.46E 14	6.41E 08
		5	0.05	1.37E 06	3.18E 09
		6	0.04	1.55E 08	8.82E 08
GE	2652	1	0.02	2.54E 10	3.23E 09
		2	0.03	1.11E 10	3.27E 09
		3	0.03	6.68E 10	3.13E 09
		4	0.35	3.17E 22	7.05E 08
		5	0.04	4.15E 08	3.50E 09
		6	0.03	1.14E 12	9.70E 08
GE	3039	1	0.01	7.02E 10	2.32E 09
		2	0.02	2.88E 10	2.36E 09
		3	0.02	2.02E 11	2.26E 09
		4	0.25	1.37E 23	5.07E 08
		5	0.02	1.44E 09	2.52E 09
		6	0.02	3.75E 12	6.98E 08

TABLEVI.1 (CONTINUED)

			ATOMIC EMISSION		ATOMIC ABSORPTION
ELEMENT	LINE	TYPE	W(OPT) MM.	N(MIN) ATOMS/CC.	N(MIN) ATOMS/CC.
HF	2890	1	0.01	1.31E 11	6.28E 10
		2	0.01	5.99E 10	6.37E 10
		3	0.02	3.14E 11	6.10E 10
		4	0.20	2.67E 21	1.37E 10
		5	0.02	4.39E 09	6.81E 10
		6	0.02	3.08E 12	1.89E 10
HF	2941	1	0.01	3.11E 10	2.80E 10
		2	0.02	1.39E 10	2.84E 10
		3	0.02	7.36E 10	2.72E 10
		4	0.25	4.14E 20	6.12E 09
		5	0.02	1.15E 09	3.04E 10
		6	0.02	7.59E 11	8.42E 09
HG	2537	1	0.03	8.82E 10	6.84E 09
		2	0.03	3.68E 10	6.94E 09
		3	0.04	2.17E 11	6.65E 09
		4	0.45	1.23E 23	1.49E 09
		5	0.04	1.55E 09	7.42E 09
		6	0.04	4.57E 12	2.06E 09
HG	4358	1	0.01	2.54E 16	5.50E 07
		2	0.02	8.18E 15	5.58E 07
		3	0.02	1.84E 17	5.35E 07
		4	0.01	2.96E 27	1.20E 07
		5	0.05	1.83E 13	5.97E 07
		6	0.04	1.81E 19	1.65E 07
IN	3039	1	0.01	3.11E 09	6.48E 09
		2	0.02	1.45E 09	6.58E 09
		3	0.02	6.91E 09	6.30E 09
		4	0.25	1.83E 19	1.42E 09
		5	0.02	1.24E 08	7.04E 09
		6	0.02	6.10E 10	1.95E 09

TABLE VI.1 (CONTINUED)

			ATOMIC EMISSION		ATOMIC ABSORPTION
ELEMENT	LINE	TYPE	W(OPT) MM.	N(MIN) ATOMS/CC.	N(MIN) ATOMS/CC.
IN	4511	1	0.01	7.10E 07	6.42E 09
		2	0.02	4.12E 07	6.51E 09
		3	0.02	1.42E 08	6.23E 09
		4	0.25	3.81E 14	1.40E 09
		5	0.05	1.91E 06	6.96E 09
		6	0.05	1.57E 08	1.93E 09
IR	2503	1	0.03	1.49E 11	9.26E 09
		2	0.04	6.15E 10	9.39E 09
		3	0.05	3.74E 11	8.99E 09
		4	0.55	2.92E 23	2.02E 09
		5	0.04	2.48E 09	1.00E 10
		6	0.04	7.56E 12	2.78E 09
IR	3221	1	0.01	4.21E 10	1.09E 10
		2	0.01	2.96E 10	1.11E 10
		3	0.01	5.37E 10	1.06E 10
		4	0.10	3.72E 20	2.38E 09
		5	0.01	2.80E 09	1.18E 10
		6	0.01	8.16E 11	3.28E 09
K	7665	1	0.65	4.67E 06	2.47E 09
		2	0.85	3.43E 06	2.50E 09
		3	0.90	5.98E 06	2.40E 09
		4	5.00	5.70E 09	5.39E 08
		5	0.85	1.31E 06	2.68E 09
		6	0.70	8.84E 06	7.41E 08
K	7699	1	0.65	9.63E 06	4.99E 09
		2	0.85	7.07E 06	5.06E 09
		3	0.90	1.23E 07	4.85E 09
		4	5.00	1.17E 10	1.09E 09
		5	0.85	2.69E 06	5.41E 09
		6	0.70	1.82E 07	1.50E 09

TABLE VI.1 (CONTINUED)

			ATOMIC EMISSION		ATOMIC ABSORPTION
ELEMENT	LINE	TYPE	W(OPT) MM.	N(MIN) ATOMS/CC.	N(MIN) ATOMS/CC.
LA	3574	1	0.02	4.96E 08	2.06E 10
		2	0.02	2.93E 08	2.09E 10
		3	0.03	9.23E 08	2.01E 10
		4	0.30	6.23E 16	4.51E 09
		5	0.03	3.22E 07	2.24E 10
		6	0.03	5.78E 09	6.21E 09
LI	6104	1	0.15	1.48E 05	1.43E 09
		2	0.20	1.02E 05	1.45E 09
		3	0.20	2.15E 05	1.39E 09
		4	2.00	6.68E 08	3.12E 08
		5	0.15	3.79E 04	1.55E 09
		6	0.15	3.42E 05	4.29E 08
LI	6708	1	1.50	1.78E 07	1.16E 10
		2	2.00	1.24E 07	1.18E 10
		3	1.50	2.88E 07	1.13E 10
		4	5.00	1.81E 11	2.54E 09
		5	1.50	4.74E 06	1.26E 10
		6	1.50	4.03E 07	3.50E 09
LU	4519	1	0.01	1.56E 08	4.55E 10
		2	0.02	9.40E 07	4.62E 10
		3	0.02	2.86E 08	4.42E 10
		4	0.25	1.32E 14	9.94E 09
		5	0.05	5.16E 06	4.94E 10
		6	0.05	2.51E 08	1.37E 10
LU	3312	1	0.01	2.67E 09	1.65E 10
		2	0.01	2.51E 09	1.68E 10
		3	0.02	4.37E 09	1.60E 10
		4	0.20	1.68E 18	3.61E 09
		5	0.01	1.64E 08	1.79E 10
		6	0.01	4.58E 10	4.96E 09

TABLE VI.1 (CONTINUED)

			ATOMIC EMISSION		ATOMIC ABSORPTION
ELEMENT	LINE	TYPE	W(OPT) MM.	N(MIN) ATOMS/CC.	N(MIN) ATOMS/CC.
MG	2852	1	0.01	5.08E 09	5.17E 09
		2	0.01	2.40E 09	5.25E 09
		3	0.02	1.31E 10	5.02E 09
		4	0.30	1.07E 20	1.13E 09
		5	0.01	2.14E 08	5.61E 09
		6	0.01	1.67E 11	1.55E 09
MG	3838	1	0.03	8.58E 11	5.11E 08
		2	0.03	4.19E 11	5.19E 08
		3	0.04	4.26E 12	4.97E 08
		4	0.30	2.22E 27	1.12E 08
		5	0.04	9.77E 09	5.54E 08
		6	0.03	1.97E 14	1.54E 08
MN	2795	1	0.01	3.81E 10	2.47E 10
		2	0.02	1.83E 10	2.51E 10
		3	0.02	1.11E 11	2.40E 10
		4	0.30	1.85E 21	5.41E 09
		5	0.02	1.52E 09	2.69E 10
		6	0.02	1.45E 12	7.44E 09
MN	4031	1	0.01	3.24E 08	4.77E 10
		2	0.01	2.15E 08	4.84E 10
		3	0.01	6.95E 08	4.63E 10
		4	0.35	1.46E 15	1.04E 10
		5	0.04	8.32E 06	5.17E 10
		6	0.03	8.35E 08	1.43E 10
MO	3133	1	0.01	3.57E 10	1.32E 10
		2	0.01	2.27E 10	1.34E 10
		3	0.01	1.31E 10	1.28E 10
		4	0.07	2.83E 19	2.87E 09
		5	0.01	1.98E 09	1.43E 10
		6	0.01	6.71E 11	3.96E 09

TABLE VI.1 (CONTINUED)

			ATOMIC EMISSION		ATOMIC ABSORPTION
ELEMENT	LINE	TYPE	W(OPT) MM.	N(MIN) ATOMS/CC.	N(MIN) ATOMS/CC.
MO	3903	1	0.01	4.49E 08	3.18E 10
		2	0.01	2.66E 08	3.23E 10
		3	0.01	9.66E 08	3.09E 10
		4	0.30	3.99E 15	6.94E 09
		5	0.04	1.13E 07	3.45E 10
		6	0.03	1.35E 09	9.56E 09
NA	5890	1	0.09	1.86E 06	6.30E 09
		2	0.10	1.22E 06	6.39E 09
		3	0.10	2.77E 06	6.12E 09
		4	1.00	4.48E 10	1.38E 09
		5	0.10	3.88E 05	6.83E 09
		6	0.10	5.59E 06	1.89E 09
NA	5896	1	0.09	3.72E 06	1.26E 10
		2	0.10	2.45E 06	1.27E 10
		3	0.10	5.54E 06	1.22E 10
		4	1.00	8.97E 10	2.74E 09
		5	0.10	7.77E 05	1.36E 10
		6	0.10	1.12E 07	3.78E 09
NA	8183	1	0.55	3.22E 10	9.61E 08
		2	0.65	1.81E 10	9.75E 08
		3	0.75	7.46E 10	9.34E 08
		4	5.00	1.90E 19	2.10E 08
		5	0.70	2.00E 09	1.04E 09
		6	0.55	6.07E 11	2.89E 08
NA	8195	1	0.55	1.63E 10	4.84E 08
		2	0.65	9.17E 09	4.91E 08
		3	0.75	3.78E 10	4.70E 08
		4	5.00	9.60E 18	1.06E 08
		5	0.70	1.01E 09	5.25E 08
		6	0.55	3.08E 11	1.45E 08

TABLEVI.1 (CONTINUED)

			ATOMIC EMISSION		ATOMIC ABSORPTION
ELEMENT	LINE	TYPE	W(OPT) MM.	N(MIN) ATOMS/CC.	N(MIN) ATOMS/CC.
NB	4059	1	0.04	3.08E 07	8.40E 09
		2	0.04	1.99E 07	8.52E 09
		3	0.04	7.12E 07	8.16E 09
		4	0.35	1.23E 15	1.83E 09
		5	0.04	3.12E 06	9.11E 09
		6	0.03	3.85E 08	2.52E 09
NB	4168	1	0.04	7.36E 07	5.50E 10
		2	0.05	5.05E 07	5.58E 10
		3	0.05	1.60E 08	5.34E 10
		4	0.30	8.59E 14	1.20E 10
		5	0.04	9.05E 06	5.97E 10
		6	0.04	6.98E 08	1.65E 10
NI	2320	1	0.03	3.21E 12	6.02E 10
		2	0.04	1.28E 12	6.10E 10
		3	0.07	6.48E 12	5.84E 10
		4	0.70	7.38E 25	1.31E 10
		5	0.07	2.69E 10	6.53E 10
		6	0.07	1.81E 14	1.81E 10
NI	3525	1	0.02	9.97E 08	4.19E 10
		2	0.02	5.75E 08	4.25E 10
		3	0.03	1.84E 09	4.07E 10
		4	0.30	1.89E 17	9.16E 09
		5	0.02	5.87E 07	4.55E 10
		6	0.03	1.11E 10	1.26E 10
NI	3619	1	0.02	2.41E 09	2.33E 10
		2	0.02	1.39E 09	2.36E 10
		3	0.03	5.07E 09	2.26E 10
		4	0.30	3.89E 18	5.08E 09
		5	0.03	1.12E 08	2.53E 10
		6	0.03	4.24E 10	7.00E 09

TABLE VI.1 (CONTINUED)

			ATOMIC EMISSION		ATOMIC ABSORPTION
ELEMENT	LINE	TYPE	W(OPT) MM.	N(MIN) ATOMS/CC.	N(MIN) ATOMS/CC.
OS	2637	1	0.02	1.40E 11	2.44E 10
		2	0.03	6.06E 10	2.48E 10
		3	0.04	3.35E 11	2.37E 10
		4	0.35	5.98E 22	5.33E 09
		5	0.03	3.33E 09	2.65E 10
		6	0.03	5.97E 12	7.34E 09
OS	3059	1	0.01	2.48E 10	2.33E 10
		2	0.01	1.92E 10	2.36E 10
		3	0.01	4.40E 10	2.26E 10
		4	0.09	1.70E 20	5.08E 09
		5	0.01	1.85E 09	2.52E 10
		6	0.01	4.83E 11	6.99E 09
P	2536	1	0.02	3.88E 15	6.62E 09
		2	0.03	1.12E 15	6.71E 09
		3	0.04	1.65E 16	6.43E 09
		4	0.01	2.96E 27	1.44E 09
		5	0.04	1.05E 13	7.18E 09
		6	0.04	2.33E 18	1.99E 09
P	2553	1	0.02	5.15E 15	1.04E 10
		2	0.03	1.52E 15	1.06E 10
		3	0.04	2.10E 16	1.01E 10
		4	0.01	2.96E 27	2.28E 09
		5	0.04	1.43E 13	1.13E 10
		6	0.04	3.13E 18	3.14E 09
PB	2170	1	0.08	5.52E 13	6.57E 10
		2	0.10	2.33E 13	6.66E 10
		3	0.15	1.65E 14	6.38E 10
		4	0.01	2.96E 27	1.43E 10
		5	0.15	4.91E 11	7.13E 10
		6	0.15	6.55E 15	1.97E 10

TABLE VI.1 (CONTINUED)

			ATOMIC EMISSION		ATOMIC ABSORPTION
ELEMENT	LINE	TYPE	W(OPT) MM.	N(MIN) ATOMS/CC.	N(MIN) ATOMS/CC.
PB	4058	1	0.04	1.53E 09	7.55E 08
		2	0.04	8.32E 08	7.66E 08
		3	0.04	5.01E 09	7.33E 08
		4	0.35	1.57E 20	1.65E 08
		5	0.04	6.34E 07	8.19E 08
		6	0.03	7.40E 10	2.27E 08
PD	2448	1	0.03	7.91E 11	4.37E 10
		2	0.04	3.35E 11	4.43E 10
		3	0.05	2.01E 12	4.25E 10
		4	0.60	3.04E 24	9.54E 09
		5	0.05	1.11E 10	4.74E 10
		6	0.05	4.55E 13	1.31E 10
PD	2476	1	0.03	4.49E 11	3.20E 10
		2	0.04	1.95E 11	3.24E 10
		3	0.05	1.17E 12	3.10E 10
		4	0.55	1.30E 24	6.98E 09
		5	0.05	6.95E 09	3.47E 10
		6	0.04	2.56E 13	9.61E 09
PD	3405	1	0.02	3.83E 09	1.14E 09
		2	0.02	2.37E 09	1.16E 09
		3	0.02	8.79E 09	1.11E 09
		4	0.25	2.60E 20	2.49E 08
		5	0.02	8.83E 07	1.24E 09
		6	0.02	1.01E 11	3.43E 08
PD	3635	1	0.02	1.61E 09	1.81E 09
		2	0.02	8.85E 08	1.83E 09
		3	0.03	3.79E 09	1.76E 09
		4	0.30	3.00E 19	3.95E 08
		5	0.03	5.66E 07	1.96E 09
		6	0.03	4.33E 10	5.44E 08

TABLE VI.1 (CONTINUED)

			ATOMIC EMISSION		ATOMIC ABSORPTION
ELEMENT	LINE	TYPE	W(OPT) MM.	N(MIN) ATOMS/CC.	N(MIN) ATOMS/CC.
PT	2659	1	0.02	1.06E 11	2.07E 10
		2	0.03	4.77E 10	2.10E 10
		3	0.03	2.91E 11	2.01E 10
		4	0.35	3.73E 22	4.51E 09
		5	0.03	2.56E 09	2.24E 10
		6	0.03	4.14E 12	6.21E 09
PT	3065	1	0.01	5.30E 10	4.25E 10
		2	0.01	3.68E 10	4.31E 10
		3	0.01	9.98E 10	4.13E 10
		4	0.07	3.50E 20	9.28E 09
		5	0.01	3.54E 09	4.61E 10
		6	0.01	1.10E 12	1.28E 10
RB	4202	1	0.04	2.04E 07	1.69E 10
		2	0.05	1.33E 07	1.71E 10
		3	0.05	4.42E 07	1.64E 10
		4	0.30	2.09E 14	3.68E 09
		5	0.04	2.55E 06	1.83E 10
		6	0.04	1.89E 08	5.07E 09
RB	4216	1	0.04	3.90E 07	3.34E 10
		2	0.05	2.54E 07	3.39E 10
		3	0.05	8.41E 07	3.25E 10
		4	0.30	3.73E 14	7.30E 09
		5	0.04	4.90E 06	3.62E 10
		6	0.04	3.57E 08	1.00E 10
RB	7800	1	0.65	2.30E 06	8.44E 08
		2	0.80	1.73E 06	8.56E 08
		3	0.90	2.92E 06	8.20E 08
		4	3.00	5.87E 09	1.84E 08
		5	0.85	6.52E 05	9.16E 08
		6	0.70	4.29E 06	2.54E 08

TABLE VI.1(CONTINUED)

			ATOMIC EMISSION		ATOMIC ABSORPTION
ELEMENT	LINE	TYPE	W(OPT) MM.	N(MIN) ATOMS/CC.	N(MIN) ATCMS/CC.
RE	3460	1	0.02	4.60E 08	8.67E 09
		2	0.02	2.68E 08	8.80E 09
		3	0.03	8.52E 08	8.42E 09
		4	0.30	1.11E 17	1.89E 09
		5	0.02	2.77E 07	9.41E 09
		6	0.02	6.20E 09	2.61E 09
RE	4889	1	0.06	3.03E 08	6.53E 11
		2	0.07	2.02E 08	6.63E 11
		3	0.07	5.80E 08	6.35E 11
		4	0.25	3.28E 14	1.43E 11
		5	0.07	4.60E 07	7.09E 11
		6	0.06	1.67E 09	1.96E 11
RH	3435	1	0.02	2.33E 09	4.50E 10
		2	0.02	1.65E 09	4.57E 10
		3	0.02	4.15E 09	4.38E 10
		4	0.25	6.24E 17	9.84E 09
		5	0.02	1.15E 08	4.89E 10
		6	0.02	3.11E 10	1.35E 10
RH	3692	1	0.02	5.80E 08	5.28E 10
		2	0.03	3.75E 08	5.36E 10
		3	0.03	1.22E 09	5.13E 10
		4	0.30	4.41E 16	1.15E 10
		5	0.03	4.25E 07	5.73E 10
		6	0.03	6.50E 09	1.59E 10
RU	3499	1	0.02	1.64E 09	4.90E 10
		2	0.02	8.72E 08	4.97E 10
		3	0.03	2.92E 09	4.76E 10
		4	0.30	2.83E 17	1.07E 10
		5	0.03	8.22E 07	5.31E 10
		6	0.02	1.88E 10	1.47E 10

TABLE VI.1 (CONTINUED)

			ATOMIC EMISSION		ATOMIC ABSORPTION
ELEMENT	LINE	TYPE	W(OPT) MM.	N(MIN) ATOMS/CC.	N(MIN) ATOMS/CC.
RU	3728	1	0.03	3.10E 08	3.65E 10
		2	0.03	1.98E 08	3.70E 10
		3	0.03	6.25E 08	3.54E 10
		4	0.30	1.98E 16	7.97E 09
		5	0.03	2.38E 07	3.96E 10
		6	0.03	3.37E 09	1.10E 10
SB	2176	1	0.07	5.56E 13	7.88E 10
		2	0.08	2.54E 13	8.00E 10
		3	0.10	1.94E 14	7.66E 10
		4	0.01	2.96E 27	1.72E 10
		5	0.15	4.52E 11	8.55E 10
		6	0.15	5.73E 15	2.37E 10
SB	2311	1	0.04	7.70E 12	1.09E 11
		2	0.05	3.22E 12	1.10E 11
		3	0.07	1.93E 13	1.06E 11
		4	0.75	2.51E 26	2.38E 10
		5	0.08	7.85E 10	1.18E 11
		6	0.07	5.49E 14	3.27E 10
SB	2529	1	0.03	9.92E 12	2.22E 09
		2	0.04	3.38E 12	2.26E 09
		3	0.04	3.52E 13	2.16E 09
		4	0.01	2.96E 27	4.86E 08
		5	0.04	6.95E 10	2.41E 09
		6	0.04	1.97E 15	6.68E 08
SB	2598	1	0.02	2.03E 12	1.79E 09
		2	0.03	7.70E 11	1.82E 09
		3	0.04	6.60E 12	1.74E 09
		4	0.40	1.51E 27	3.92E 08
		5	0.04	1.91E 10	1.95E 09
		6	0.03	3.23E 14	5.39E 08

TABLE VII (CONTINUED)

			ATOMIC EMISSION		ATOMIC ABSORPTION
ELEMENT	LINE	TYPE	W(OPT) MM.	N(MIN) ATOMS/CC.	N(MIN) ATOMS/CC.
SC	3907	1	0.03	1.41E 07	6.02E 09
		2	0.04	9.77E 06	6.11E 09
		3	0.04	3.04E 07	5.85E 09
		4	0.30	4.63E 14	1.31E 09
		5	0.04	1.41E 06	6.53E 09
		6	0.03	1.66E 08	1.81E 09
SC	4020	1	0.04	9.86E 06	6.63E 09
		2	0.04	6.73E 06	6.73E 09
		3	0.04	2.21E 07	6.44E 09
		4	0.35	2.03E 14	1.45E 09
		5	0.04	1.07E 06	7.19E 09
		6	0.03	1.10E 08	1.99E 09
SE	1960	1	1.00	8.80E 15	4.65E 10
		2	1.50	3.78E 15	4.72E 10
		3	2.00	4.00E 16	4.52E 10
		4	0.01	2.96E 27	1.02E 10
		5	2.00	5.72E 13	5.05E 10
		6	2.00	2.51E 18	1.40E 10
SE	2075	1	0.75	1.17E 16	7.12E 11
		2	0.80	5.28E 15	7.23E 11
		3	1.00	4.63E 16	6.92E 11
		4	0.01	2.96E 27	1.56E 11
		5	1.50	6.93E 13	7.73E 11
		6	1.00	2.14E 18	2.14E 11
SI	2516	1	0.03	8.36E 10	1.32E 10
		2	0.04	3.37E 10	1.34E 10
		3	0.04	2.11E 11	1.28E 10
		4	0.50	1.59E 23	2.87E 09
		5	0.04	1.41E 09	1.43E 10
		6	0.04	4.39E 12	3.96E 09

TABLEVII (CONTINUED)

			ATOMIC EMISSION		ATOMIC ABSORPTION
ELEMENT	LINE	TYPE	W(OPT) MM.	N(MIN) ATOMS/CC.	N(MIN) ATCMS/CC.
SI	2524	1	0.03	1.12E 11	2.02E 10
		2	0.04	4.52E 10	2.05E 10
		3	0.04	2.80E 11	1.96E 10
		4	0.50	1.75E 23	4.41E 09
		5	0.04	1.93E 09	2.19E 10
		6	0.04	5.67E 12	6.06E 09
SM	4297	1	0.04	6.92E 07	4.62E 09
		2	0.05	4.23E 07	4.69E 09
		3	0.05	1.70E 08	4.49E 09
		4	0.30	1.30E 16	1.01E 09
		5	0.05	5.99E 06	5.01E 09
		6	0.04	1.05E 09	1.39E 09
SN	2840	1	0.01	4.17E 10	2.12E 09
		2	0.01	1.78E 10	2.15E 09
		3	0.02	1.15E 11	2.06E 09
		4	0.25	1.77E 22	4.63E 08
		5	0.01	1.28E 09	2.30E 09
		6	0.01	2.28E 12	6.37E 08
SN	2863	1	0.01	1.68E 10	8.18E 09
		2	0.01	7.64E 09	8.30E 09
		3	0.02	4.05E 10	7.95E 09
		4	0.25	3.41E 20	1.79E 09
		5	0.01	7.29E 08	8.88E 09
		6	0.01	5.43E 11	2.46E 09
SR	4607	1	0.05	3.36E 06	7.22E 09
		2	0.06	2.18E 06	7.33E 09
		3	0.05	6.73E 06	7.02E 09
		4	0.25	9.27E 12	1.58E 09
		5	0.05	4.78E 05	7.84E 09
		6	0.05	2.23E 07	2.17E 09

TABLE VI.1 (CONTINUED)

			ATOMIC EMISSION		ATOMIC ABSORPTION
ELEMENT	LINE	TYPE	W(OPT) MM.	N(MIN) ATOMS/CC.	N(MIN) ATOMS/CC.
TA	2647	1	0.02	1.09E 11	2.12E 10
		2	0.03	4.91E 10	2.15E 10
		3	0.03	2.74E 11	2.06E 10
		4	0.35	4.31E 22	4.63E 09
		5	0.04	2.30E 09	2.30E 10
		6	0.02	6.42E 12	6.37E 09
TA	2661	1	0.02	9.89E 11	6.83E 09
		2	0.03	4.06E 11	6.93E 09
		3	0.03	3.03E 12	6.64E 09
		4	0.35	3.26E 25	1.49E 09
		5	0.04	1.27E 10	7.41E 09
		6	0.02	1.25E 14	2.05E 09
TE	2143	1	0.90	4.49E 14	4.57E 10
		2	1.00	1.90E 14	4.64E 10
		3	1.50	1.46E 15	4.44E 10
		4	0.01	2.96E 27	9.99E 09
		5	1.50	5.10E 12	4.96E 10
		6	1.50	6.25E 16	1.37E 10
TE	2386	1	0.03	1.53E 13	2.34E 10
		2	0.04	5.84E 12	2.38E 10
		3	0.06	4.51E 13	2.28E 10
		4	0.01	2.96E 27	5.12E 09
		5	0.07	1.15E 11	2.54E 10
		6	0.06	1.81E 15	7.04E 09
TH	3719	1	0.02	2.63E 08	1.90E 10
		2	0.03	1.73E 08	1.93E 10
		3	0.03	5.35E 08	1.84E 10
		4	0.30	1.73E 16	4.15E 09
		5	0.03	1.99E 07	2.06E 10
		6	0.03	2.59E 09	5.71E 09

TABLE VI.1 (CONTINUED)

			ATOMIC EMISSION		ATOMIC ABSORPTION
ELEMENT	LINE	TYPE	W(OPT) MM.	N(MIN) ATOMS/CC.	N(MIN) ATOMS/CC.
TH	3803	1	0.03	1.81E 08	2.09E 10
		2	0.03	1.26E 08	2.12E 10
		3	0.04	3.87E 08	2.03E 10
		4	0.30	9.22E 15	4.57E 09
		5	0.05	1.08E 07	2.27E 10
		6	0.03	2.02E 09	6.29E 09
TI	3654	1	0.02	2.13E 08	2.19E 10
		2	0.03	1.40E 08	2.22E 10
		3	0.03	4.45E 08	2.13E 10
		4	0.30	2.14E 16	4.78E 09
		5	0.03	1.49E 07	2.38E 10
		6	0.03	2.39E 09	6.58E 09
TI	3949	1	0.03	6.90E 07	3.15E 10
		2	0.04	4.45E 07	3.20E 10
		3	0.04	1.47E 08	3.06E 10
		4	0.35	1.86E 15	6.88E 09
		5	0.04	7.06E 06	3.42E 10
		6	0.03	7.23E 08	9.48E 09
TL	2768	1	0.01	3.32E 10	9.43E 09
		2	0.02	1.36E 10	9.57E 09
		3	0.02	9.12E 10	9.16E 09
		4	0.20	3.26E 21	2.06E 09
		5	0.02	1.20E 09	1.02E 10
		6	0.02	1.28E 12	2.83E 09
TL	3776	1	0.03	1.44E 08	1.52E 10
		2	0.03	9.62E 07	1.54E 10
		3	0.03	3.00E 08	1.47E 10
		4	0.30	7.67E 15	3.31E 09
		5	0.03	1.18E 07	1.64E 10
		6	0.03	1.63E 09	4.56E 09

TABLE VI.1 (CONTINUED)

			ATOMIC EMISSION		ATOMIC ABSORPTION
ELEMENT	LINE	TYPE	W(OPT) MM.	N(MIN) ATOMS/CC.	N(MIN) ATOMS/CC.
TL	5350	1	0.07	1.46E 08	2.54E 09
		2	0.09	7.92E 07	2.57E 09
		3	0.09	3.10E 08	2.47E 09
		4	0.35	2.10E 16	5.54E 08
		5	0.09	1.12E 07	2.75E 09
		6	0.07	1.78E 09	7.63E 08
TM	4094	1	0.04	2.33E 07	9.58E 09
		2	0.05	1.47E 07	9.72E 09
		3	0.05	4.78E 07	9.31E 09
		4	0.35	3.46E 14	2.09E 09
		5	0.04	2.53E 06	1.04E 10
		6	0.04	2.19E 08	2.88E 09
U	3871	1	0.03	3.61E 07	5.68E 09
		2	0.04	2.45E 07	5.77E 09
		3	0.04	7.92E 07	5.52E 09
		4	0.30	1.37E 15	1.24E 09
		5	0.04	3.47E 06	6.17E 09
		6	0.03	4.16E 08	1.71E 09
V	3183	1	0.01	7.44E 09	6.06E 09
		2	0.01	4.08E 09	6.15E 09
		3	0.01	9.89E 09	5.89E 09
		4	0.06	8.29E 18	1.32E 09
		5	0.01	7.40E 08	6.58E 09
		6	0.01	2.00E 11	1.82E 09
V	4385	1	0.01	1.45E 08	1.40E 10
		2	0.02	8.49E 07	1.42E 10
		3	0.02	3.01E 08	1.36E 10
		4	0.25	1.25E 15	3.06E 09
		5	0.05	3.54E 06	1.52E 10
		6	0.04	3.90E 08	4.21E 09

TABLE VI.1 (CONTINUED)

			ATOMIC EMISSION		ATOMIC ABSORPTION
ELEMENT	LINE	TYPE	W(OPT) MM.	N(MIN) ATOMS/CC.	N(MIN) ATOMS/CC.
W	4009	1	0.03	3.06E 08	1.45E 10
		2	0.04	1.84E 08	1.47E 10
		3	0.04	7.12E 08	1.41E 10
		4	0.35	7.20E 16	3.16E 09
		5	0.04	2.42E 07	1.57E 10
		6	0.03	4.88E 09	4.35E 09
W	4295	1	0.04	3.34E 08	3.85E 10
		2	0.05	2.08E 08	3.91E 10
		3	0.05	7.89E 08	3.74E 10
		4	0.30	2.65E 16	8.42E 09
		5	0.05	3.03E 07	4.18E 10
		6	0.04	4.35E 09	1.16E 10
Y	3621	1	0.02	2.07E 08	1.04E 10
		2	0.02	1.34E 08	1.06E 10
		3	0.03	4.21E 08	1.01E 10
		4	0.30	3.34E 16	2.27E 09
		5	0.03	1.35E 07	1.13E 10
		6	0.03	2.60E 09	3.13E 09
Y	4077	1	0.04	1.91E 07	1.05E 10
		2	0.05	1.20E 07	1.06E 10
		3	0.05	3.92E 07	1.02E 10
		4	0.35	3.02E 14	2.29E 09
		5	0.04	2.06E 06	1.14E 10
		6	0.04	1.81E 08	3.15E 09
Y	4102	1	0.04	2.08E 07	8.67E 09
		2	0.05	1.30E 07	8.80E 09
		3	0.05	4.33E 07	8.42E 09
		4	0.35	4.58E 14	1.89E 09
		5	0.04	2.16E 06	9.40E 09
		6	0.04	2.09E 08	2.61E 09

TABLE VI.1 (CONTINUED)

			ATOMIC EMISSION		ATOMIC ABSORPTION
ELEMENT	LINE	TYPE	W(OPT) MM.	N(MIN) ATOMS/CC.	N(MIN) ATOMS/CC.
YB	3464	1	0.02	7.91E 08	1.41E 10
		2	0.02	4.72E 08	1.43E 10
		3	0.02	1.43E 09	1.37E 10
		4	0.30	1.75E 17	3.08E 09
		5	0.02	4.37E 07	1.53E 10
		6	0.02	1.01E 10	4.24E 09
YB	3988	1	0.03	1.48E 07	4.19E 09
		2	0.04	9.33E 06	4.25E 09
		3	0.04	3.10E 07	4.07E 09
		4	0.35	3.45E 14	9.14E 08
		5	0.04	1.52E 06	4.54E 09
		6	0.03	1.58E 08	1.26E 09
ZN	2139	1	0.10	3.56E 12	3.70E 09
		2	0.15	1.54E 12	3.75E 09
		3	0.20	1.15E 13	3.59E 09
		4	1.50	2.72E 27	8.07E 08
		5	0.20	3.05E 10	4.01E 09
		6	0.20	4.83E 14	1.11E 09
ZN	3345	1	0.02	2.47E 16	6.56E 08
		2	0.01	1.33E 16	6.65E 08
		3	0.02	1.67E 17	6.37E 08
		4	0.01	2.96E 27	1.43E 08
		5	0.02	8.38E 13	7.11E 08
		6	0.02	5.06E 19	1.97E 08
ZN	4811	1	0.02	2.26E 14	2.94E 08
		2	0.02	7.54E 13	2.98E 08
		3	0.02	1.32E 15	2.85E 08
		4	0.01	2.96E 27	6.42E 07
		5	0.06	3.84E 11	3.19E 08
		6	0.05	3.33E 16	8.83E 07

TABLE VI.1 (CONTINUED)

			ATOMIC EMISSION		ATOMIC ABSORPTION
ELEMENT	LINE	TYPE	W(OPT) MM.	N(MIN) ATOMS/CC.	N(MIN) ATOMS/CC.
ZR	3520	1	0.02	6.02E 08	2.20E 10
		2	0.02	3.46E 08	2.23E 10
		3	0.03	1.08E 09	2.14E 10
		4	0.30	9.80E 16	4.81E 09
		5	0.02	3.53E 07	2.39E 10
		6	0.02	7.00E 09	6.61E 09

APPENDIX VII

FACTORS CONCERNING THE CONVERSION OF ATOMIC CONCENTRATION TO SOLUTION CONCENTRATION

Winefordner and Vickers (29) have derived an expression which can be used to convert from atomic concentration in atoms/cm.^{3} to solution concentration in moles/l.

$$C = 3.3 \times 10^{-22} \frac{n_T \; T \; Q \; N}{n_{298} \; \phi \epsilon \beta} , \qquad \text{(VII.1)}$$

where the constant term results from unit conversions, n_T/n_{298} is the ratio of moles of flame gas products at temperature T to moles at 298°K, T is the flame temperature in °K, Q is the flow rate of unburned gases in cm.^{3}/sec., ϕ is the flow rate at which the sample is introduced into the flame in cm.^{3}/min., N is the atomic concentration in atoms/cm.^{3}, C is the solution concentration in moles l., ϵ is the efficiency of aspiration of the solution into the flame, and β is the fraction of the species which exists in the atomic form.

All of the parameters in this equation are known to a good degree of accuracy except $\epsilon \beta$. Methods for determining $\epsilon \beta$ and β are discussed in the following sections of this appendix.

Experimental Determination of $\epsilon\beta$. The theoretical derivation of equations relating i, the current at the photoanode, to N, the atomic concentration have been given for atomic emission by Winefordner and Vickers (29)

$$i = \gamma T_f W H \Omega_e I \quad , \tag{VII.2}$$

where

$$I = \frac{10^{-7} h \nu_o NL A_t g_u}{4\pi g_l} e^{-E_u/kT} \tag{VII.3}$$

for low atomic concentrations. Thus, if the current due to a known solution concentration is measured, the atomic concentration causing i can be calculated under the condition that the concentration is in the linear (low concentration) portion of the analytical growth curve. This is a condition which can be experimentally verified by measuring several concentrations and plotting an analytical curve. Once the atomic concentration is calculated by means of equations VII.2 and VII.3, $\epsilon\beta$ can be calculated from VII.1 by substituting the appropriate values for the particular flame used in the measurement.

A second method for the calculation of $\epsilon\beta$ is by measuring $i^o - i_t$ in atomic absorption flame spectrometry, that is, the current due to the incident radiation transmitted by the flame gases with no sample minus the current due to the radiation transmitted by the flame gases with sample. This value has also been related to N by Winefordner and Vickers (30).

$$i^{o} - i_{t} = \gamma T_{f}\, W\, H\, \Omega_{e}(I_{A}^{\circ} - I_{t}) \quad , \tag{VII.4}$$

where I_t is given by

$$I_{t} = I_{A}^{\circ}\, e^{-\rho k^{\circ} L} = I_{A}^{\circ} \rho k^{o} L \quad , \tag{VII.5}$$

where the last form of equation VII.5 is true for low values of NL, and the term k^o is given by

$$k^{o} = \frac{0.037\, \lambda_{o}^{2}\, g_{u}\, NA_{t}}{g_{l}\, \Delta \nu_{D}} \quad . \tag{VII.6}$$

Thus when the signal due to absorption, that is $(i^o - i_t)$, due to a known solution concentration is measured (if is known), N can be calculated, and therefore $\epsilon\beta$ can also be calculated using equation VII.1.

A third method of $\epsilon\beta$ calculation can be accomplished from atomic fluorescence flame spectrometry measurements; however, in this method the Φ_T value must be known. Since Φ_T is not usually known, this method is not recommended. Because Φ_T is an important parameter in atomic fluorescence flame spectrometry, and in some cases a difficult parameter to experimentally determine, a simple method for estimating its value would be to measure $\epsilon\beta$ by atomic emission or atomic absorption flame spectrometry and to solve for Φ_T using equation 3.2 after measuring the current due to the corresponding concentration by atomic fluorescence flame spectrometry. (Of course, the same experimental conditions would be used for both measurements.)

Measurement of ϵ. To date the only method for measurement of the aspiration efficiency was described by Winefordner, Mansfield, and Vickers (23). Their method was based on atomic absorption of the Zn 2139 Å line when a 50 ppm solution of Zn as $ZnCl_2$ was introduced into various flames. In their method it was necessary to assume that the zinc species were completely atomized. It was also necessary to assume that a solution flow rate of 0.1 milliliter per minute gave 100 per cent aspiration efficiency. Thus, the absorption of zinc for a desired set of flame conditions was related to the aspiration efficiency by taking the ratio of the absorbance of zinc resulting for various solution flow rates of the 50 ppm Zn solution to the absorbance of the 50 ppm zinc solution introduced into the same flame at a rate of 0.1 milliliter per minute multiplied times the increase in flow rate factor.

A somewhat simpler method of measuring the aspiration efficiency is described here. This method is based on a comparison of the measurements of the light intensity reflected at a 90° angle from the water droplets aspirated from the burner without the flame. Dean and Carnes (6) have reported that the mean droplet diameter of water aspirated from a total-consumption aspirator-burner is about 20 microns when no flame is on. Therefore, the intensity of light reflected in the visible wavelength region by water droplets when no flame is on should be directly proportional to the total amount of solution being aspirated provided all solution droplets in the region of observation are within the solid angle of the incident radiation. Furthermore, when this intensity is compared with the light intensity reflected when the flame is on, the ratio will be the fraction of the introduced and dispersed solution which consists of droplets having diameters larger than the wavelength of observation. If this fraction is subtracted from unity, the fraction of the introduced and dispersed solution with droplets smaller than the wavelength of observation is obtained, and this fraction, if the wavelength is sufficiently small, is a direct measurement of the aspiration efficiency. A wavelength of 0.55 microns is suggested because droplets smaller than this would most likely be capable of complete evaporation, and a negligible interference signal due to Rayleigh scattering would be observed.

The procedure for ϵ measurements would be as follows: the burner being studied would be positioned at the desired height with respect to the monochromator entrance slit, the aspirating gas flow would be adjusted, and distilled deionized water would be aspirated into the burner; the reflected light signal would be measured over the background signal (the signal remaining when the shutter is placed between the source of excitation and the flame cell); then the fuel gas would be turned on, and the flame ignited; the reflected light signal would then be measured over the flame background signal; and ϵ is determined as discussed above.

Thus, the β factor can be calculated by dividing $\epsilon\beta$ obtained from equation VII.1 by β, and the transition from N to C is possible.

A FORTRAN IV program has been designed to perform the calculations of N, $\epsilon\beta$, and β by the atomic emission flame spectrometric method described above and is presented in Appendix VIII.

APPENDIX VIII

COMPUTER PROGRAMS

FORTRAN IV programs were designed to perform all of the calculations made for this manuscript. In this appendix each program will be discussed and the input and output formats for each will be given. This discussion will assume some knowledge of FORTRAN terminology.

Program I. This program is designed to calculate each r.m.s. noise term, the total r.m.s. noise, and $N_{min.}$ as a function of W for atomic fluorescence, atomic emission, and atomic absorption flame spectrometry for a specific set of flame conditions. Four cases are considered for atomic fluorescence flame spectrometry; they are the cases when either a continuous or narrow line source of excitation is used with either a D.C. or an A.C. amplifier-readout system. Only the case of a D.C. system is considered for atomic emission flame spectrometry, and both A.C. and D.C. systems are considered for atomic absorption flame spectrometry.

The data which concerns only the flame conditions are read into the program in the form of a subroutine, ACE1. The information contained in ACE1 is T, L, ξ , and Γ_R. The complete input format for Program I is as follows:

A. Read in the type of system assumed for atomic fluorescence flame spectrometry, CONDB, e.g., ATOMIC FLUORESCENCE, LINE SOURCE, A.C. SYSTEM, etc.

B. Read in the flame conditions, CONDA, e.g., FUEL RICH FLAME, 6CM. ABOVE BURNER.

C. Read in CONDC, ATOMIC EMISSION.

D. Read CONDD, atomic absorption AC. and D.C., e.g., ATOMIC ABSORPTION, D.C. SYSTEM, etc.

E. Read in the number of wavelengths to be considered, N.

F. Read in the parameters for each, γ, I_c, Φ_T, I°, I_L, g_u, g_l, A_t, E_u, $\Delta\nu_D$, and the element symbol.

G. Read in ρ_R for each wavelength.

The output of this program is as follows:

```
       CONDA

              ELEMT         WAVE

       CONDB or CONDC or CONDD

SLIT       SHOT     FLAME    SCATTER[1]   ELECT.    TOTAL     N(MIN)
 MM        NOISE    NOISE     NOISE       NOISE     NOISE    ATOMS/CC

0.01   x.xxE-xx x.xxE-xx x.xxE-xx x.xxE-xx  x.xxE-xx x.xxExx
0.02
  .
  .
0.10                   etc.
0.15
  .
  .
0.90
1.00
1.50
2.00
  .
  .
12.50
```

[1] This column will read SCATTER NOISE FOR CONDB;

Translation of the FORTRAN symbols to those used in the text is as follows:

XK is k, the Boltzmann constant in eV.;

EC is e_c, the charge on an electron in coulombs;

BM is BM the characteristic phototube factor times the amplification factor of the multiplier phototube (no units);

XID is i_d, the dark current of the phototube in amps.;

OMEGE is Ω_e, the solid angle over which the monochromator gathers in light in ster.;

OMEGA is Ω_a, the solid angle of incident radiation which is imaged on the flame cell in ster.;

TF is T_f, the transmittancy of the monochromator (no units);

H is H, the monochromator slit height in cm.;

RD is R_d, the reciprocal linear dispersion of the monochromator in $m\mu$/cm.;

SC is s_c, the minimum resolving spectral band width in $m\mu$;

DELF is Δf, the frequency response band width of the amplifier-readout system in sec.^{-1};

RHO is ρ, the correction factor to account for hyerpfine structure of the source and absorption line in atomic absorption flame spectrometry (no units);

---

1 (cont'd) it will be blank for CONDC; and it will read SOURCE NOISE for CONDD.

XLDEL is δ, the factor to account for line broadening other than Doppler broadening in atomic absorption flame spectrometry (no units);

CL is c, the speed of light in cm./sec.;

CHI is χ, the source flicker factor in sec.$^{1/2}$;

PI is π, 3.1416 (no units);

ZETA is ζ, the amplifier-readout noise factor in sec.$^{1/2}$;

T is T, the flame temperature in °K;

XL is L, the path length of the flame cell in cm.;

SQUIG is ξ, the flame background flicker factor in sec.$^{1/2}$;

GAMR is Γ_R, the reflection plus Rayleigh scattering from water droplet flicker factor in sec.$^{1/2}$;

GAMMA is γ, the photoanodic sensitivity of the photodetector in amps./watt;

XIC is I_c, the intensity of the flame background in watts/cm.^{2}ster.mμ ;

PHI is Φ_T, the power efficiency for atomic fluorescence flame spectrometry (no units);

WAVE is λ_o, the wavelength of the transition of concern in cm.;

XIOC is I°, the intensity of the continuous source of excitation in watts/cm.^{2}ster.mμ;

GUP is g_u, the statistical weight of the upper energy level (no units);

XIOL is I_L, the intensity of a narrow line source of excitation in watts/cm.^{2}ster.;

GLOW is g_1, the statistical weight of the ground energy level (no units);

AT is A_t, the transition probability of the transition of concern in sec.$^{-1}$;

EU is E_u, the energy of excitation for the energy level of concern in eV.;

DOPP is $\Delta \nu_D$, the Doppler half-width of the line of concern in sec.$^{-1}$;

ELEMT is the symbol of the elements of concern;

RHOR is ρ_R, the fraction of light reflected from water droplets in the flame (no units);

XIOA is I°_A, the intensity of the source of excitation in atomic absorption flame spectrometry in watts/cm.^{2}ster.;

FREQ is ν_o, the frequency of the transition of concern in sec.$^{-1}$;

W is W, the monochromator slit width in cm.;

SHOAC is the root-mean-square (r.m.s.) photoanodic shot noise, $\overline{\Delta i_p}$, in atomic fluorescence flame spectrometry using a continuous source of excitation with an A.C. system in amps.;

SHODC is the r.m.s. photoanodic shot noise, $\overline{\Delta i_p}$, in atomic fluorescence flame spectrometry using a continuous source with a D.C. system in amps.;

SHODL is the r.m.s. photoanodic shot noise, $\overline{\Delta i_p}$, in atomic fluorescence flame spectrometry using a narrow line source with a D.C. system in amps.;

SHOAL is the r.m.s. photoanodic shot noise, $\overline{\Delta i}_p$, in atomic fluorescence flame spectrometry using a narrow line source with an A.C. system in amps.;

FLAME is the r.m.s. flame background noise, $\overline{\Delta i}_c$, in atomic fluorescence flame spectrometry in amps.;

SCATC is the r.m.s. reflection noise in atomic fluorescence flame spectrometry using a continuous source of excitation in amps.;

SCATL is the r.m.s. reflection noise in atomic fluorescence flame spectrometry, $\overline{\Delta i}_R$, using a narrow line source of excitation in amps.;

ELEDC is the r.m.s. amplifier-readout noise in at9mic fluorescence flame spectrometry, $\overline{\Delta i}_e$, using a continuous source with a D.C. system, in amps.;

ELEAC is the r.m.s. amplifier-readout noise in atomic fluorescence flame spectrometry, $\overline{\Delta i}_e$, using a continuous source with an A.C. system in amps.;

ELEDL is the r.m.s. amplifier-readout noise in atomic fluorescence flame spectrometry, $\overline{\Delta i}_e$, using a narrow line source with a D.C. system in amps.;

ELEAL is the r.m.s. amplifier-readout noise in atomic fluorescence flame spectrometry, $\overline{\Delta i}_e$, using a narrow line source with an A.C. system in amps.;

TOTN is the total r.m.s. noise calculated for all three flame spectrometric methods, $\overline{\Delta i}_T$, in amps.;

XMIN is $N_{min.}$ calculated for all three flame spectrometric methods in atoms/cm.^{3};

ESHOT is the r.m.s. shot noise in atomic emission flame spectrometry, $\overline{\Delta i}_p$, in amps.;

EFLAM is the r.m.s. flame background noise in atomic emission flame spectrometry, $\overline{\Delta i}_c$, in amps.;

EELEC is the r.m.s. amplifier-readout noise in atomic emission flame spectrometry, $\overline{\Delta i}_e$, in amps.;

ASHDC is the r.m.s. shot noise, $\overline{\Delta i}_p$, in atomic absorption flame spectrometry using a D.C. system in amps.;

ASHAC is the r.m.s. shot noise, $\overline{\Delta i}_p$, in atomic absorption flame spectrometry using an A.C. system in amps.;

AFLAM is the r.m.s. flame background noise in atomic absorption flame spectrometry, $\overline{\Delta i}_c$, in amps.;

ASORC is the r.m.s. source noise in atomic absorption flame spectrometry, $\overline{\Delta i}^o$, in amps.;

AELDC is the r.m.s. amplifier-readout noise, $\overline{\Delta i}_e$, in atomic absorption flame spectrometry using a D.C. system in amps.; and

ALEAC is the r.m.s. amplifier-readout noise, $\overline{\Delta i}_e$, in atomic absorption flame spectrometry using an A.C. system in amps.

See Appendix I for a complete definition of the symbols used in the text.

The FORTRAN program follows:

```
C
C     CALCULATION OF NOISES AND N(MIN) VS. W FOR ATOMIC
C     EMISSION, ABSORPTION, AND FLUORESCENCE FLAME
C     SPECTROMETRY
C
      DIMENSION GAMMA(10),XIC(10),PHI(10),WAVE(10),XIOC(10),
     1XIOL(10),ELEMT(10),GUP(10),GLOW(10),AT(10),EU(10),DOPP
     1(10),FREQ(10),Q1(10),Q2C(10),Q2L(10),Q4(10),Q5(10),Q8(
     110),Q9(10),Q10(10),Q11(10),Q12(10),SHODC( 50 ),SHODL(
     150 ),FLAME(100 ),SCATC(100 ),SCATL(100 ),ELEDC(50 ),EL
     1EAC(50 ),ELEDL(50 ),ELEAL(50 ),ESHOT(50 ),EFLAM(50 ),E
     1ELEC(50 ),ASHDC( 50),AFLAM(50 ),ASORC(50 ),AELDC( 50),
     1W(50  ),XMIN(50  ),XIOA(10),BCOND(11,4),ACOND(11),CCON
     1D(11),DCOND(11,2),TOTN(50),SHOAC(50 ),SHOAL(50 ),ASHAC
     1( 50),AELAC( 50),RHOR(10),Q6(10)
      COMMON T,XL,SQUIG,GAMR
C
C     SINGLE VALUED CONSTANTS
C
      XK=8.618*10.**(-5)
      EC=1.6*10.**(-19)
      BM=2.86*10.0**6
      XID=3.3*10.**(-10)
      OMEGA=7.1*10.**(-2)
      OMEGE=3.7*10.0**(-2)
      TF=0.5
      H=1.0
      RD=33.0
      SC=4.*10.**(-2)
      DELF=1.0
      RHO=1.0
      XLDEL=1.0
      CL=3.0*10.**10
      CHI=10.**(-2)
      PI=3.1416
      ZETA=10.**(-3)
      Q3=2.0*EC*DELF*BM
      Q7=DELF*ZETA**2
C
C     CONSTANTS WHICH CHANGE WITH FLAME CONDITIONS
C
      CALL ACE1
      READ(5,100) ((BCOND(L,J),L=1,11),J=1,4)
      READ(5,100) (ACOND(M),M=1,11)
      READ(5,100) (CCOND(M),M=1,11)
      READ(5,100) ((DCOND(M,J),M=1,11),J=1,2)
C
C     CONSTANTS WHICH VARY WITH WAVELENGTH
C
      READ(5,104) N
      READ(5,105)(GAMMA(I),XIC(I),PH1(I),WAVE(I),XIOC(I),XIC
     1L(I),GUP(I),GLOW(I),AT(I),EL(I),DOPP(I),ELEMT(I),I=1,N
     1)
      READ(5,131) (RHOR(I),I=1,N)
C
C     CALCULATION OF NEW CONSTANTS THAT VARY WITH WAVELENGTH
C
      WRITE(6,106)
      WRITE(6,107) Q3,Q7
      WRITE(6,130)
      DO 10 I=1,N
      FREQ(I)=CL/WAVE(I)
      XIOA(I)=8.9*10.0**(-4)
      Q1(I)=GLOW(I)/(GAMMA(I)*TF*H*OMEGE*OMEGA*PHI(I)*WAVE(I
     1)**2*GUP(I)*AT(I)*XL)
     1
      Q2C(I)=64.0*10.0**(-7)*PI**2*CL/(XIOC(I)*WAVE(I)**2)
      Q2L(I)=671.9*DOPP (I)/XIOL(I)
      Q4(I)=GAMMA(I)*TF*H
      Q5(I)=XIC(I)*RD*OMEGE
      Q6(I)=OMEGE*OMEGA*RHOR(I)/(4.0*PI)
      Q8(I)=XIOC(I)*RD
      Q9(I)=XIOL(I)*GAMR
      Q10(I)=XIC(I)*OMEGE
      Q11(I)=ALOG(3.8*10.0**34)+ALOG(GLOW(I)/(FREQ(I)*GUP(I)
     1*AT(I)*XL*TF*H*OMEGE*GAMMA(I)))+EU(I)/(XK*T)
     1
      Q11(I)=EXP(Q11(I))
      Q12(I)=53.5*DOPP(I)*GLOW(I)/(Q4(I)*OMEGE   *  XIOA(I)*
     1RHO*WAVE(I)**2*GUP(I)*AT(I)*XLDEL*XL)
     1
      WRITE(6,108) ELEMT(I),Q1(I),Q2C(I),Q2L(I),Q4(I),Q5(I),
     1Q6(I),Q8(I),Q9(I),Q10(I),Q11(I),Q12(I)
     1
   10 CONTINUE
C
C      CALCULATION OF NOISES AND N(MIN) VS. W FOR ATOMIC
C      FLUORESCENCE FLAME SPECTROMETRY
C
      DO 25 I=1,N
      DO 25 J=1,4
      WRITE(6,109) (ACOND(M),M=1,11),ELEMT(I),WAVE(I)
      WRITE(6,110) (BCOND(L,J),L=1,11)
      WRITE(6,111)
      DO 20 K=1,50
      IF(K-9)11,11,12
   12 IF(K-26)13,13,14
   11 W(K)=FLOAT (K)*0.001
      GO TO 15
   13 W(K)=FLOAT (K)*0.005-0.04
      GO TO 15
   14 W(K)=FLOAT (K)*0.05-1.25
   15 SHODC(K)=SQRT (Q3*(XID+Q4(I)*(Q5(I)+Q6(I)*Q8(I))*W(K)*
     1*2))
      SHOAC(K)=SQRT (Q3*(XID+Q4(I)*(Q5(I)+Q6(I)*Q8(I)/2.0)*W
     1(K)**2))
      SHODL(K)=SQRT (Q3*(XID+Q4(I)*(Q5(I)*W(K)+Q6(I)*XIOL)*W
     1(K)))
      SHOAL(K)=SQRT (Q3*(XID+Q4(I)*(Q5(I)*W(K)+Q6(I)*XIOL/2.
     10)*W(K)))
      FLAME(K)=Q4(I)*W(K)**2*SQRT (DELF)*SQUIG*Q5(I)
      SCATC(K)=SQRT (DELF)*Q4(I)*Q6(I)*Q8(I)*GAMR*W(K)**2
```

```
    SCATL(K)=SQRT (DELF)*Q4(I)*Q6(I)*Q9(I)*W(K)
    ELEDC(K)=SQRT (Q7)*(XID+Q4(I)*(Q5(I)+Q6(I)*Q8(I))*W(K)
   1**2)
    ELEAC(K)=SQRT (Q7)*(Q4(I)*Q6(I)*Q8(I)*W(K)**2/2.0)
    ELEDL(K)=SQRT (Q7)*(XID+Q4(I)*(Q5(I)*W(K)+XIOL(I)*Q6(I
   1))*W(K))
    ELEAL(K)=SQRT (Q7)*(Q4(I)*XIOL(I)*Q6(I)*W(K)/ 2.0)
    GO TO (16,17,18,19),J
 16 TOTN(K)=SQRT (SHODC(K)**2+FLAME(K)**2+SCATC(K)**2+ELED
   1C(K)**2)
    XMIN(K)=Q1(I)*Q2C(I)/W(K)*TOTN(K)
    GO TO 20
 17 TOTN(K)=SQRT (SHOAC(K)**2+FLAME(K)**2+(SCATC(K)/2.0)**
   12+ELEAC(K)**2)
   1
    XMIN(K)=Q1(I)*Q2C(I)*2.0/W(K)*TOTN(K)
    GO TO 20
 18 TOTN(K)=SQRT (SHODL(K)**2+FLAME(K)**2+SCATL(K)**2+ELED
   1L(K)**2)
    XMIN(K)=Q1(I)*Q2L(I)/W(K)*TOTN(K)
    GO TO 20
 19 TOTN(K)=SQRT (SHOAL(K)**2+FLAME(K)**2+(SCATL(K)/2.0)**
   12+ELEAL(K)**2)
   1
    XMIN(K)=Q1(I)*Q2L(I)*2.0/W(K)*TOTN(K)
 20 CONTINUE
    GO TO (21,22,23,24), J
 21 WRITE(6,112) (W(K),SHODC(K),FLAME(K),SCATC(K),ELEDC(K)
   1,TOTN(K),XMIN(K),K=1,50)
   1
    GO TO 25
 22 DO 50 K=1,50
    SCATC(K)=SCATC(K)/2.0
 50 CONTINUE
    WRITE(6,112) (W(K),SHOAC(K),FLAME(K),SCATC(K),ELEAC(K)
   1,TOTN(K),XMIN(K),K=1,50)
   1
```

```
      GO TO 25
   23 WRITE(6,112) (W(K),SHODL(K),FLAME(K),SCATL(K),ELEDL(K)
     1,TOTN(K),XMIN(K),K=1,50)
     1
      GO TO 25
   24 DO 60 K=1,50
      SCATL(K)=SCATL(K)/2.0
   60 CONTINUE
      WRITE(6,112) (W(K),SHOAL(K),FLAME(K),SCATL(K),ELEAL(K)
     1,TOTN(K),XMIN(K),K=1,50)
     1
   25 CONTINUE
C
C     CALCULATION OF NOISES AND N(MIN) FOR ATOMIC EMISSION
C
      DO 35 I=1,N
      WRITE(6,109) (ACOND(M),M=1,11),ELEMT(I),WAVE(I)
      WRITE(6,110)(CCOND(M),M=1,11)
      WRITE(6,118)
      DO 34 K=1,50
      IF(K-9)26,26,27
   27 IF(K-26)28,28,29
   26 W(K)=FLOAT (K)*0.001
      GO TO 30
   28 W(K)=FLOAT (K)*0.005-0.04
      GO TO 30
   29 W(K)=FLOAT (K)*0.05-1.25
   30 ESHOT(K)=SQRT (Q3*(XID+Q4(I)*Q10(I)*W(K)*(RD*W(K)+SC))
     1)
      EFLAM(K)=SQRT (DELF*(Q4(I)*Q10(I)*SQUIG*W(K))**2*(RD*W
     1(K)+SC)**2)
      EELEC(K)=SQRT (Q7*(XID+Q4(I)*Q10(I)*W(K)*(RD*W(K)+SC))
     1**2)
      TOTN(K)=SQRT (ESHOT(K)**2+EFLAM(K)**2+EELEC(K)**2)
      XMIN(K)=Q11(I)/W(K)*TOTN(K)
   34 CONTINUE
      WRITE(6,119) (W(K),ESHOT(K),EFLAM(K),EELEC(K),TOTN(K),
     1XMIN(K),K=1,50)
     1
   35 CONTINUE
C
C      CALCULATION OF NOISES AND N(MIN) FOR ATOMIC ABSCRPTION
C
      DO 48 I=1,N
      DO 48 J=1,2
      WRITE(6,109) (ACOND(M),M=1,11),ELEMT(I),WAVE(I)
      WRITE(6,110) (DCOND(M,J),M=1,11)
      WRITE(6,122)
      DO 44 K=1,50
      IF(K-9)36,36,37
   37 IF(K-26)38,38,39
   36 W(K)=FLOAT (K)*0.001
      GO TO 40
   38 W(K)=FLOAT (K)*0.005-0.04
      GO TO 40
   39 W(K)=FLOAT (K)*0.05-1.25
   40 ASHDC(K)=SQRT (Q3*Q4(I)*OMEGE*W(K)*(XIOA(I)+XIC(I)*RD*
     1W(K)))
      ASHAC(K)=SQRT (Q3*Q4(I)*OMEGE*W(K)*(XIOA(I)/2.0+XIC(I)
     1*RD*W(K)))
      AFLAM(K)=SQRT (DELF)*Q4(I)*Q5(I)*SQUIG*W(K)**2
      ASORC(K)=SQRT (DELF)*Q4(I)*OMEGE*CHI*XIOA(I)*W(K)
      AELDC(K)=SQRT (Q7)*Q4(I)*OMEGE*W(K)*(XICA(I)+RD*XIC(I)
     1*W(K))
      AELAC(K)=SQRT (Q7)*Q4(I)*XIOA(I)*OMEGE*W(K)/2.0
      GO TO (41,42),J
   41 TOTN(K)=SQRT (ASHDC(K)**2+AFLAM(K)**2+ASORC(K)**2+AELD
     1C(K)**2)
      XMIN(K)=Q12(I)*TOTN(K)/W(K)
      GO TO 44
   42 TOTN(K)=SQRT (ASHAC(K)**2+AFLAM(K)**2+ASORC(K)**2/2.0+
     1AELAC(K)**2)
      XMIN(K)=2.0*Q12(I)*TOTN(K)/W(K)
   44 CONTINUE
      GO TO (45,46),J
```

```
 45 WRITE(6,112) (W(K),ASHDC(K),AFLAM(K),ASORC(K),AELDC(K)
   1,TOTN(K),XMIN(K),K=1,50)
   1
    GO TO 48
 46 DO 70 K=1,50
    ASORC(K)=ASORC(K)/2.0
 70 CONTINUE
    WRITE(6,112) (W(K),ASHAC(K),AFLAM(K),ASORC(K),AELAC(K)
   1,TOTN(K),XMIN(K),K=1,50)
   1
 48 CONTINUE
100 FORMAT (11A5)
104 FORMAT (I5)
105 FORMAT ((3E8.1,E10.0,2E8.1,2F4.1/E8.1,F5.2,E8.1,A5))
131 FORMAT (E10.2)
106 FORMAT (1H1)
107 FORMAT (1H0/1X5HQ3 = ,1PE10.2,3X5HQ7 =
   1   ,1PE10.2/)
   1
130 FORMAT (1H0//10X2HQ1,7X3HQ2C,6X3H2QL,6X2HQ4,7X2HQ5,7X2
   1HQ6,7X2HQ8,7X2HQ9,7X3HQ10,6X3HQ11,6X3HQ12)
   1
108 FORMAT (1H0/(A5,1P11E9.2))
109 FORMAT (1H1,10X11A5//25XA5,10X4PE10.0)
110 FORMAT (1H0,11X11A5/)
111 FORMAT (1H0,10X4HSLIT,8X4HSHOT,4X5HFLAME,4X7HSCATTER,3
   1X6HELECT.,5X5HTOTAL,5X6HN(MIN)/12X2HMM,9X5HNOISE,3X5HN
   1OISE,5X5HNOISE,4X5HNOISE,6X5HNOISE,4X8HATOMS/CC)
   1
112 FORMAT(1H0/(9X1PF5.2,6X4E9.2,1XE10.2,1XE10.2))
118 FORMAT (1H0,10X4HSLIT,8X4HSHOT,4X5HFLAME,4X6HELECT.,3X
   15HTOTAL,5X6HN(MIN)/12X2HMM,9X5HNOISE,3X5HNOISE,4X5HNOI
   1SE,4X5HNOISE,4X8HATOMS/CC)
   1
119 FORMAT(1H0/(9X1PF5.2,6X4E9.2,1XE9.2))
122 FORMAT(1H0,10X4HSLIT,8X4HSHOT,4X5HFLAME,5X6HSOURCE,3X6
   1HELECT.,5X5HTOTAL,5X6HN(MIN)/12X2HMM,9X5HNOISE,3X5HNOI
   1SE,5X5HNOISE,4X5HNOISE,6X5HNOISE,4X8HATOMS/CC)
```

```
1
 RETURN
 END
```

Program II. This program was designed to determine $N_{min.}$ at $W_{opt.}$ for atomic emission flame spectrometry and to calculate $N_{min.}$ for atomic absorption flame spectrometry. It is further designed to print in table form, suitable for direct use, from the computer output, the spectral parameters and the calculated values discussed above.

The input format is as follows:

A. Read in the number of flame types to be considered, J.

B. Read in the number of spectral lines to be considered, N.

C. Read in the element symbol, the molecular weight of the element, λ_o, g_u, g_l, A_t, E_u, and γ.

D. Read in I_c for each wavelength of each flame type.

E. Read in T, L, and ξ for each flame type.

F. Read in the wavelength again in 'fixed-point' notation.

The output format is given in Appendix IV, Table IV.1 for the spectral parameters and in Appendix VI, Table VI.1 for the calculated values. All of the FORTRAN symbols have already been translated with the following exceptions:

XMOL is the molecular weight of the element of concern in atomic mass units;

XAVE is the wavelength of the element of concern in 'fixed-point' notation;

XAT is the transition probability, A_t, times 10^{-8};

ANMIN is the minimum detectible atomic concentration in atomic absorption flame spectrometry in atoms/cm.^{3};

ENMIN is the minimum detectible atomic concentration in atomic emission flame spectrometry in atoms/cm.^{3}; and

WOPT is $W_{opt.}$ for atomic emission flame spectrometry in cm. (it should be noted that $W_{opt.}$ is printed out in mm.).

The FORTRAN IV program follows:

```
C      CALCULATION OF SIGNALS, NOISES, W(OPT), AND N(MIN)
C      FOR SOME ANALYTICALLY USEFUL LINES OBSERVED UNDER
C      SEVERAL FLAME CONDITIONS IN ATOMIC EMISSION AND
C      ATOMIC ABSORPTION FLAME SPECTROMETRY
C
       INTEGER X,XAVE
       DIMENSION T(10),XL(10),SQUIG(10),GAMMA(140),XIC(140,6)
      1,WAVE(140),XAVE(140),ELEMT(140),XMOL(140),GUP(140),GLO
      1W(140),AT(140),EU(140),FREQ(140),DOPP(140,6),Q1(140,6)
      1,Q4(140),Q13(140,6),ACOND(11,6),BCOND(11),CCOND(11),W(
      135),XMIN(35,6),ESHOT(35,6),EFLAM(35,6),EELEC(35,6),TOT
      1N(35,6),EWOPT(140,6),AWOPT(140,6),ENMIN(140,6),ANMIN(1
      140,6),XAT(140),Q5(140,6)
      1
C
C      SINGLE VALUED CONSTANTS
C
       XK=8.618*10.**(-5)
       EC=1.6*10.**(-19)
       BM=2.86*10.0**6
       XID=3.3*10.0**(-10)
       OMEGE=3.7*10.0**(-2)
       TF=0.5
       H=1.0
       RD=33.0
       SC=4.*10.**(-2)
       CL=3.0*10.**10
       DELF=1.0
       RHO=1.0
       XLDEL=1.0
       L=0
       CHI=10.0**(-2)
       ZETA=10.**(-3)
       Q3=2.0*EC*DELF*BM
       Q7=DELF*ZETA**2
       XIOL=8.9*10.0**(-4)
C
```

```
C     READ IN ALL DATA
C
C     J IS THE NUMBER OF FLAME TYPES TO BE CONSIDERED
C
      READ(5,101)J
C
C     N IS THE NUMBER OF SPECTRAL LINES TO BE OBSERVED
C
      READ(5,101)N
      READ(5,102)(ELEMT(I),XMOL(I),WAVE(I),GUP(I),GLOW(I),AT
     1(I),EU(I),GAMMA(I),I=1,N)
     1
      READ(5,103)((XIC(I,X),I=1,N),X=1,J)
      READ(5,104)(T(X),XL(X),SQUIG(X),X=1,J)
      READ(5,101)(XAVE(I),I=1,N)
C
C     WRITE OUT ATOMIC SPECTRAL CONSTANTS
C
      DO 2 I=1,N
      XAT(I)=    (AT(I)*10.0**(-8))
      IF (L-39)8,9,8
    8 IF(I-1)7,6,7
    9 WRITE(6,105)
      L=0
    5 WRITE(6,106)
      WRITE(6,107) ELEMT(I),XAVE(I),GUP(I),GLOW(I),XAT(I),EU
     1(I)
      GO TO 3
    7 WRITE(6,107) ELEMT(I),XAVE(I),GUP(I),GLOW(I),XAT(I),EU
     1(I)
      GO TO 3
    6 WRITE(6,150)
      GO TO 5
    3 L=L+1
    2 CONTINUE
      WRITE(6,170)
C
```

```
C     CALCULATION OF CONSTANTS WHICH VARY WITH WAVELENGTH
C
      DO 10 I=1,N
      FREQ(I)=CL/WAVE(I)
      Q4(I)=GAMMA(I)*TF*H
   10 CONTINUE
C
C     MASTER DO LOOP TO VARY FLAME TYPE
C
      DO 90 X=1,J
C
C     CALCULATIONS OF CONSTANTS WHICH VARY WITH BOTH
C     WAVELENGTH AND FLAME TYPE
C
      DO 20 I=1,N
      DOPP(I,X)=7.16*10.0**(-7)*FREQ(I)*SQRT(T(X)/XMCL(I))
      Q1(I,X)=XIC(I,X)*OMEGE
      Q5(I,X)=XIC(I,X)*RD*OMEGE
      Q13(I,X)=ALOG(3.8*10.0**34)+ALOG(GLOW(I)/(FREQ(I)*GUP(
     1I)*AT(I)*XL(X)*TF*H*OMEGE*GAMMA(I)))+EU(I)/(XK*T(X))
     1
      Q13(I,X)=EXP(Q13(I,X))
   20 CONTINUE
C
C     CALCULATION OF N(MIN) VS. W AND NOISE DATA FOR ATOMIC
C     EMISSION AND ABSORPTION FLAME SPECTROMETRY
C
      DO 30 I=1,N
      ANMIN(I,X)=53.5*DOPP(I,X)*GLOW(I)/(RHO*XL(X)*WAVE(I)**
     12*GUP(I)*AT(I)*XLDEL)*CHI
     1
      ENMIN(I,X)=1.00*10.0**29
      DO 30 K=1,35
      IF(K-9)26,26,27
   27 IF(K-26)28,28,29
   26 W(K)=FLOAT(K)*0.001
      GO TO 25
   28 W(K)=FLOAT(K)*0.005-0.04
```

```
      GO TO 25
   29 W(K)=FLOAT(K)*0.05-1.25
   25 ESHOT(K,X)=SQRT(Q3*(XID+Q4(I)*Q1(I,X)*W(K)*(RD*W(K)+SC
     1)))
      EFLAM(K,X)=SQRT(DELF*(Q4(I)*Q1(I,X)*SQUIG(X)*W(K))**2*
     1(RD*W(K)+SC)**2)
     1
      EELEC(K,X)=SQRT(Q7*(XID+Q4(I)*Q1(I,X)*W(K)*(RD*W(K)+SC
     1))**2)
      TOTN(K,X)=SQRT(ESHOT(K,X)**2+EFLAM(K,X)**2+EELEC(K,X)*
     1*2)
      XMIN(K,X)=Q13(I,X)/W(K)*TOTN(K,X)
      IF(XMIN(K,X).LT.ENMIN(I,X))ENMIN(I,X)=XMIN(K,X)
      IF(XMIN(K,X).EQ.ENMIN(I,X))EWOPT(I,X)=W(K)
   30 CONTINUE
   90 CONTINUE
C
C     WRITE OUT W(OPT) AND N(MIN) UNDER  SEVERAL FLAME
C     CONDITIONS FOR BOTH ATOMIC EMISSION AND ABSCRPTION
C     FLAME SPECTROMETRY
C
      L=0
      DO 80 I=1,N
      IF(L-5)82,83,82
   82 IF(I-1)84,85,84
   83 WRITE(6,116)
      L=0
   88 WRITE(6,117)
      WRITE(6,118)ELEMT(I),XAVE(I),(X,EWOPT(I,X),ENMIN(I,X),
     1ANMIN(I,X),X=1,J)
     1
      GO TO 89
   84 WRITE(6,118)ELEMT(I),XAVE(I),(X,EWOPT(I,X),ENMIN(I,X),
     1ANMIN(I,X),X=1,J)
     1
      GO TO 89
   85 WRITE(6,119)
```

```
      GO TO 88
   89 L=L+1
   80 CONTINUE
  101 FORMAT (I5)
  102 FORMAT (A5,F6.2,E10.0,2F4.1,E10.2,F5.2,E10.1)
  103 FORMAT (E9.1)
  104 FORMAT (E10.3,F5.0,E10.1)
  105 FORMAT (1H1/////////35X20HTABLE I. (CONTINUED)//////)
  106 FORMAT (1X,23X7HELEMENT,2X4HLINE,3X4HG(1),2X4HG(2),4X4
     1HA(T),4X4HE(U))
     1
  107 FORMAT (1X,24XA5,3XI4,2XF4.1,2XF4.1,5XF4.2,3XF5.2)
  116 FORMAT (1H1 ////////38X20HTABLE I. (CONTINUED)////////
     1/)
  117 FORMAT(1H0/40X15HATOMIC EMISSION,2X17HATOMIC ABSORPTIO
     1N//19X7HELEMENT,2X4HLINE,2X4HTYPE,2X6HW(OPT),2X6HN(MIN
     1),           8X6HN(MIN)/41X3HMM.,3X9HATOMS/CC.,
     1 5X9HATOMS/CC.)
  118 FORMAT(1H0,18XA5,4XI4,3X I1,3X1PF5.2,2X1PE9.2,
     1 5X1PE9.2/(35XI1,3X1PF5.2,2XE9.2,      5XE9.2))
     1
  119 FORMAT (1H1////////43X8HTABLE I.//19X54HCALCULATED VAL
     1UES FOR THE MINIMUM ATOMIC CONCENTRATION/15X63HAT THE
     1OPTIMUM SLIT WIDTH FOR SOME ANALYTICALLY IMPORTANT LIN
     1ES/17X58HOF SIXTY ELEMENTS UNDER SEVERAL FLAME TYPES A
     1ND CONDITIONS/16X60HFOR ATOMIC EMISSION AND ATOMIC ABS
     1ORPTION FLAME SPECTROMETRY//)
     1
  150 FORMAT (1H1/////////40X8HTABLE I.//26X35HVALUES OF ATO
     1MIC SPECTRAL CONSTANTS//16X55HFOR SOME ANALYTICALLY IM
     1PORTANT LINES OF SIXTY ELEMENTS///)
     1
  170 FORMAT(1H1)
      RETURN
      END
```

Program III. This program was designed to calculate the atomic concentration (N_i) corresponding to the point of intersection of the low and high concentration segments of analytical growth curves in atomic emission and atomic fluorescence flame spectromety using a continuous source of excitation. These calculations are made under the assumption that the a parameter is equal to unity (see Chapter IV). This calculation can be made for any number of spectral lines under any number of flame conditions. The input format is as follows:

A. Read in the number of flame types, J.

B. Read in the number of spectral lines, N.

C. Read in the element symbol, molecular weight of the element, λ_o, g_u, g_l, A_t, E_u, and γ for each line.

D. Read in L and $\Delta \nu_D$ for each flame type.

The output is as follows:

```
ELEMT                  WAVE
FLAME                  N(I)
  1                   x.xxExx
  2
  3
  .
  .
  J
```

All FORTRAN symbols have been translated except the following:

XNI is N_i the atomic concentration corresponding to the point of intersection in atoms/cm.^{3}.

The FORTRAN IV program follows:

```
C     CALCULATION OF N(I) FOR ATOMIC EMISSION
C     AND ATOMIC FLUORESCENCE FLAME SPECTROMETRY
C
      INTEGER X
      DIMENSION GUP(10),GLOW(10),AT(10),XMOL(10),GAMMA(10),W
     1AVE(10),XL(10,8),DOPP(10,8),ELEMT(10),EU(10),XNI(10,8)
     1
      A=1.0
C
C     READ IN DATA
C     J IS THE NUMBER OF FLAME CONDITIONS
C     N IS THE NUMBER OF WAVELENGTHS
      READ(5,100)J
      READ(5,100)N
      READ(5,102)(ELEMT(I),XMOL(I),WAVE(I),GUP(I),GLOW(I),AT
     1(I),EU(I),GAMMA(I),I=1,N)
     1
      READ(5,103)((XL(I,X),DOPP(I,X),I=1,N),X=1,J)
      DO 10 I=1,N
      WRITE(6,106) ELEMT(I),WAVE(I)
      WRITE(6,104)
      DO 10 X=1,J
      XNI(I,X)=60.0*A*DOPP(I,X)*GLOW(I)/(AT(I)*XL(I,X)*WAVE(
     1I)**2*GLOW(I))
     1
      WRITE(6,105)X,XNI(I,X)
   10 CONTINUE
  100 FORMAT(I5)
  102 FORMAT (A5,F6.2,E10.0,2F4.1,E10.2,F5.2,E10.1)
  103 FORMAT(F5.1,E10.1)
  104 FORMAT(1H0///25X5HFLAME,5X4HN(I)//)
  105 FORMAT(1X/27XI1,2X1PE10.2)
  106 FORMAT(1H1/25XA5,3X4PE10.0)
      RETURN
      END
```

Program IV. This program was designed to calculate $\epsilon\beta$ and β by the atomic emission method described in Appendix VII as a function of height above the burner tips. The program is set up for an aspirating gas flow rate of 3.0 l./min., a solution flow rate of 1.3 m./min., and an expansion factor, n_T/n_{298}, of 1.2; however, these values can easily be changed to suit other conditions by changing only three cards in the program.

The input format is as follows:

A. Read in the number of spectral lines plus the number of concentrations (or number of times the measurement was made) being considered, N.

B. Read in the number of flame types being considered, J.

C. Read in the flame types, ACOND, e.g., AN AIR-HYDROGEN FLAME.

D. Read in the element symbol, molecular weight of the element, λ_o, g_u, g_l, A_t, E_u, and γ for each spectral line. (This card must be repeated for each separate concentration or for each separate measurement of the same concentration.)

E. Read in T, L, and ϵ for each flame type at 1, 2, 3, and 4 cm. above the tip of the burner.

F. Read in the signal current and the concentration in p.p.m. for each line under each flame type at 1, 2, 3, and 4 cm. above the tip of the burner.

The output is as follows:

```
ELEMT                WAVE

ACOND

CONC.     CONC.     CURRENT    ATOMS      EB       B      HEIGHT
 PPM     MOLES/L.    AMPS.    PER CC.                       CM.

x.xxExx  x.xxE-xx  x.xxE-xx  x.xxExx  x.xxE-xx x.xxE-xx 1
                                                         2
                                                         3
                                                         4
                          etc.
```

All FORTRAN symbols have been translated except the following:

Q is Q, the flow rate of the unburned gases in cm.^{3}/sec.;

PHI is Φ , the solution flow rate in cm.^{3}/min.;

ROFN is n_T/n_{298}, the expansion factor (no units);

HT is the height above the tip of the burner in cm.;

XN is N, the atomic concentration corresponding to the measured current in atoms/cm.^{3};

IX is i, the signal current due to the solution concentration C in amps.;

CONP is the solution concentration in p.p.m.;

CONM is C, the solution concentration in moles/l.;

E is ϵ , the aspiration efficiency (no units); and

B is β, the fraction of the species in the atomic form (no units).

The FORTRAN IV program follows:

```
C
C      CALCULATION OF BETA AS A FUNCTION OF FLAME TYPE
C      AND HEIGHT ABOVE THE BURNER TIP
C
       INTEGER X
       DIMENSION GLOW(10),FREQ(10),GUP(10),AT(10),XL(6,4),GAM
      1MA(10),EU(10),T(6,4),WAVE(10),ELEMT(10),Q2(10,6,4),XN(
      110,6,4),ACOND(11,4),E(6,4),XMOL(10),CONM(10,6,4),CONP(
      110,6,4),XI(10,6,4),HT(4),EB(10,6,4),B(10,6,4)
      1
       COMMON W
C
C      SINGLE VALUED CONSTANTS
C
       Q1=3.8*10.0**34
       Q3=3.3*10.0**(-22)
       TF=0.50
       OMEGE=3.7*10.0**(-2)
       XK=8.618*10.0**(-5)
       H=1.0
       Q=50.0
       PHI=1.3
       ROFN=1.2
       CL=3.0*10.0**10
C
C      READ IN ALL DATA
C
C      N IS THE NUMBER OF SPECTRAL LINES PLUS THE NUMBER
C      OF DIFFERENT CONCENTRATIONS BEING CONSIDERED
C
       READ(5,100)N
C
C      J IS THE NUMBER OF FLAME TYPES BEING CONSIDERED
C
       READ(5,100)J
       READ(5,101)((ACOND(M,L),M=1,11),L=1,J)
C
```

```
C     A SEPARATE DATA CARD FOR THE SPECTRAL PARAMETERS MUST
C     BE INCLUDED FOR EACH CONCENTRATION WHICH IS CONSIDERED
C
      READ(5,102)(ELEMT(I),XMOL(I),WAVE(I),GUP(I),GLOW(I),AT
     1(I),EU(I),GAMMA(I),I=1,N)
     1
      READ(5,103)((T(L,X),XL(L,X),E(L,X),X=1,4),L=1,J)
      READ(5,110)(((XI(I,L,X),CONP(I,L,X),X=1,4),L=1,J),I=1,
     1N)
C
C     CALCULATIONS
C
      DO 10 I=1,N
      FREQ(I)=CL/WAVE(I)
   10 CONTINUE
      CALL BETA1
      DO 50 I=1,N
      WRITE(6,104)ELEMT(I),WAVE(I)
      DO 50 L=1,J
      WRITE(6,105)(ACOND(M,L),M=1,11)
      WRITE(6,106)
      DO 50 X=1,4
      HT(X)=FLOAT(X)
      Q2(I,L,X)=ALOG(Q1)+ALOG(GLOW(I)/(FREQ(I)*GUP(I)*AT(I)*
     1XL(L,X)*TF*HT(X)*OMEGE*GAMMA(I)))+EU(I)/(XK*T(L,X))
     1
      Q2(I,L,X)=EXP(Q2(I,L,X))
      XN(I,L,X)=Q2(I,L,X)*XI(I,L,X)/(2.0*W)
      CONM(I,L,X)=CONP(I,L,X)/XMOL(I)*10.0**(-3)
      EB(I,L,X)=Q3           /(CONM(I,L,X)*PHI)*RCFN*T(  L,X)
     1*XN(I,L,X)*Q
      B(I,L,X)=EB(I,L,X)/E(L,X)
      WRITE(6,111)CONP(I,L,X),CONM(I,L,X),XI(I,L,X),XN(I,L,X
     1),EB(I,L,X),B(I,L,X),X
     1
   50 CONTINUE
  100 FORMAT(I5)
```

```
101 FORMAT(11A5)
102 FORMAT (A5,F6.2,E10.0,2F4.1,E10.2,F5.2,E10.1)
103 FORMAT(F10.0,F5.1, F5.2)
110 FORMAT(E10.2,F10.0)
104 FORMAT(1H1///20XA5,5X4PE10.0)
105 FORMAT(1H0/20X11A5)
106 FORMAT(1H0/15X5HCONC.,5X5HCONC.,3X7HCURRENT,4X5HATOMS,
   15X2HEB,7X1HB,5X6HHEIGHT/16X3HPPM,3X8HMOLES/L.,4X5HAMPS
   1.4X7HPER CC.,21X3HCM.)
111 FORMAT(1H0,10X1PE10.2,1PE10.2,1PE10.2,1PE9.2,1PE9.2,1P
   1E9.2,2XI1)
    RETURN
    END
    SUBROUTINE ACE2
    COMMON W
    W=0.01
    RETURN
    END
```

Some general comments should be made about the programs. It is a simple matter to add or subtract from any of these programs in order to make them more useful for more general or more specific calculations. This is true because of the similar nature of both the parameters involved and the input formats. These programs were developed to be able to handle a variety of flame types and any number of spectral lines; thus, it is felt that these programs should meet many of the needs of theoretical calculations for all three methods of flame spectrometry in the future.

LITERATURE CITED

1. Alkemade, C.T.J., "Proceedings of the Xth Colloquium Spectroscopicum Internationale," E.R. Lippincott and M. Margoshes, eds., Spartan Books, Washington, D.C., 1963.

2. Boumans, P.W.J.M., "Enkele Fundemtele Aspecten van de Spectrochemische Analyse Met de Gelykstroomboog," Ph.D. Thesis, University of Amsterdam, 1961.

3. Clinton, O.E., Spectrochim. Acta, 16, 985(1960).

4. Corliss, C.H. and Bozman, W.R., "Experimental Transition Probabilities for Spectral Lines of Seventy Elements," N.B.S. Monograph 53, Washington, D.C., 1962.

5. Crosswhite, H.M., "The Spectrum of Iron I," Johns Hopkins Spectroscopic Rept. 13, August, 1958.

6. Dean, J.A. and Carnes, W.J., Anal. Chem., 34, 192(1962).

7. Goldman, S., "Frequency Analysis Modulation and Noise," McGraw-Hill, New York, 1948.

8. Herrmann, R. and Alkemade, C.T.J., "Chemical Analysis by Flame Photometry," trans. by P.T. Gilbert, Jr., Interscience Publishers, New York, 1963.

9. Hofmann, F.W. and Kohn, H., J. Opt. Soc. Am., 51, 512 (1961).

10. Kolb, A.C. and Streed, E.K., Austr. J. Phys., 20, 1872 (1952).

11. Lion, K.S., "Instrumentation in Scientific Research," McGraw-Hill, New York, 1959.

12. McCarthy, W.J., Parsons, M.L., and Winefordner, J.D., Spectrochim. Acta (submitted for publication).

13. Mansfield, J.M., Winefordner, J.D., and Veillon, C., Anal. Chem., 37, 1049(1965).

14. Mavrodineanu, R. and Boiteux, H., "Flame Spectroscopy," John Wiley and Sons, New York, 1965.

15. Mitchell, A.C.G. and Zemansky, M.W., "Resonance Radiation and Excited Atoms," University Press, Cambridge, 1961.

16. Moore, C.E., "Atomic Energy Levels," Vols. 1-3, Circular of the N.B.S. 467, Washington, D.C.

17. Remington, L.D., "Factors Which Influence the Signal-to-Noise Ratio in Atomic Emission Flame Spectrometry," Ph.D. Thesis, University of Florida, Gainesville, April, 1966.

18. Rodda, S., "Photoelectric Multipliers," Macdonald and Co., Ltd., London, 1953.

19. Slavin, W., Sprague, S. and Manning, D.C., Atomic Absorption Newsletter, No. 18, 1964.

20. Unsöld, A., "Physik der Sternatmosphere," Springer Vorlag, Berlin, 1955.

21. Veillon, C., Mansfield, J.M., Parsons, M.L. and Winefordner, J.D., Anal. Chem., 38, 204(1966).

22. Vickers, T.J., "The Calculation of Limits of Detectability and Optimum Condition for Atomic Emission and Absorption Flame Spectrometry," Ph.D. Thesis, University of Florida, Gainesville, April, 1964.

23. Winefordner, J.D., Mansfield, C.T. and Vickers, T.J., Anal. Chem., 35, 1607(1963).

24. Winefordner, J.D., Mansfield, C.T. and Vickers, T.J., Anal. Chem., 35, 1611(1963).

25. Winefordner, J.D. and Staab, R.A., Anal. Chem., 36, 165(1964).

26. Winefordner, J.D. and Staab, R.A., Anal. Chem., 36, 1367(1964).

27. Winefordner, J.D. and Veillon, C., Anal. Chem., 37, 416(1965).

28. Winefordner, J.D. and Vickers, T.J., Anal. Chem., 36, 161(1964).

29. Winefordner, J.D. and Vickers, T.J., Anal. Chem., 36, 1939(1964).

30. Winefordner, J.D. and Vickers, T.J., Anal. Chem., 36, 1947(1964).

31. Winefordner, J.D., Vickers, T.J. and Remington, L.D., Anal. Chem., 37, 1216(1965).

BIOGRAPHICAL SKETCH

Michael (Mike) Loewen Parsons was born in Oklahoma City, April 20, 1940, reared in Lawton, Oklahoma, and was graduated from Lawton High School in 1958. He married Karen O. Bridwell in the summer of 1958, and Stephen Michael Parsons was born in August, 1962.

He spent three years at Austin College, Sherman, Texas and finished his senior year at Kansas State College of Pittsburg, Kansas, where he received his B.A. degree in 1962. In 1963, he received a M.S. degree in analytical chemistry at K.S.C. and started to work on a Ph.D. degree at the University of Florida. In 1966, he accepted his first professional position as a research chemist with Phillips Petroleum Company at Bartlesville, Oklahoma.

He is a charter member of the Oklahoma Junior Academy of Science, a member of the American Chemical Society, the Society for Applied Spectroscopy, and Alpha Chi Sigma.

While at Austin College he received the Honor Award, and he was an N.S.F. Undergraduate Research Fellow at K.S.C.

This dissertation was prepared under the direction of the chairman of the candidate's supervisory committee and has been approved by all members of that committee. It was submitted to the Dean of the College of Arts and Sciences and to the Graduate Council, and was approved as partial fulfillment of the requirements for the degree of Doctor of Philosophy.

June 21, 1966

E. Ruffin Jones
Dean, College of Arts and Sciences

Dean, Graduate School

Supervisory Committee:

J. D. Winefordner
Chairman

A. P. Black

J. M. Pearce

R. C. Stoufer

W. V. Wilmot J.